University of Padova

Department of Surgery, Oncology and Gastroenterology

PhD Course in Oncology and Surgical Oncology

29th series

Role of miR-182 in neoplastic progression of colorectal cancer

Coordinator and Supervisor: Prof. Paola ZANOVELLO

PhD Student: Dr. Lisa PERILLI

INDEX

ABSTRACT

Numerous studies have demonstrated that aberrant expressions of specific microRNAs (miRNAs) are involved in many cancer types including colorectal cancer (CRC). In particular, in a previous study we integrated miRNA and target gene expression data obtained from chip array by comparing normal colon tissue, primary tumor and liver metastasis, and we focused our attention on post-transcriptional regulatory networks with differentially expressed miRNAs and their supported relations with target genes. We demonstrated that miR-182 was one of the most up-regulated miRNAs in primary CRC compared to normal colon mucosa.

Starting from these premises, the project was focused on the following tasks:

1) Identification of miRNA biomarkers for CRC monitoring and screening in colon cancer patients;

2) Analysis of the functional effects of miR-182 inhibition in CRC cell lines characterized by a different *in vivo* tumorigenic behavior.

Regarding the first task in my first year of PhD we published a paper (68, Appendix 1) to confirm the involvement of miR-182 in CRC development and progression. In particular, a total of 240 histopathological and 51 plasma samples were included in this study. We observed a significant overexpression of miR-182 in CRC primary tumor compared to normal colon mucosa, which is also maintained in CRC liver metastases. Then, we also demonstrated that plasma miR-182 levels are significantly higher in CRC patients than in healthy controls. Moreover, miR-182 plasma levels were significantly reduced in post-operative samples after radical hepatic metastasectomy, compared to pre-operative samples. These results indicated that the evaluation of circulating miR-182 levels could be a promising approach to improve the repertoire of non-invasive blood based biomarkers for CRC monitoring and screening.

To strengthen these evidences, we carried out a prospective study in stage I-II (N0 M0) colon cancer. We preselected four strongly up-regulated miRNAs involved in the same post-transcriptional sub-network (miR-18a, miR-21, miR-182 and miR-183) and the most down-regulated miRNA (miR-139) and we confirmed that all the selected miRNAs are significantly modulated in colon cancer compared to normal colon mucosa. Moreover, we observed that miR-182, miR-183 and miR-139 were not modulated in inflammatory tissue compared to colon mucosa; by contrast miR-18a and miR-21 are significantly up-regulated also in the

inflammation-related process. To investigate whether the selected miRNAs could be useful to predict tumor relapse the patients were subdivided in Recurrent and Non Recurrent groups within 55 months. We calculated 10 ratios between the expression values of all possible miRNA pairs, applying the miRNA ratio approach both in the tumor tissue and in the adjacent normal mucosa. None of the miRNA ratios resulted predictive when evaluated in the colon cancer tissue, instead three miRNA ratios evaluated in the tumor-adjacent mucosa were found to be significant predictors of relapse by 55 months from resection: miR-21/miR-183, miR-18a/miR-182 and miR-18a/miR-183. *Manuscript submitted*.

Regarding the second task, to gain insights in the functional role played by miR-182 in the tumorigenesis we investigated the effects of miR-182 inhibition. To this end, we used two CRC cell lines as *in vitro* models: MICOL-14$^{h\text{-}tert}$ (an *in vivo* non-tumorigenic cell line derived from a lymph node metastasis of rectal cancer) and its *in vivo* tumorigenic variant MICOL-14^{tum} (or TC22). We carried out transfection experiments for the transient inhibition of miR-182 and we observed a significant increase of cell apoptosis in both cell lines after the treatment. We confirmed the results with cleaved PARP and Caspase-3 proteins detection by Western Blot.

Therefore, we evaluated the effect of miR-182 inhibition on *in vivo* tumor growth. To this end, we injected subcutaneously the TC22 cells treated with the anti-miR-182 in NOD/SCID mice and, after a week, we performed also an *in vivo* intra-tumor injection of miR-182 inhibitor to maintain the silencing. Interestingly, the inhibition of miR-182 significantly reduced the size of the tumor, and the obtained mass exhibited a pattern of features as less aggressive tumors compared to controls. *Manuscript in preparation*.

In conclusions:

- ✓ miR-182 expression levels can be followed in tissues and plasma of CRC patients. In particular, circulating miR-182 evaluation could be a promising approach to enhance the repertoire for blood based biomarkers in non-invasive CRC monitoring and screening;
- ✓ the panel of selected miRNAs were significantly regulated also in the early phases of the CRC tumor process extending to stage I-II the results obtained in our previous work in stage IV CRC;
- ✓ not a single miRNA, but rather a coordinated alteration of four miRNAs may be useful to predict recurrence after resection in early CRC when evaluate in the normal mucosa adjacent to tumor;

- ✓ in CRC cell lines the expression level of miR-182 is higher in *in vivo* tumorigenic variant, suggesting a role of this miRNA in tumor aggressiveness. MiR-182 seems to be involved in increasing the survival of cancer cells and enhance the tumor growth.

INTRODUCTION

1. Colorectal cancer

1.1 Epidemiology of CRC. Colorectal cancer (CRC) is still one of the most worldwide cancer type, in both men and women (1). The relative survival rate for CRC is 65% at 5 years following diagnosis and 58% at 10 years. Only 39% of CRC patients are diagnosed with localized-stage disease, for which the 5-year survival rate is 90%; survival declines to 71% and 14% for patients diagnosed with regional and distant stages, respectively (American Cancer Society: Cancer Facts and Figures 2017-2019. Atlanta). CRC incidence is higher in developed regions compared to less developed regions, which may reflect an increased exposure to risk factors such as smoking, unhealthy diet, physical inactivity, obesity, and other lifestyle factors (3). The opposite is observed for mortality rates and is mainly caused by late diagnosis due to lack of symptoms at an early stage, and thus many patients present at diagnosis with advanced disease and metastasis. Despite the ongoing development of novel anti-tumor agents and therapeutic principles as we enter the era of personalized cancer medicine, systemic chemotherapy continues to be the cornerstone for treatment of CRC patients (4).

1.2 Classification and disease staging. The TNM Classification of Malignant Tumours (TNM) is a cancer staging notation system that describes the stage of a cancer which originates from a solid tumor with alphanumeric codes and it is the most widely used and recommended system for CRC staging (5). TNM classification is based on the extent of the disease at diagnosis, which provides an important estimation of prognosis in CRC (6). It includes clinical findings (cTNM) and radiologic imaging (rTNM) prior to diagnosis, and pathological examination of resected tumor specimens or perioperative findings (pTNM, or ypTNM) when staging is made after neoadjuvant treatment) (7). Specifically, the T stage describes the depth of invasion of the primary tumor through the layers of the intestinal wall, N stage describes spread to regional lymph nodes, and the M stage describes the occurrence of distant metastases. TNM stages are classified in stage groups (stage I-IV) where increasing stage corresponds to a more advanced disease, e.g. lymph node involvement (stage III) and metastasis (stage IV) (8). In particular:

Stage 0: The cancer is found only in the innermost lining of the colon or rectum. "Carcinoma in situ" is considered to be Stage 0 colon cancer.
Stage I: The tumor has grown into the inner wall of the colon or rectum. The tumor has not grown through the wall.
Stage II: The tumor extends more deeply into or through the wall of the colon or rectum. It may have invaded nearby tissue, but cancer cells have not spread to the lymph nodes.
Stage III: The cancer has spread to nearby lymph nodes, but not to other parts of the body.
Stage IV: The cancer has spread to other parts of the body, such as the liver or lungs.

Based on microscopic features, CRCs are graded in terms of resemblance to the tissue from which it originated and the proportion of gland formation by the tumor (9). Tumor differentiation grade range from highly differentiated tumors with >95% gland formation, to undifferentiated tumors with less than 5% glandular structures. Histopathological differentiation grade is an important prognostic factor in CRC as low differentiation grade is associated with poorer outcome (10, 11).

1.3 Molecular basis of CRC. During colorectal adenocarcinoma development, epithelial cells from gastrointestinal trait acquire sequential genetic and epigenetic mutations in specific oncogenes and/or tumor suppressor genes, conferring them a selective advantage on proliferation and self-renewal (12). Normal epithelium becomes hyper-proliferative mucosa and subsequently gives rise to a benign adenoma that evolves into carcinoma and metastasis in about 10 years (13). Sporadic CRC, due to somatic mutations, account for about 70% of all CRCs.
Normal gastrointestinal epithelium is organized along a crypt-villus axis. A pool of colon stem and progenitor cells, the most undifferentiated cell types that are able of self-renewal and pluripotency, are located at the bottom of the crypt. These cells migrate along the crypt-villus axis, simultaneously differentiating in all epithelial colon lineages, such as Paneth, goblet, enterocytes and enteroendocrine cells (14). In about two weeks they arrive at the top of the villus and undergo apoptosis (15, 16). This process is orchestrated from gradients of proteins, such as Wnt, BMP and TGF-β, together with extracellular matrix and stromal cells that form the cell niche (17).

At the molecular level, CRCs are a very heterogeneous group of diseases as consequence of multistep tumorigenesis of several genetic and epigenetic events **(Figure 1)**. The well known

"adenoma-carcinoma" sequence in CRC has made this disease a popular model for a multihit cancer (18). There are three most important molecular pathways leading to CRC development: 1) Somatic or germ line derived genomic instability due to inactivation of several tumor suppressor genes such as APC, SMAD4 and TP53; aberrant DNA methylation, DNA repair defects induced by mutations in mismatch repair genes (MMR); 2) Mutational inactivation of tumor suppressor genes (e.g., APC, TP53, TGFβ, and MMR genes); and 3) Over activation of oncogenic pathways including BRAF, RAS (KRAS and NRAS), Phosphatidylinositol 3-kinase (PIK-3) (19).

In colorectal epithelial cell transformation play a significant role other involved mechanisms, as chromosomal instability (CIN), microsatellite instability (MSI), CpG island methylator phenotype (CIMP), DNA polymerase mutations (POLE), aberrant DNA methylation and DNA repair defects (20-23). These alterations confer individual susceptibility to cancer, and are responsible for responsiveness or resistance to antitumor agents.

As regard, an international consortium named CRC Subtyping Consortium (CRCSC) dedicated to large-scale data sharing recently suggests a disease stratification to resolve inconsistencies among the reported gene expression and facilitate clinical translation (24). The result is in four consensus molecular subtypes (CMSs) of CRC with distinguishing features:

CMS1 (MSI immune, 14%): hypermutation, MSI, and strong immune activation.

CMS2 (Canonical, 37%): epithelial, with CIN and prominent WNT and MYC signaling activation.

CMS3 (Metabolic, 13%): epithelial, with metabolic dysregulation.

CMS4 (Mesenchymal, 23%): with prominent TGF-β activation, stromal invasion and angiogenesis.

A remaining 13% possibly represent a transition phenotype or intratumoral heterogeneity.

This is considered the most robust classification system currently available for CRC.

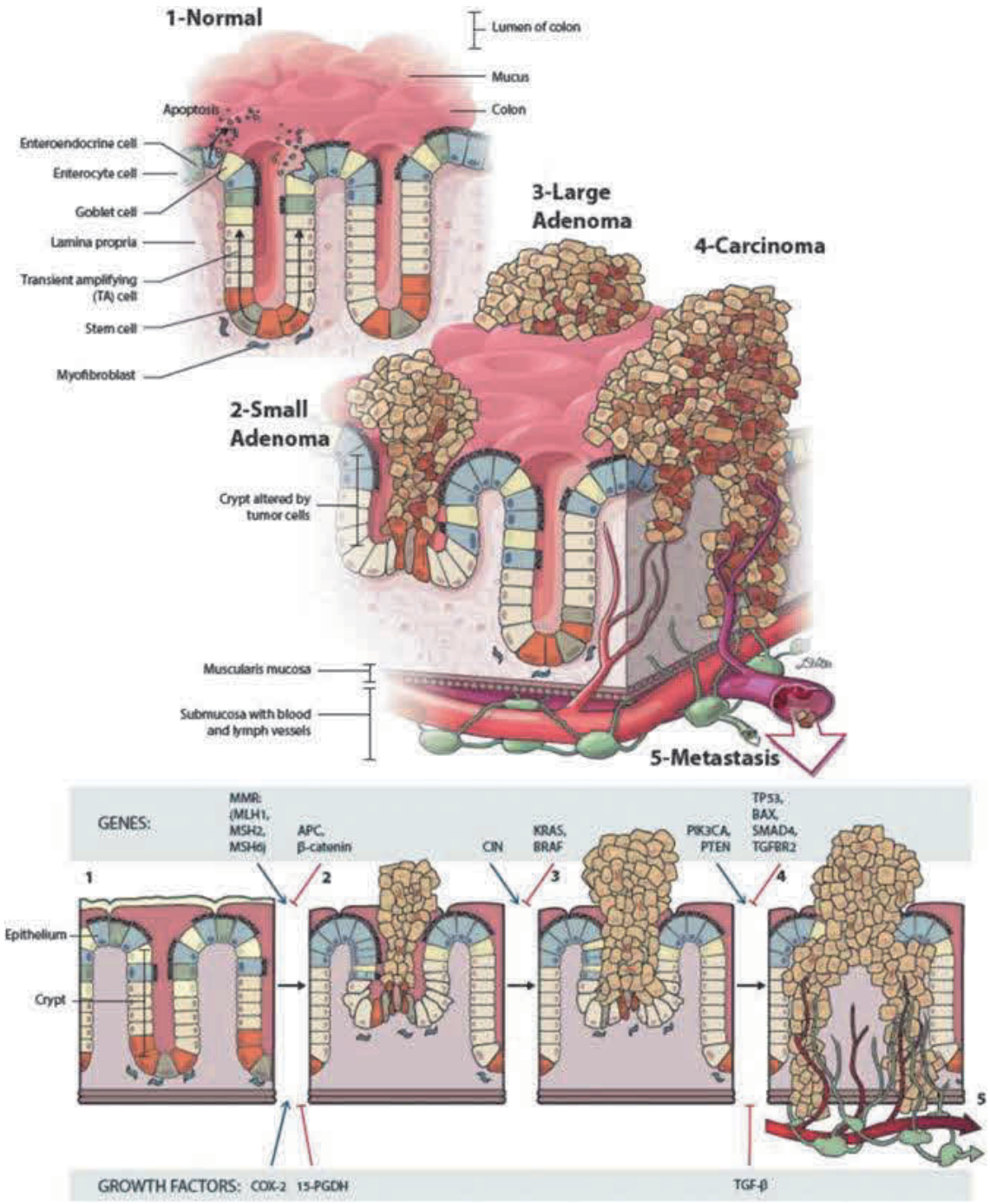

Figure 1: A multihit scenario for colorectal cancer, showing the mutational events that correlates with each step of "adenoma-carcinoma" sequence. CRC development is a multistep process that begins when normal epithelium forms aberrant crypts and further advances into stages of early and late adenomatous polyps, invasive carcinoma, and metastasis. Some of the most frequently affected genes and pathways are shown. The arrows show the oncogenes that are turned on, while the red blocked arrows denote the tumor suppressor genes that are turned off at different stages of CRC development. APC, adenomatous polyposis coli; COX2, cyclooxygenase 2; DCC, deleted in colorectal cancer; EGFR, epithelial growth factor receptor; MLH1, 2, mutL homologue (mismatch repair) genes; MSH2, 3, 6, mutS homologue (mismatch repair) genes; TP53, multi-function tumour-suppressor gene; PRL3, (also known as PTP4A3, a metastasis-associated gene); Ras, signalling protein; SMAD3 and SMAD4, signalling proteins downstream of TGFbeta; TGFbeta, transforming growth factor beta; TGFbetaRII, transforming growth factor receptor beta type II. (from Thergiory Irrazábal et al., The Multifaceted Role of the Intestinal Microbiota in Colon Cancer. 2014).

1.4 Biomarkers in CRC. The continuing CRC incidence and the increasing disease associated morbidity and mortality are in part due to the lack of efficient early detection; therefore, earlier diagnosis and more efficient treatment could play a key role in reducing CRC mortality. Obviously, there is an urgent need for reliable biomarkers with prognostic and predictive value, which are able to discriminate cancer patients from healthy individuals, as well as different CRC subgroups from each other.

Cancer related molecular and cellular markers can be classified as:

Diagnostic markers, used for risk stratification and early detection;

Prognostic marker, give an indication of the likely progression of the disease;

Predictive markers, predict treatment response;

Surveillance markers, used to monitor disease recurrence.

As summarized in **Figure 2**, several biomarker classes have been evaluated in CRC screening and have all shown potential in early phase biomarkers studies: MSI, CIN, DNA mutations, KRAS mutations, BRAF mutations, TP53 mutations, APC/β catenin mutations, DNA methylation (aberrant DNA hypermethylation, genome-wide DNA hypomethylation), tumor specific gene or microRNA expression pattern, telomere length dynamics, angiogenesis biomarkers, inflammatory biomarkers, stool and blood non-invasive biomarkers (circulating tumor cells, cell-free DNA, microRNA and proteins) (19). In particular, these last biomarkers derived from biological fluids and so easily accessible could be considered as practical tools for CRC detection and monitoring to improve patients' prognosis, treatment response prediction and possible recurrence risk.

Actually, the most widely used biomarker in CRC is CEA (carcinoembryonic antigen), a set of highly related glycoproteins involved in cell adhesion that are secreted from cancer cells into the bloodstream. Elevated levels at diagnosis are associated with increased tumor stage a poor prognosis (25), but the test is compromised by low sensitivity and specificity and high rate of false positive. Indeed, CEA levels are lower in early stage, and high levels are found in other cancer types, non-malignant conditions, and smokers (26-29), making it insufficient for early detection and screening. In addition, other circulating proteins are often measured, as carbohydrate antigens (CA19-9, CA50, CA72-4), soluble Fas ligand (FasL), p53, and VEGF.

Despite the disadvantages, CEA is the more non-invasive and inexpensive test with a strong prognostic impact useful to monitor CRC patients (30).

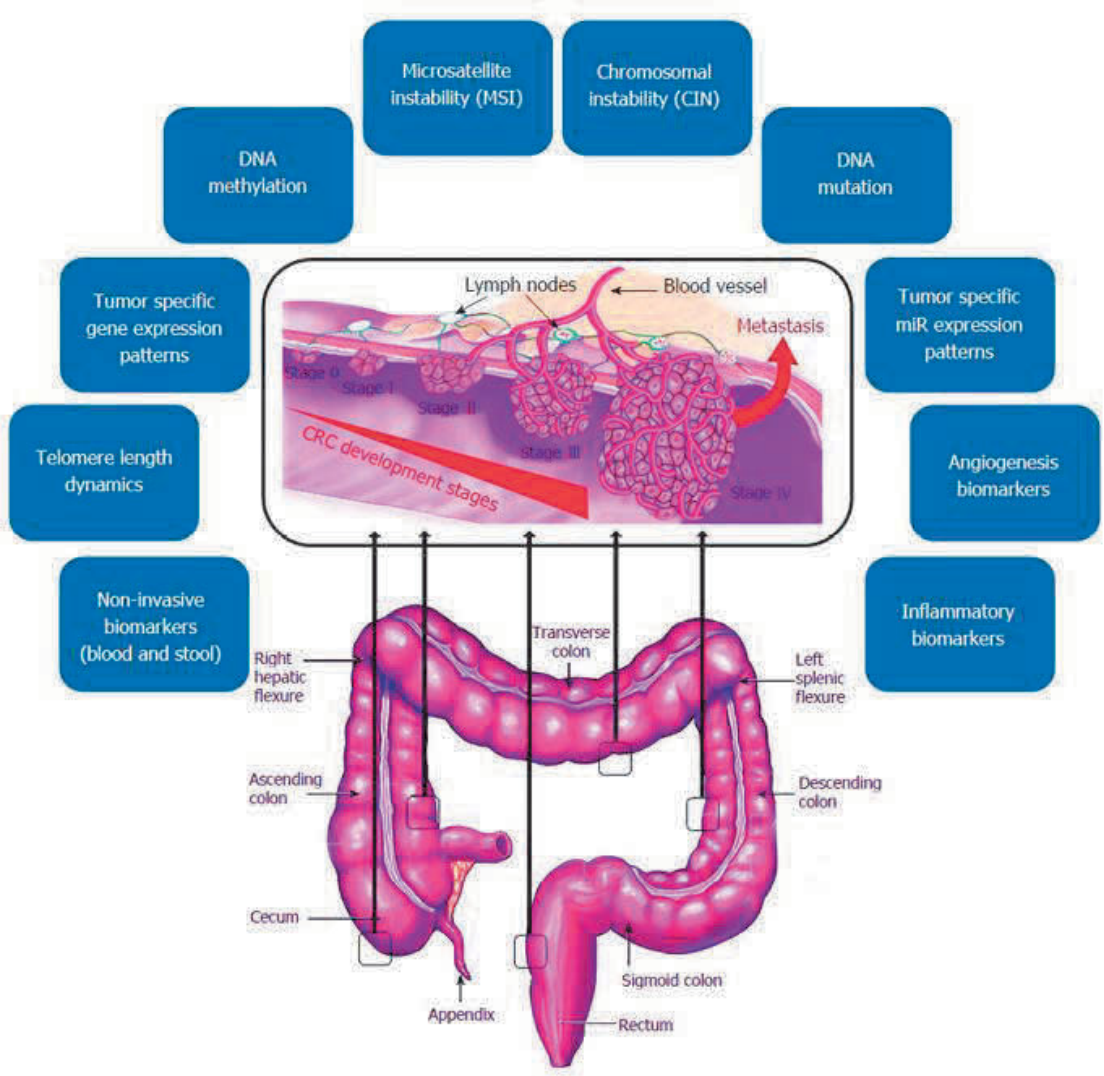

Figure 2: Different classes of colorectal cancer associated molecular and cellular biomarkers. (from Aghagolzadeh P et al . Molecular and cellular biomarkers for CRC).

Therefore, new biomarkers are needed to early identify colon cancer patients. In particular, they should be able to stratify patients into risk groups to support the therapeutic choice. The evaluation of biomarkers in body fluids of cancer patients will be in the next future a novel mini-invasive tool for an earlier personalized cancer diagnosis and to predict prognosis and response to therapy of CRC.

2. MicroRNAs

2.1 miRNAs biogenesis. MiRNAs are small non-coding RNAs that function as guide molecules in RNA silencing. Targeting most protein-coding transcripts, miRNAs are involved in nearly all developmental and physiological processes. The biogenesis is regulated at multiple levels and is under tight temporal and spatial control, and their dysregulation is associated with many human diseases, particularly cancer. MiRNAs genes are generally transcribed by RNA polymerases II and III, generating precursors that undergo a series of cleavage events to form mature miRNA. As described in **Figure 3**, the conventional biogenesis pathway consists of two cleavage events, one nuclear and one cytoplasmic (31). The transcription by RNA Polymerase II (Pol II) in the nucleus forms large pri-miRNA transcripts, which are capped and polyadenylated. These pri-miRNA transcripts are processed by the RNase III enzyme DROSHA and its co-factor, PASHA, to release the ~70-nucleotide pre-miRNA precursor product. RAN–GTP and exportin 5 transport the pre-miRNA into the cytoplasm and subsequently, another RNase III enzyme, DICER, processes the pre-miRNA to generate a transient ~22-nucleotide miRNA: miRNA duplex. This duplex is then loaded into the miRNA-associated multiprotein RNA-induced silencing complex (miRISC), which includes the Argonaute proteins, and the mature single-stranded miRNA is preferentially retained in this complex. Then, the mature miRNA binds to complementary sites in the mRNA target to negatively regulate gene expression by grade of complementarity between the miRNA and its target gene. miRNAs that bind with imperfect complementarity block target gene expression at the level of protein translation usually affect mRNA stability and bind in the 3' UTRs. Instead, miRNAs that bind to their mRNA targets with perfect (or nearly perfect) complementarity induce target-mRNA cleavage and were generally found in the coding sequence or open reading frame (ORF) of the target (32).

Non-canonical pathways for miRNA biogenesis, including those that are independent of Drosha or Dicer, are also emerging (33).

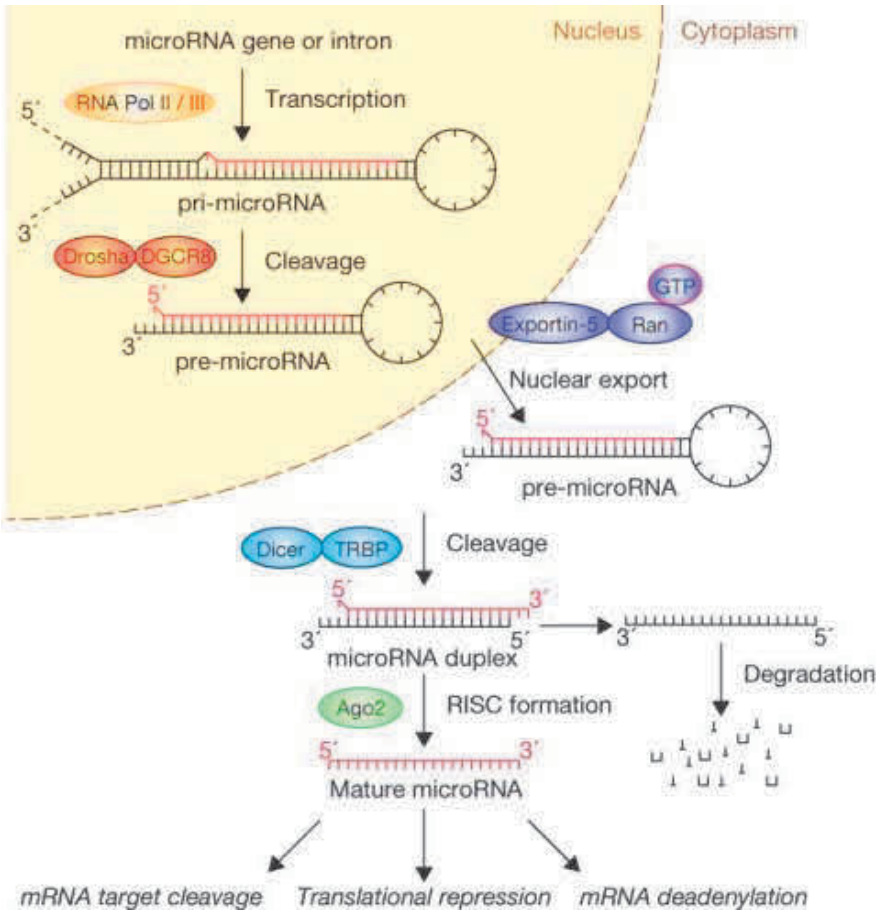

Figure 3: Overview of canonical miRNA biogenesis pathway. MiRNA genes are transcribed as primary miRNAs (pri-miRNAs) by RNA polymerase II (Pol II) in the nucleus. The long pri-miRNAs are cleaved by Microprocessor, which includes DROSHA and DiGeorge syndrome critical region 8 (DGCR8), to produce the 60–70-nucleotide precursor miRNAs (pre-miRNAs). The pre-miRNAs are then exported from the nucleus to the cytoplasm by exportin 5 (XPO5) and further processed by DICER1, a ribonuclease III (RIII) enzyme that produces the mature miRNAs. The functional strand of the mature miRNA is loaded together with Argonaute (Ago2) proteins into the RNA-induced silencing complex (RISC), where it guides RISC to silence target mRNAs through mRNA cleavage, translational repression or deadenylation, whereas the passenger strand (black) is degraded.

2.2 miRNAs in CRC. miRNAs are critical regulators of gene expression. Amplification and overexpression of individual 'oncomiRs' or genetic loss of tumour suppressor miRNAs are associated with human cancer and are sufficient to drive tumorigenesis in mouse models. Moreover, global miRNA depletion caused by genetic and epigenetic alterations in components of the miRNA biogenesis machinery is oncogenic. Aberrant miRNA biogenesis in cancer occurs at different steps during miRNA maturation: genetic alterations, epigenetic modifications, oncogenes and tumour suppressors negatively or positively regulate pri-miRNA transcription. Numerous oncogenic mutations are recently identified in core miRNA biogenesis genes (34) **(Figure 4)**, but there are multiple mechanisms by which cancer cells inactivate the miRNA 'guardian' of differentiation, proliferation and metabolic reprogramming. This, together with the recent identification of novel miRNA regulatory factors and pathways, highlights the importance of miRNA dysregulation in cancer.

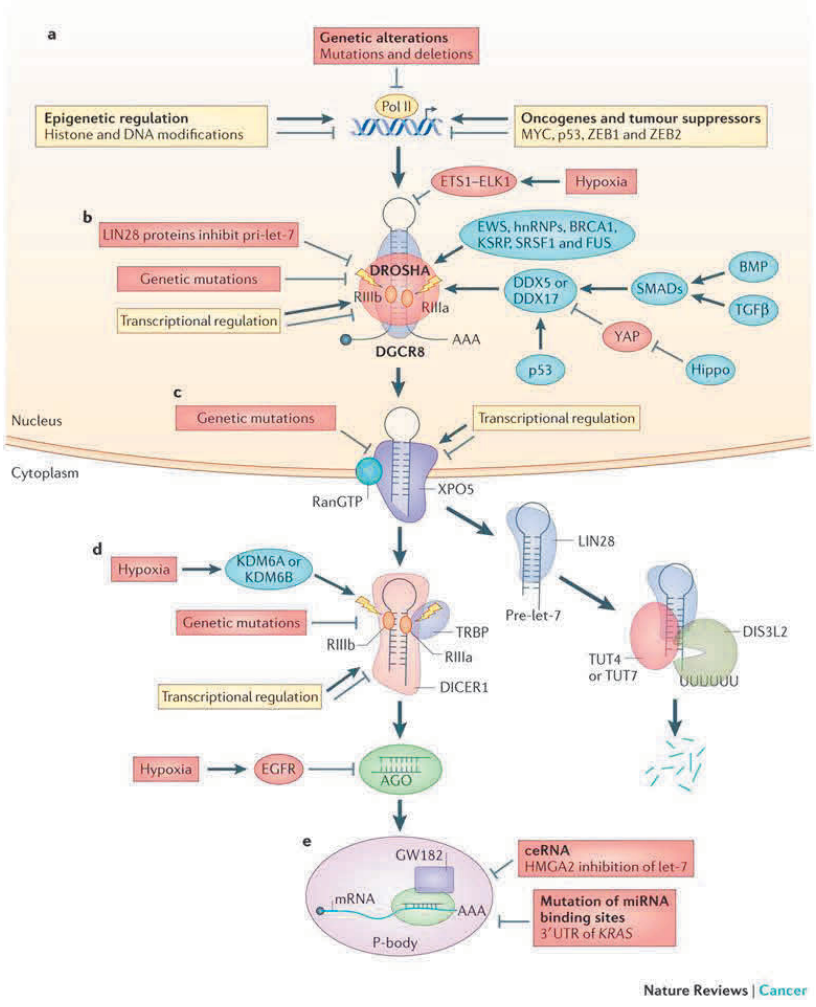

Figure 4: Dysregulated miRNA biogenesis in cancer. Aberrant miRNA biogenesis in cancer occurs at different steps during miRNA maturation.

MiR-143 and miR-145 were the first miRNA associated with CRC. Michael and colleagues observed a significant down-regulation of these miRNAs in tumor tissue compared to normal tissue (35), which was later shown to elicit tumor suppressor activity (36) and mainly expressed in the stroma (37). Since then, a range of altered expressed miRNAs has been associated with development and progression of this tumor type.

In CRC, miRNAs have shown involvement in, or directly regulating, oncogenic signaling pathways, such as Wnt, Ras, TGF-β, and NF-kB/AKT/STAT3 (38). In addition, they are also involved in the regulation of the stemness of cancer cells, epithelial-mesenchymal transition (EMT), and metastasis (**Figure 5**).

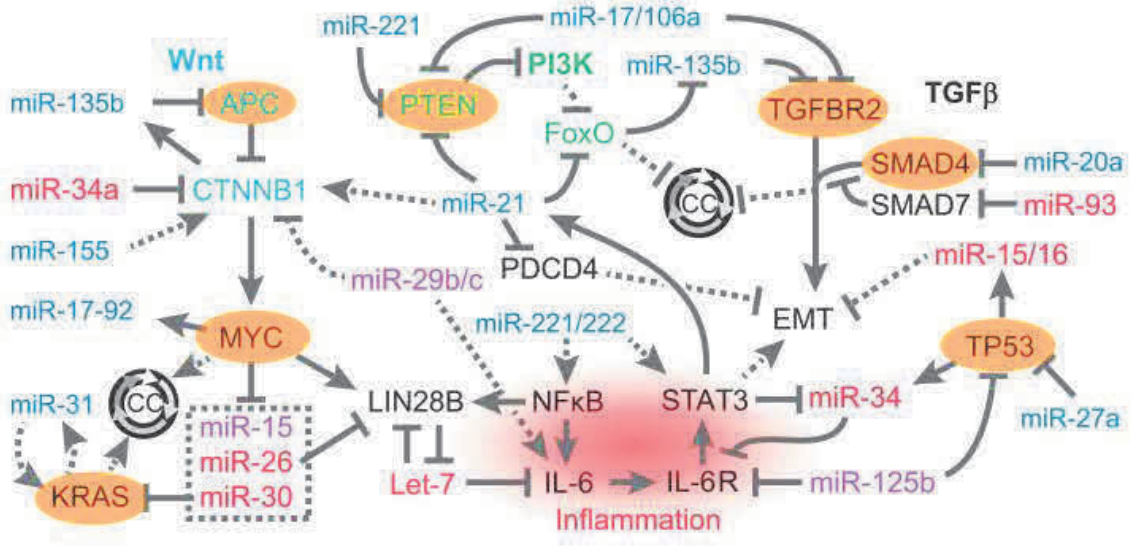

Figure 5: Genes frequently mutated in CRC and their relationships with miRNAs. Oncogenic miRNAs are depicted in blue, tumor-suppressive miRNAs in red, and miRNAs with reported pleiotropic effects in purple. Direct relationships are shown with solid lines, while indirect relationships are illustrated with dotted lines. The Wnt pathway is augmented by miR-135b, miR-21 and miR-155, and inhibited by miR-34a, miR-29b/c. Downstream of Wnt, MYC transcriptionally activates the miR-17-92 locus, but represses expression of miR-15, miR-26 and miR-30. KRAS augments expression of miR-31. In the PI3K pathway, which is negatively regulated by PTEN, miR-135b is augmented by PI3K inhibition of FoxO transcription factors. MiR-221, miR-21 and miR-17/106 enhance activation of PI3K signaling by repressing negative regulators of this pathway. MiRNAs also modulate inflammatory pathways mediated by the transcription factors NFKB and STAT3 by directly inhibiting IL-6 (via Let-7 miRNAs, which are inhibited by LIN28B) or the IL-6 receptor (via miR-34 and miR-125b). MiR-221/222 and miR-29b/c can also augment this pathway via indirect stimulatory effects on IL-6, NFKB, and STAT3. The TGF-β pathway is also antagonized by several miRNAs, including miR-17/106, miR-135b, and miR-20a through effects on TGFBR2 and SMAD4. The miRNA miR-93 can stimulate the TGF-β pathway by repressing the inhibitory SMAD7, although the effect of miR-93 is inhibitory of Wnt signaling through inhibition of SMAD7, which can augment nuclear accumulation of β-catenin. Lastly, several miRNAs have effects on EMT in CRC tumorigenesis, with miR-15/16 and miR-34 inhibiting this process, while miR-21 enhances EMT. CC, cell cycle.

2.3 miRNAs as diagnostic and prognostic tools. Screening and early detection of cancer is the main approach for prevention. MiRNAs are observed to function in positive- or negative-feedback loops highlighting their relevance in self-sustaining epigenetic switches that can change or reinforce cellular aberrant phenotype. As consequence, they are undoubtedly strong drivers and modulators of colon tumorigenesis with a potential as biomarkers and therapeutic targets.

Studies on the prognostic value of miRNAs have demonstrated their association with clinicopathological features of CRC patients. MiR-21 is a highly relevant miRNA in CRC and its up-regulation have been related to decreased disease-free survival (39) and suggested also as blood-based biomarker (40). Other miRNAs that have been demonstrated to correlate with poor survival rates are miR-185, miR-221, miR-182, miR-17-3p, miR-34a, miR-106a, when expressed at high levels, and miR-133b, miR-150, miR-378, when down-regulated (41-47). Moreover, potential miRNAs biomarkers to predict metastasis and recurrence are also indicated: miR-10b, miR-885-5p, miR-210, and miR-155 (48, 49). Since several alterations confer individual susceptibility to cancer, and are responsible for responsiveness or resistance to antitumor agents, it is crucial to identify biomarkers to predict the effect of chemotherapy allowing a more personalized approach to the management of CRC. Several miRNAs have been associated with a different response to chemotherapy, as miR-21, miR-320a, miR-150 and miR-129 (50-53).

Biomarker discovery for CRC based on the personalized genotype and clinical information could facilitate the classification of patients with certain types and stages of cancer to tailor preventive and therapeutic approaches. These cancer-related biomarkers should be highly sensitive and specific in a wide range of specimens as tumor tissues, patients' fluids or stool. Reliable biomarkers, which enable the early detection of CRC, could improve early diagnosis, prognosis, treatment response prediction, and recurrence risk.

3. Previous results obtained in our lab

3.1 miRNA regulatory network in colorectal carcinogenesis and metastasis

In our previous studies (54) we analyzed the expression profiles in 158 samples from 46 patients with CRC and we identify changes in both miRNA and gene expression levels among normal colon mucosa, primary tumor and liver metastasis samples. We observed that most changes in miRNA and gene expression levels had already established in the primary tumors and they remain almost stably in the subsequent primary tumor-to-metastasis transition. Specifically, while only few mRNAs were found to be differentially expressed between primary colorectal carcinoma and liver metastases, miRNA expression profiles can classify primary tumors and metastases well. A preliminary survival analysis considering differentially expressed miRNAs (DEM) suggested a possible link between miR-10b expression in metastasis and patient survival. In addition, we integrated expression data obtained from chip array by comparing normal colon mucosa, primary tumor and CRC liver metastasis, and we focused our attention on post-transcriptional regulatory networks with DEM, and their supported relations with target genes. Indeed, we identified a combination of interconnected miRNAs, which are organized into sub-networks, including several regulatory relationships with differentially expressed genes and specific mixed circuits with transcription factors.

In particular, two network components are observed involving respectively 6 up-regulated and 17 down-regulated DEM. The component regarding 6 up-regulated miRNAs was smaller, but a large fraction of genes appeared to be modulated by miR-182 (miR-182-5p; sequence: UUUGGCAAUGGUAGAACUCACACU). Other miRNAs upregulated in the same network were miR-18a (miR-18a-5p; sequence: UAAGGUGCAUCUAGUGCAGAUAG), miR-18b (miR-18b-5p; sequence: UAAGGUGCAUCUAGUGCAGUUAG), miR-183 (miR-183-5p; sequence: UAUGGCACUGGUAGAAUUCACU), miR-21 (miR-21-5p; sequence: UAGCUUAUCAGACUGAUGUUGA), and miR-1246 (sequence: AAUGGAUUUUUGGAGCAGG) (**Figure 6**). Interestingly, the large majority of miRNAs and genes with varied expression in the comparison among primary tumors and normal tissue remained stable after metastasis development. This similarity in miRNAs expression in later stage of tumor progression may reflect the need to maintain the tumor-specific processes required for tumorigenesis and cancer progression. So, we described the interplay of miRNA groups in regulating gene expression important for tumor development, and demonstrated that

miR-182 was one of the most up-regulated miRNA in primary CRC compared to normal colon tissue.

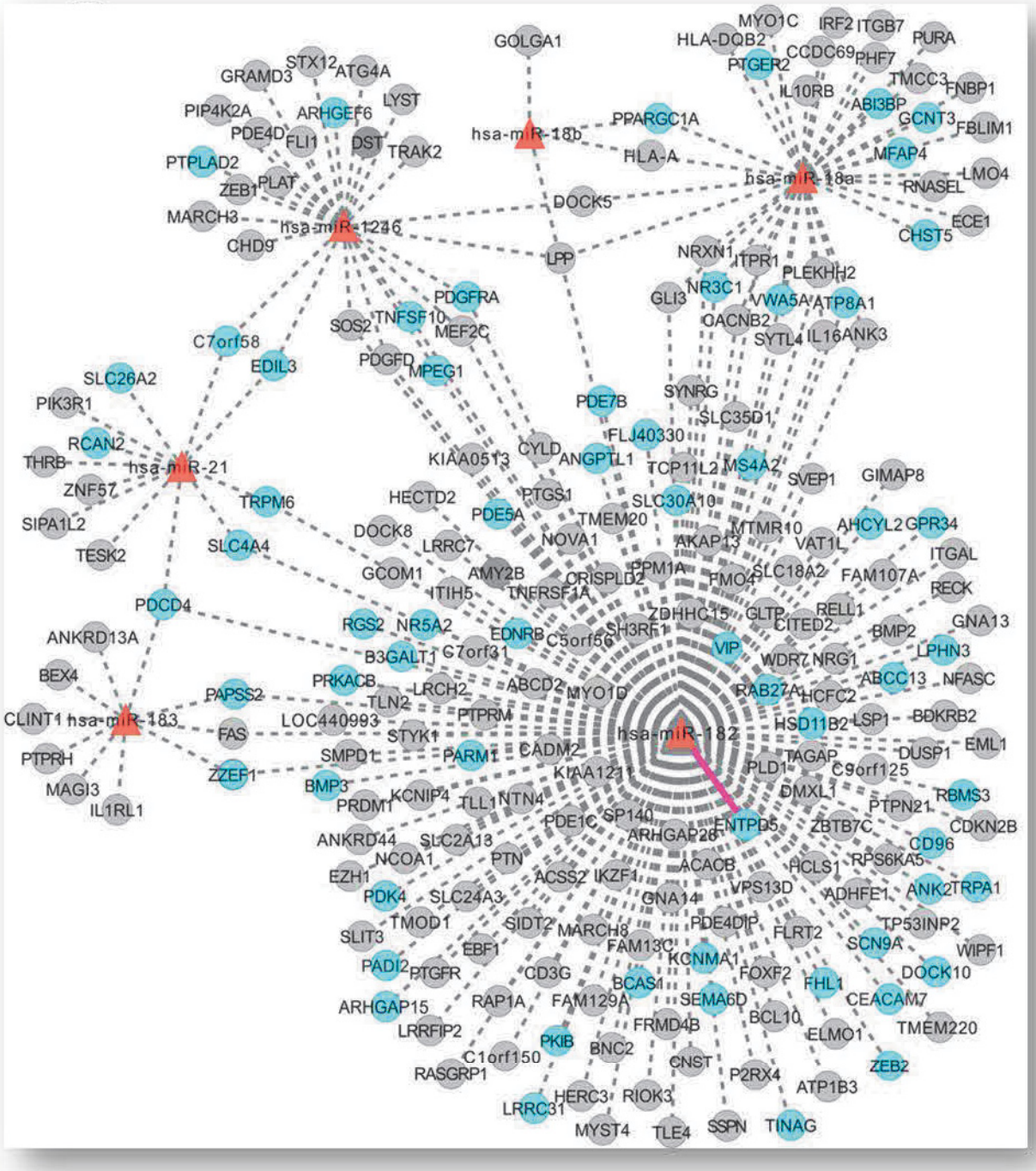

Figure 6: Post-transcriptional regulatory network of miRNAs up-modulated in primary CRC tumor *vs* normal colon mucosa contrast. The network represents DEMs up-modulated in tumor *vs* normal mucosa comparison (red triangles), supported target genes (circles) and their relations (gray dotted lines). Target DEGs are shown in blue, other genes in grey. The pink solid line outlines the experimentally validated miR-182/ENTPD5 relation.

3.2 MICOL-14 and MICOL-14^{tum}, a model of tumor dormancy and its tumorigenic variant

The MICOL-14$^{h\text{-}tert}$ (or MICOL-14) cell line was derived from a metastatic colorectal cancer (55) and was initially unstable because telomerase-negative, although their parental tumor tissue sample score as hTERT-positive. Dalerba P. *et al* demonstrated that the lack of telomerase activity was due to lack of hTERT transcription and that the reconstitution of telomerase enzymatic activity in this unstable CRC primary culture by transduction with an hTERT-encoding retroviral vector allows immortalization of these short-lived cultures. This cell line contained mutations in APC and KRAS, and more importantly, the set of detected mutations corresponded to that of the original tumor tissue proving that the primary culture was representative of the tumor cell population that formed the original *in vivo* metastatic tumor mass.

As previously reported (56), MICOL-14 cells remained viable, although poorly tumorigenic in non-obese diabetic severe combined immunodeficient (NOD/SCID) mice following subcutaneous injection. A tumorigenic variant of MICOL-14 cells, termed MICOL-14^{tum} (or TC22), was obtained from Indraccolo S. group after subcutaneous injection of parental MICOL-14 cells in Matrigel plus angiogenic factors. As consequence, this cell variant was able to generate large vascularized tumors by 6 weeks from injection (**Figure 7A**) and this feature may in part depend on the higher angiogenic potential of MICOL-14^{tum} compared with MICOL-14 cells (**Figure 7B**). As reported by Serafin V. *et al.* (57), in agreement with this, the numbers of Ki67^{+} proliferating cells were significantly higher in aggressive than in dormant tumors (**Figure 7C**). Moreover, it seems that the activation and increased expression of several components of Notch pathway is a feature of aggressive xenografts. Instead, the apoptosis levels were low and comparable in both tumor entities.

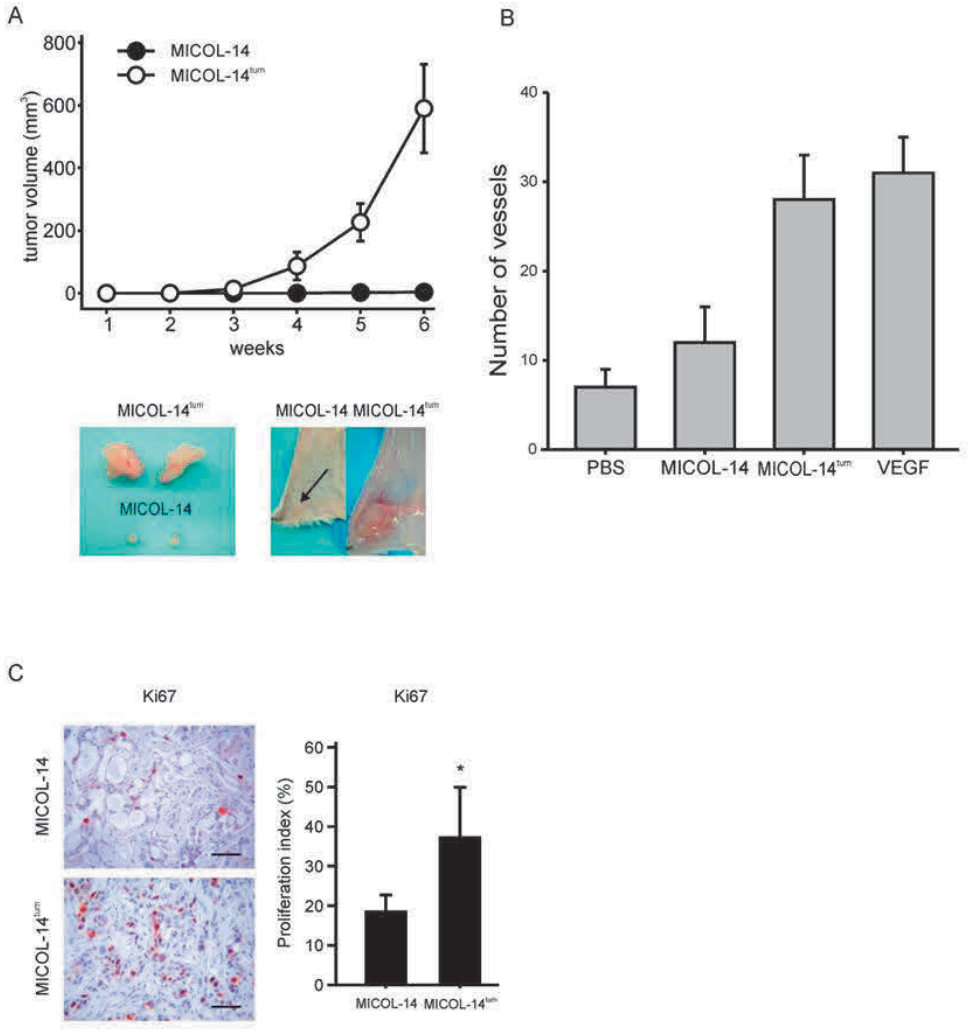

Figure 7. MICOL-14 and MICOL-14^{tum} exhibited different tumorigenic capacities in NOD/SCID mice. A. MICOL-14 cells behaved as dormant when injected into the subcutaneous tissue of the mice, whereas their tumorigenic variant MICOL-14^{tum}, formed aggressive tumors. **B.** MICOL-14^{tum} showed an high angiogenic potential as were able to generate large vascularized mass. **C.** The numbers of Ki67^{+} proliferating cells were significantly higher in aggressive than in dormant tumors.

To confirm whether the cell lines have maintained the original different biological behavior we initially carried out the experiment of subcutaneous injection of MICOL-14$^{h\text{-}tert}$ and MICOL-14^{tum} (or TC22) in mice. We observed that MICOL-14 cells behaved as dormant, instead TC22 developed aggressive tumors (**Figure 8**).

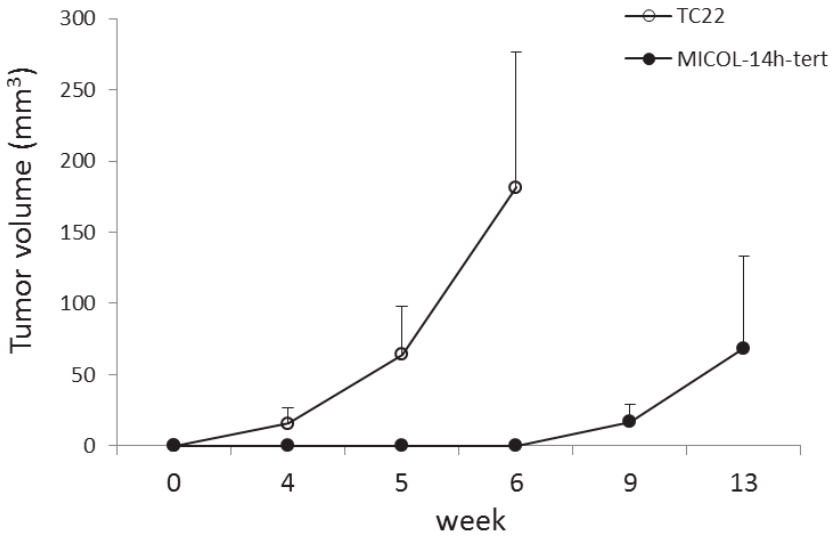

Figure 8. MICOL-14$^{h\text{-}tert}$ and TC22 confirmed their different *in vivo* biological behaviour. The volume of tumors were significantly different after s.c. injection of the CRC cell lines.

3.3 MICOL-14$^{h\text{-}tert}$ and TC22 present the same STR profiling

The Short Tandem Repeat (STR) profile is one of the most useful methods used to compare specific loci on DNA from two or more samples. A STR is a microsatellite and the polymorphic nature of the STR regions that are analyzed intensifies the discrimination between one DNA profile and another. So, we analyzed the profile of CRC cell lines to obtain a specific genetic fingerprint, which permit us to monitor them in the time and avoid cell line misidentification (58, 59). DNA profiles of the CRC cell lines studied were reported in **Supplementary Table 1**. Notably, MICOL14$^{h\text{-}tert}$ and its tumorigenic variant TC22 present the same STR loci number, thus confirming that these cell lines have the same origin.

AIMS OF THE PhD PROJECT:

miRNAs are optimal biomarkers owing to high stability under storage and handling conditions and their presence in body fluids. The detection of circulating miRNA levels has the potential for an earlier cancer diagnosis and to predict prognosis and response to therapy. We demonstrated that miR-182 was one of the most up-regulated miRNAs in primary CRC compared to normal colon mucosa, and a large fraction of genes appears to be modulated by this miRNA.

Starting from these premises, my PhD project was focused on the following tasks:

1) Identification of miRNA biomarkers for monitoring and screening of colon cancer patients. To this end, we investigating plasma, and both matched normal colon mucosa and tumor tissues in carcinogenesis cascade.

Furthermore, we focused on the localized colon cancer (pTNM stage I/II, N0 M0) because within 5 years from surgery up to 20% of these patients develop extranodal metastases and no predictive biomarker able to identify the population at high-risk of relapse after curative treatment is presently available.

2) Analysis of the functional impact of miR-182 inhibition on CRC cell lines characterized by a different *in vivo* tumorigenic behavior. In particular, we used MICOL-14$^{h\text{-}tert}$ and TC22 cells as CRC model of tumor dormancy and its tumorigenic variant, respectively. We also investigated the effect of miR-182 inhibition on *in vivo* TC22 cell growth. We extended the analysis to explore the transcriptome profiles and regulatory mechanisms involved in miR-182 modulation.

MATERIALS AND METHODS

Task 1

Patients. Forty-eight patients with stage I-II colon adenocarcinomas, who underwent radical surgical treatment between January 2003 and October 2008, were selected from the institutional database where clinico-histopathological data of all patients were recorded. The surgical procedure was standardized according to the cancer's location, minimizing any variability in technique. Pathological cancer staging (pTNM) was done according to the 7th Edition of the TNM classification. This study focuses on patients at TNM stages I or II, with no regional lymph node metastases (N0) and no distant metastases (M0), and none of them received neoadjuvant or adjuvant therapy.

In order to reduce variability, it was mandatory to exclude: patients with a known history of a hereditary colorectal cancer syndrome, rectal cancers, cases with special histotype, *in situ* carcinomas.

Consistently with patients' follow-up (recurrence and survival data) two groups were collected and Recurrence-free survival (RFS) was defined as the length of time from radical primary tumor resection until the detection of loco-regional or distant recurrence or decease due to any cause:

-Recurrent (R) group: 23 patients with RFS less than 55 months;

-Non-Recurrent (NR) group: 25 patients with RFS greater than 55 months;

All patients were followed up every 6 months for the first 2 years after their surgical treatment and every 12 months from the 3rd to the 5th year thereafter. Further patients' details are reported in **Table 1**.

Finally, also 10 patients affected by a form of Inflammatory Bowel Disease (IBD), in particular moderate Ulcerative Colitis (UC), were independently evaluated.

Approval for the use of all human tissues was obtained from the research Ethics Commitee of the University Hospital of Padua and informed consent was obtained from all the patients involved.

The collection and selection of patients were performed in collaboration with Professor Rugge's group (Surgical Pathology and Cytopathology Unit, DIMED, University of Padova).

Characteristics		R	NR
		n=23	n=25
Age at resection (years)	Median	72	69
	Range	55-85	50-90
Sex	M	16 (70%)	10 (40%)
	F	7 (30%)	15 (60%)
Tumor site	Cecum, colon ascending, hepatic (right) flexure	7	6
	transverse colon	3	4
	Splenic (left) flexure, colon descending, sigmoid colon	13	15
	Rectum	0	0
TNM stage	I	6	7
	II	17	18
T(n)	T1	2	1
	T2	4	6
	T3	15	18
	T4	2	0
N(n)	N0	23(100%)	25(100%)
M(n)	M0	23 (100%)	25 (100%)
Grading (n)	G1	5	4
	G2	15	17
	G3	3	4
	G4	0	0

Table 1: Clinical characteristics of relapsing (R) and non-relapsing (NR) patients.

Histopathological FFPE samples. All the considered samples were fixed in formalin for 18-24h. Original slides or serial sections (4-6 μm thick) obtained from archival paraffine-embedded tissue samples were jointly re-assessed by two expert gastrointestinal pathologists according to current criteria (WHO 2010). For each patient, a sample of CRC-adjacent, morphologically normal colon mucosa was dissected from the proximal tumor resection margin, with a minimum distance of 3 centimeters from the primary tumor. At least 3 cancer samples were obtained from all the cases considered (range 3-8, depending on the size of the cancer).

RNA isolation and quantitative RT-PCR. Hematoxylin and eosin (H&E) stained sections of each specimen were prepared and evaluated, and only samples with more than 70% of vital tumor tissue were considered for RNA extraction. Total RNA was isolated from FFPE

(Formalin Fixed Paraffin Embedded) samples using the RecoverAll Total Nucleic Acid Isolation Kit (Ambion, Austin, TX), according to the manufacturer's instructions, and optimizing the protocol for ensure the recovery of smaller RNA fragments as miRNAs. The concentration of RNA was quantified by NanoDrop 1000 Spectrophotometer (NanoDrop Technologies, Waltham, MA).

Total RNA was used for first-strand cDNA synthesis in a 15µl reaction volume, using the TaqMan miRNA Reverse Transcription kit and miRNA-specific stem-loop primers (Thermo Fisher Scientific, Foster City, CA, USA). We performed qRT-PCR experiments amplifying cDNA for 45 cycles using TaqMan miRNA primers and probes (Thermo Fisher Scientific) and LightCycler 480 PCR Master Mix (Roche Diagnostics, Mannheim, Germany). All reactions were conducted in triplicates, including no template controls, using LightCycler 480 II Real-Time System (Roche Diagnostics).

Data normalization. RNU44 and miR-200c were tested as candidate normalizers. MiR-200c, already identified as most stable miRNA in metastatic CRC (54), was confirmed as best normalizer also in localized CRC. Relative expression of target miRNAs was calculated as $\Delta Ct_{miR} = Ct_{miR} - Ct_{normalizer}$. The miRNA ratio (60, 61) was used to find molecular markers of relapse. The Ct value of each miRNA was converted into the corresponding expression level (2^{-Ct}). The miRNA ratios between all possible miRNA pairs (e.g. miR-x/miR-y ratio) were calculated as $2^{-\Delta Ct} = 2^{-(CtmiR\text{-}x - CtmiR\text{-}y)}$.

Statistical analysis. A one-tailed Wilcoxon signed-rank sum test was used to identify miRNAs significantly different between matched tumor tissue and adjacent normal mucosa. A univariate logistic regression model was built to evaluate the ability of each miRNA ratio on $\log_2$-scale to predict the relapse by 55 months. Odds ratios and 95% confidence intervals were estimated for the fitted logistic regression models. Receiver operating characteristic (ROC) curves were plotted and the area under the ROC curve (AUC) was estimated to compare the most significant miRNA ratios.

Statistical analysis were performed in the R environment using a customized code and the pROC package for ROC curve analysis.

Data normalization and statistical analysis were performed in collaboration with Dott. A. Grassi (Oncology and Immunology Division, DiSCOG, University of Padova).

Task 2

Cell lines and *in vitro* culture. The classical immortalized human colorectal adenocarcinoma cell lines Caco2 and HT29 were purchased from Banca Biologica and Cell Factory Core Facility of IRCCS AOU San Martino - IST Istituto Nazionale per la Ricerca sul Cancro - Genova. MICOL-$14^{h\text{-}tert}$ and CG-758 cell lines were a gift from Dalerba P. group, instead the tumorigenic variant MICOL-14^{tum} (named also TC22) were obtained and characterized in our Department from Indraccolo S. lab.
The cells were grown in RPMI-1640 medium (Invitrogen, Milan, Italy) supplemented with 10% fetal bovine serum (FBS; Gibco, Invitrogen), L-glutamine, Pen/Strep and HEPES, and used within 6 months from thawing and resuscitation. The cells were harvested with trypsin-EDTA in their exponentially growing phase and maintained in a humidified incubator at 37 °C with 5% CO2.

RNA extraction, reverse transcription and quantitative RT-PCR analysis. RNAs were extracted from cells after 24, 48 and 72h of transfection using Trizol reagent (Thermo Fisher Scientific), according to the manufacturer's instructions. RNA concentration and purity were measured with Nanodrop (Bio-Tek Instruments, Winooski, VT, USA) and Agilent (Agilent Technologies, Santa Clara, CA, USA).
To study miRNA expression levels, the Taqman microRNA reverse transcription synthesis Kit and miRNA-specific stem-loop primers (Thermo Fisher Scientific) were used according to the manufacturer's instructions.
First-strand cDNA synthesis from total RNA (1µg) was performed using the SuperScript™ II Reverse Transcriptase kit (Thermo Fisher Scientific) to detect and quantify mRNA.
A LightCycler 480 PCR Master Mix (Roche Diagnostics) was used with specific Taqman assay to detect miRNAs or transcripts. The Lightcycler II (Roche) instrument was used for realtime PCR experiments for 40 cycles and the relative expression level was calculated using the $2^{-\Delta\Delta CT}$ method. Expression data were normalized using as reference RNU44 for miRNAs, and HPRT1 for genes.

Transient transfection for *in vitro* miRNA silencing. Cells were plated at the concentration of $1{,}5x10^5$ cells/well on normal adhesion 6-well dishes with RPMI complete medium for 24h. Then, the RPMI medium was replaced with Opti-MEM® I Reduced Serum Medium (Thermo

Fisher Scientific) and specific anti-miR (hsa-mir-182, or hsa-miR-183) mirVana™ miRNA inhibitor (Ambion by Thermo Fisher Scientific) was added to a total of 150 pmol/well; to allow cell transfection, Lipofectamine RNAiMAX transfection reagent (Invitrogen) was mixed with the miRNA inhibitor, as protocol instructions. The mixture was incubated in a dark room for 5 min at room temperature and then added to each well. Similarly, an equal number of cells were treated with an anti-miR-NC (mirVana™ miRNA inhibitor Negative Control #1; Ambion), to use as a control for data normalization on anti-mir-182 or anti-miR-183 independent transfection effects. Moreover, to monitor antagomiR uptake efficiency by flow cytometry analysis, the same number of cells were transfected with a carboxyfluorescein-labeled RNA oligonucleotide (FAM™-labeled Anti-miR™ Negative Control; Ambion). After an overnight incubation, the Opti-MEM medium supplemented with miRNA inhibitors was replaced with normal complete RPMI medium, and the miRNA silencing was evaluated by qRT-PCR at time point considered. At each time point the cells were also harvested to perform all the experiments for miRNA function investigation. In all reported silencing experiments, transfection efficiency was highest than 80%, and miRNA expression levels showed a significant decrease in transfected cells compared to controls. The controls for all the experiments were: Non-Treated (NT) cells and anti-miR-NC treated cells. In particular, the NT cells were plated in the medium used for the transfection, but without treatments.

Apoptosis and cell cycle assay, flow cytometry. For the detection of apoptosis and necrosis, an Annexin-V-FLUOS staining kit (Roche, Mannheim, Germany) was used according to the manufacturer's instructions. Briefly, the cells were seeded in triplicate in six-well plates at a density of 1.5×10^5 cells per well in RPMI with 10% FBS. After 24 h incubation, the procedure was performed at 24, 48 and 72 h after transfection. Also the cell culture medium containing floating cells was collected. Adherent cells were rinsed with PBS and collected after trypsin-EDTA incubation. After the cells were visibly detached, at least 5 ml of complete growth medium was added and cells were resuspended. Afterward, both floating and adherent cells were pooled and rinsed twice with PBS. The resulting suspension was poured into a flow cytometry tube and centrifuged for 5 min at 200 g at 4 °C. Then, the cell pellets were resuspended in 100 µl incubation buffer with 2 µl Annexin-V and 2 µl propidium iodide (PI) for 15 min in a dark room at 4 °C. For cell cycle analysis, cells were fixed with cold ethanol and then incubated for 1 h in a PI/RNAse solution. The method is based on

cellular DNA content, which discriminates resting/quiescent cell populations (G0 cells) and quantifies cell cycle distribution (G1, S or G2/M, respectively). Then, the samples were analyzed by using a FACS Calibur flow cytometer (Becton-Dickinson Immunocytometry Systems) with excitation/emission wavelengths of 488/525 and 488/675 nm for Annexin-V and PI, respectively.

Migration assay. Cells were plated into 6-well dishes, transfected after 24h, and allowed to grow for another 24h, after which a scratch was created. A scratch was applied directly on the monolayer by means of a sterile pipette tip. The ability of cells to move and fill in the gap was evaluated by optical microscopy immediately (0hr) and at 18-24-36hr after the scratch. Data represents mean ± standard deviation (SD) from three independent experiments.

Western blot analysis. Cell lysates were obtained into RIPA buffer containing protease inhibitor. Proteins were quantified using Quantum Micro Protein Assay Kit (Euroclone, Milan, Italy). Lysates were denatured, boiled and then fractionated using SDS-PAGE gel (Invitrogen). After blotting onto PVDF membrane and blocking with a 5% non-fat dry milk or BSA solution, blots were incubated at 4°C with the primary antibody overnight. The following rabbit primary antibodies from Cell Signaling Technology, were used: Cleaved Caspase-3 #9661 1:1000, PARP #9542 1:1000. Mouse antibody *vs* β-actin (sc-47778 1:1000 Santa Cruz Biotechnologies, CA, USA) served as an internal control. Antibody binding to the membrane was detected using a secondary antibody (goat anti-rabbit IgG 1:5000; Perkin Elmer or goat anti-mouse IgG 1:5000 Calbiochem) conjugated to horseradish peroxidase and visualized using Supersignal West Pico Chemiluminescent Substrate Kit (Thermo Fisher Scientific) with the Chemidoc XRS System (Bio-Rad) and Quantity One 4.6.9 software (Bio-Rad, CA, USA). Densitometric analysis was performed with the ImageJ software (NIH). Data are shown as the mean ± SD of the mean of three different experiments performed in triplicate. Results are representative of three independent experiments.

***In vivo* tumorigenesis assay.** Nonobese diabetic/severe combined immunodeficiency (NOD/SCID) mice were obtained from internal breeding. Procedures involving animals and their care conformed to institutional guidelines that comply with national and international laws and policies (EEC Council Directive 86/609, OJ L 358, 12 December 1987). TC22 cells were seeded in complete medium and treated with miR-182 inhibitor or anti-miR-NC. For

tumor establishment, 7-wk-old to 9-wk-old mice were injected subcutaneously (s.c.) with exponentially growing TC22 NT or treated cells washed and resuspended in PBS. $1x10^6$ cells in a 200µl total volume were inoculated in combination with Matrigel in both dorsolateral flanks.

After 1 week the mirVana™ miR-182 inhibitor *in vivo* ready (Life Technologies by Thermo Fisher Scientific) or negative control combined with Invivofectamine 2.0 Reagent (Life Technologies) were used for intratumoral injection to maintain the *in vivo* miRNA silencing. The resulting tumor mass were inspected twice weekly and measured by caliper. Tumor volume was calculated with the following formula: tumor volume (mm^3) = L X l^2 X 0.5, wherein L is the longest diameter, l is the shortest diameter, and 0.5 is a constant to calculate the volume of an ellipsoid. At the end of the experiments the mice were sacrificed by cervical dislocation and the tumors were harvested by dissection and either snap-frozen or fixed in formalin and embedded in paraffin for further analysis. H&E staining were performed using automated system. This part was performed in collaboration with Dott. M. Curtarello of the S. Indraccolo's group (Oncology and Immunology Division, DiSCOG, University of Padova,).

In addition we investigated the CRC Grading and Mitotic index of tumor mass. The 2010 WHO scores the CRC Grading in G1 well differentiated cancer, G2 moderate differentiated cancer and G3 poorly differentiated cancer based upon the percentage of glands formation (> 75%; 35%-75% and <35%, respectively). Main growth patterns are, in order from tipically less aggressive to more aggressive: glandular, trabecular and solid. Mitotic index is the number of mitosis counted in 10 fields at 40X magnification (n. x10 hpf). Usually, a typical CRC has a mean mitotic index higher than 20 mitosis x10hpf. This part was performed in collaboration with Dott. L. Albertoni of the Professor Rugge's group (Surgical Pathology and Cytopathology Unit, DIMED, University of Padova).

Statistical analysis. Student's t-test was performed on parametric groups. Values were considered significant at *$p \leq 0.05$ and **$p \leq 0.01$. Values are reported as mean ± SD. All analysis were performed by using SigmaPlot (Systat Software Inc).

Gene expression analysis. Human gene expression microarray data were generated using the Affymetrix GeneChip PrimeView Human Gene Expression Array (Affymetrix by Thermo Fisher Scientific). Total RNA, after specific quality controls, was isolated from MICOL-$14^{h\text{-}tert}$ and TC22 transfected with anti-miR-182 or anti-miR-NC. For transcriptome analysis, we

performed 4 chip array for each cell line condition. Statistical and bioinformatic analysis were conducted to find out significant gene expression differences due to miR-182 inhibition. Raw data quality controls has been performed using the R package 'affyQCreport' (62) to examine and compare boxplots and histograms of intensities, percent present call rate and 3'/5' hybridization intensity ratios.

Expression matrix reconstruction was obtained by 'affy' package (63) using RMA for data summarization and normalization (background correction, quantile normalization, log-transformation of values). Dataset description was based on different unsupervised analyses providing on sample correlation values (Pearson correlation method, complete clustering method) and PCA analyses. Additional cluster analyses and heatmaps (Pearson correlation method, complete cluster method) of selected sample and gene subsets were obtained using R package 'gplots'.

Transcript-level annotation of probesets, based on Ensembl (release 88), was obtained with R package 'primeviewcdf'. Probesets were also associated to UniGene ID, official gene symbol and gene description, EntrezGene ID, RefSeq Transcript ID and OMIM ID.

Differential expression tests were conducted using Limma package (64), using FDR method for multiple testing correction and setting significant threshold for adjusted p-value to 0.05.

Functional enrichment tests. Pathway enrichment analysis of differentially expressed genes has been conducted using DAVID (Database for Annotation, Visualization and Integration Discovery, release 6.8 (65). Significant GO terms, PIR keywords, and KEGG and Reactome pathways have been selected considering p-values adjusted (Benjamini-Hochberg) at most 0.05.

Collection of predicted and validated targets of miR-182 in MICOL-14$^{h\text{-}tert}$ and TC22. Target predictions for miR-182, consisting of predicted target gene transcripts (Ensembl) and the corresponding prediction scores (Aggregate Pct, Cumulative Context ++ score and Total Cumulative Context ++), have been downloaded from TargetScanHuman (release 7.1 (66). Predicted target prioritization was based on the Total Cumulative Context ++ score.

Experimentally validated miR-182 targets were downloaded from MirTarBase release 6.0 (67). Two validation evidence strength categories, based on validation methods, were considered: strong (luciferase reporter assay, western blot, qPCR) and less strong (microarray, NGS, pSILAC).

Among probesests significantly up-regulated after miR-182 silencing, those with average expression lower than 3 and a fold change lower or equal to 0.3 in both contrasts were filtered out. Selected up-regulated probests were matched with transcripts being predicted or validated miR-182 targets.

The bioinformatic analysis of gene expression were performed in collaboration with Professor Bortoluzzi's group (Department of Molecular Medicine, University of Padova, Italy).

RESULTS

Task 1: miR-182 as possible biomarker of CRC progression

ABSTRACT OF PUBLISHED RESULTS (see APPENDIX 1 for details)

Regarding the first task, in my first year of PhD we published the attached paper (68, Appendix 1) to confirm the involvement of miR-182 in CRC development and progression, and to investigate its possible role as prognostic biomarker. In particular, we analyzed in this study a total of 240 histopathological and 51 plasma samples. We observed by qRT-PCR a progressive and significant over-expression of miR-182 along with the carcinogenesis cascade (**Figure 1A**). We then analyzed miR-182 dysregulation in CRC liver metastases, by investigating its expression levels in a series of stage IV CRCs. A significant overexpression of miR-182 was observed in primary CRCs and CRC liver metastases compared to normal tissues (**Figure 1B**) demonstrating that miR-182 up regulation starts at the beginning of colon carcinogenesis and is maintained in the metastatic process. We also investigated miR-182 expression by ISH (*In situ* hybridization) in 5 cases of stage IV CRCs and a consistently significant overexpression was confirmed in paired primary tumors and CRC liver metastasis in comparison to normal colon mucosa (**Figure 1C**).

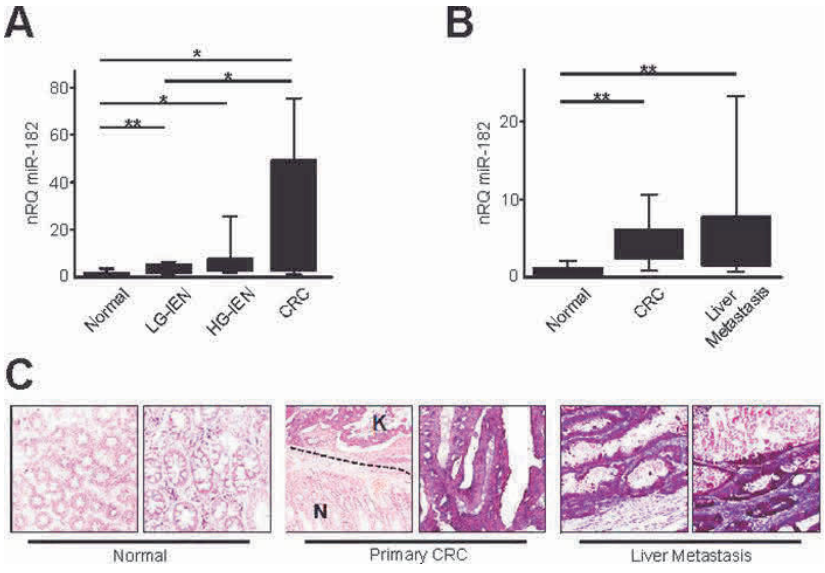

Figure 1: miR-182 is up-regulated during colon carcinogenesis. A. miR-182 expression was evaluated by qRT-PCR in FFPE samples of colon normal mucosa, tubular adenomas low-grade [LG] and high-grade [HG] intraepithelial neoplasia [IEN, formerly known as dysplasia] and CRCs. **B.** miR-182 expression was evaluated by qRT-PCR in matched surgical samples of normal colon mucosa, primary CRC and liver metastatis. **C.** Representative ISH evaluation of miR-182 in matched tissue sections of normal colon, primary tumor and metastatic CRC (N= normal colon mucosa; K= primary CRC). The presence of miR-182 is shown by a grainy blue cytoplasmic stain; slides counterstained in fast red. (Original magnifications 10x and 20x). Significance (Student's t test); *p<0.05; **p<0.01. nRQ, normalized Relative Quantity. Data were expressed as mean values ± SD.

To further strengthen these results, we also evaluated the prognostic impact of miR-182 expression on a large number of CRCs in The Cancer Genome Atlas (TCGA) CRC series (n=393). The miR-182 expression was significantly higher in CRCs presenting lymph node or liver metastases at diagnosis. Furthermore, in univariate analysis, and considering the median miR-182 value as a cut-off limit, miR-182 expression levels negatively correlated with the overall survival of patients (Mantel-Cox log-rank test, p=0.035).

We then investigated whether the up-regulation of miR-182 expression in primary and metastatic CRC tissues could influence miR-182 concentration in the plasma of CRC patients. We demonstrated by qRT-PCR that plasma miR-182 concentrations were significantly higher in CRC patients than in healthy controls or patients with colic polyps at endoscopy (**Figure 2A**). Considering tumor staging, miR-182 plasma expression level in both early and advanced CRC patients was significantly higher than in controls (**Figure 2B**). Finally, we analyzed paired pre- and post-operative samples from 11 CRC patients who underwent curative liver metastasectomy, and we observed that miR-182 plasma levels were significantly reduced one month after surgery (**Figure 2C**).

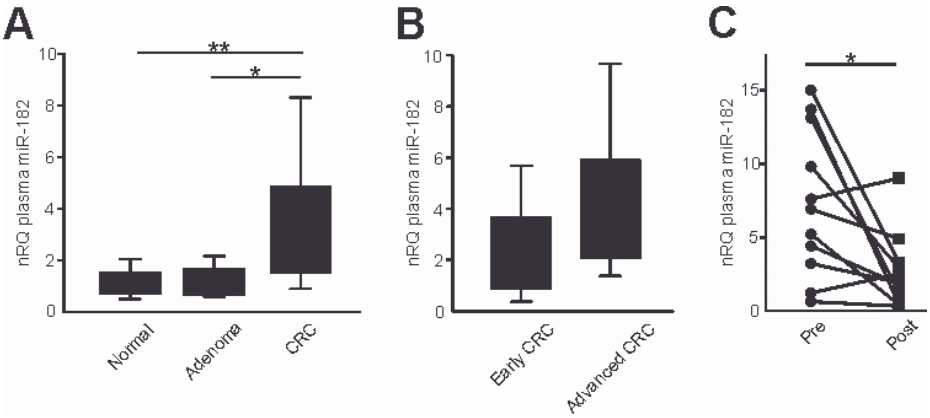

Figure 2: miR-182 plasma levels are significantly elevated in CRC patients. A. miR-182 plasma levels were analyzed in 10 healthy volunteers, 10 patients with colic adenomas at endoscopy, 10 early stages and 10 late stages CRC patients. **B.** miR-182 plasma expression in advanced CRC patients and in early CRC patients. **C.** Plasma miR-182 concentration before and after curative liver metastasectomy (p=0.020). Significance (Student's t test); *p<0.05; **p<0.01. nRQ, normalized Relative Quantity. Data were expressed as mean values ± SD.

These results indicate the potential of circulating miR-182 as a novel non-invasive blood based biomarker for CRC patients monitoring.

This part of the PhD project was carried out in collaboration with Proff. M. Rugge's group (Surgical Pathology and Cytopathology Unit, DIMED, University of Padova) and A. Scarpa's group (Department of Diagnostics and Public Health, ARC-NET Research Center, University and Hospital Trust of Verona).

Differentially expressed microRNAs in stage I-II colon cancer between tumor and matched normal colon mucosa.

We evaluated by qRT-PCR in 48 localized colon cancer (stage I-II) the expression levels of five preselected miRNAs that resulted strongly modulated in primary advanced tumor (stage IV) versus normal colon mucosa in our previous work. The four up-regulated miRNA (miR-18a, miR-21, miR-182 and miR-183) resulted involved in the same post-transcriptional network, while miR-139-5p (miR-139; sequence: UCUACAGUGCACGUGUCUCCAGU) was the most down-regulated. MiR-200c was confirmed to be the most stable normalizer and was used as a reference for the calculation of $-\Delta Ct$.

Interestingly, our analysis confirmed that all of them are significantly regulated also in the early phases of the CRC tumor process. Specifically, miR-18a, miR-21, miR-182 and miR-183 were strongly up-regulated ($p << 0.001$) in cancer tissue versus normal mucosa, whereas miR-139 was strongly down-regulated ($p << 0.001$), see **Figure 1**. This result is important because it shows that these five miRNAs accompany the CRC tumor process, from initial stages to advanced tumorigenesis.

To then evaluate whether the modulations of these miRNAs were tumor-specific or the effect of tumor-associated inflammation, we checked their expression levels also in a situation of chronic inflammation. Specifically, we tested their expression levels in 10 patients affected by Ulcerative Colitis, a form of inflammatory bowel disease characterized by chronic and widespread inflammation of the colorectal mucosa. The comparison was performed analyzing the inflamed mucosa versus matched normal colon mucosa.

Although with a limited sample size, our data support the fact that, among the up-regulated miRNAs, miR-182 and miR-183 are more specific of the tumor process, whereas miR-18a and miR-21 appear weakly modulated also in the chronic inflammatory process. Also the down-regulated miR-139 seems specific of the tumor process. MiR-18a and miR-21 appeared weakly up-regulated with p-value of 0.053 and 0.042, respectively, suggesting that the strong up-regulation of these two miRNAs in the tumor could be partially due to inflammation. On the contrary, miR-182, miR-183 and miR-139 were not significantly modulated in inflamed bowel tissue (**Figure 2**).

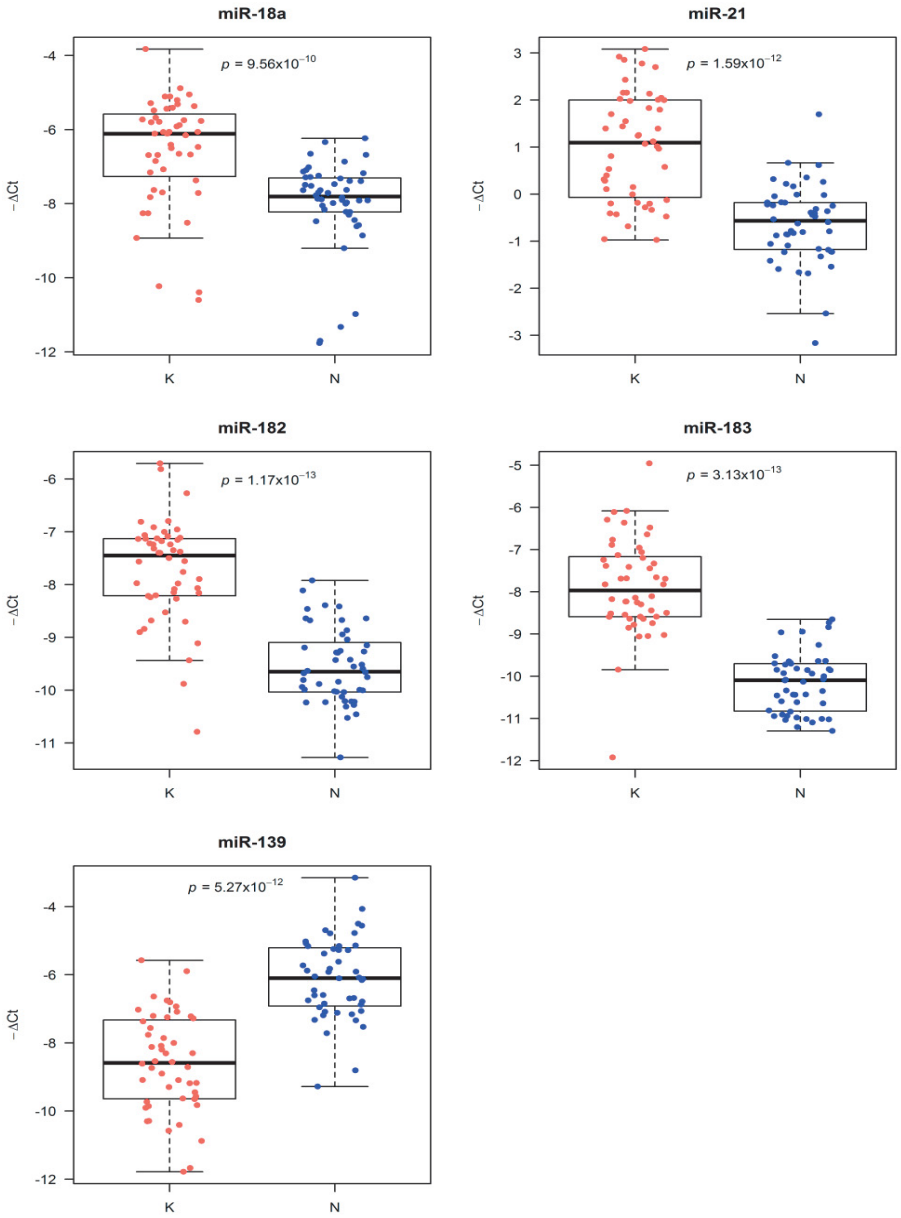

Figure 1: Boxplots of the distribution of –ΔCt values in tumor tissue versus matched normal mucosa for miR-18a, miR-21, miR-182, miR-183 and miR-139. Each dot represents a patient sample. –ΔCt values were calculated using miR-200c as a reference. Differences between cancer tissue (K) and matched normal mucosa (N) samples were analyzed using one-tailed Wilcoxon signed-rank sum test.

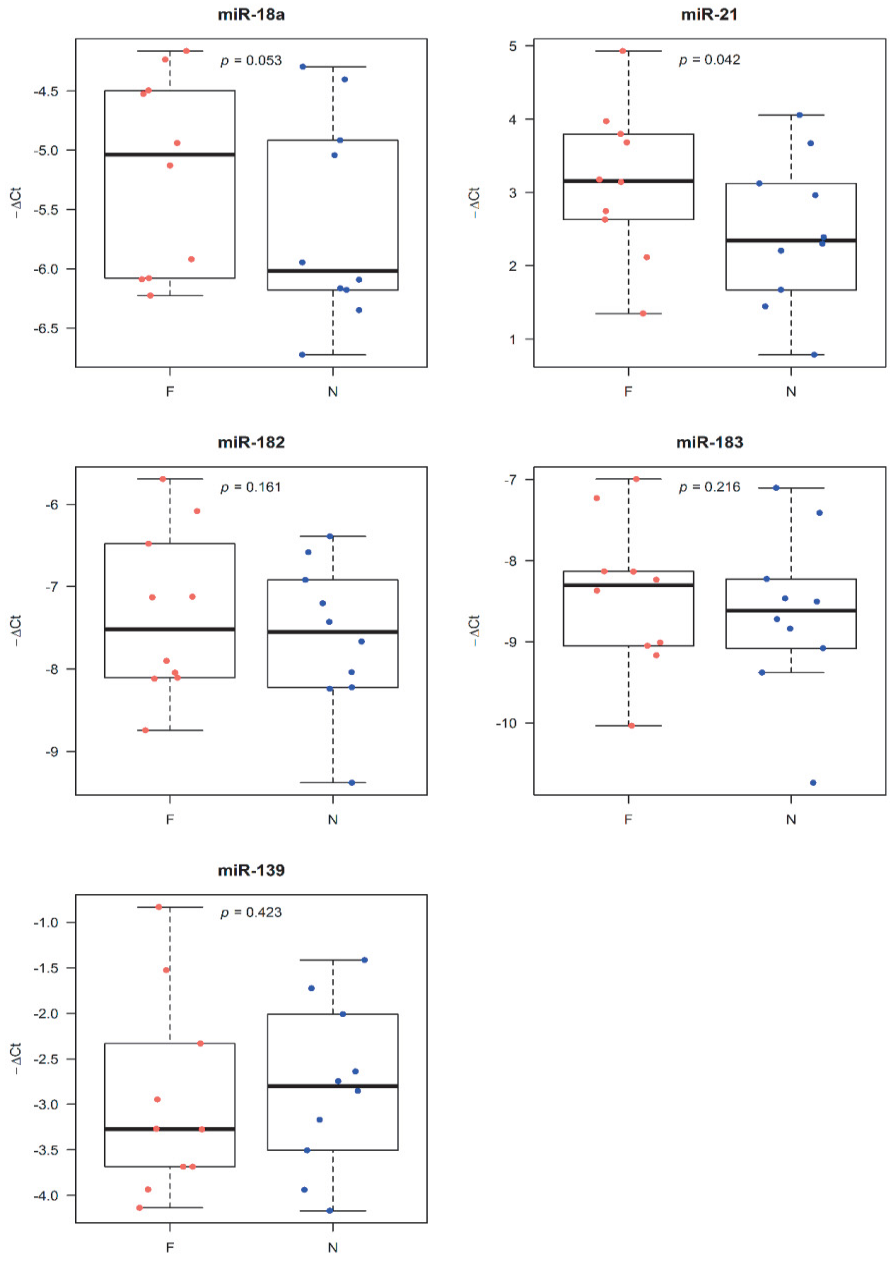

Figure 2: Boxplots of the distribution of –ΔCt values in inflamed tissue versus matched normal mucosa for miR-18a, miR-21, miR-182, miR-183 and miR-139. Each dot represents a patient sample. –ΔCt values were calculated using RNU44 as a reference, which was proven to be more stable than miR-200c in these samples. Differences between inflamed bowel tissue (F) and matched normal mucosa (N) from patients affected by moderate ulcerative colitis were analyzed using one-tailed Wilcoxon signed-rank sum test.

A coordinate deregulation of miRNAs as possible biomarkers of relapse

To find possible biomarkers of relapse, the patients of the study were subdivided into a Recurrent group (R) and a Non-Recurrent group (NR) (see Table 1 in Materials and Methods section for details), and we tested on our data the miRNA ratio approach proposed by Boeri and colleagues (60).

We thus calculated 10 ratios between the expression values of all possible miRNA pairs, both in the tumor tissue and in the adjacent normal mucosa, and assessed their capability to predict relapse through univariate logistic regression analysis. Complete results are reported in **Table 2** for both matched normal mucosa and tumor tissue.

Three miRNA ratios, evaluated in the mucosa adjacent to tumor, were found to be significant predictors of relapse by 55 months from resection: miR-21/miR-183 (p=0.0011), miR-18a/miR-182 (p=0.0053) and miR-18a/miR-183 (p=0.0099), see **Figure 3**. Corresponding areas under ROC curves (AUC) were 0.83 (miR-21/miR-183), 0.76 (miR-18a/miR-182) and 0.78 (miR-18a/miR-183), see **Figure 4**. None of the miRNA ratios resulted significant in colon cancer tissue.

Interestingly, the miRNA ratio approach was useful to show that not a single miRNA, but rather a coordinated alteration of four miRNAs (i.e. miR-21, miR-18a, miR-182 and miR-183) from the same regulatory network, may be useful to predict recurrence after resection when evaluated in the tumor-adjacent mucosa and not in the tumor tissue.

This result, apparently counterintuitive, is in line with previous findings reported in CRC (69) and also in other tumors (70). Indeed, in a recent study (69) it was demonstrated that a number of genes related to the presence of the tumor were activated in adjacent mucosa of CRC patients. Moreover, these activated genes were enriched in transcription factors, indicating the existence of a transcriptional program driving the observed altered expression pattern in normal mucosa. At a higher level, we expect that also microRNAs are involved in regulating TFs and, in cascade, the genes activated in adjacent mucosa.

Our results, if confirmed in an ample cohort of patients, may help to identify patients with localized CRC at high-risk of recurrence who would benefit most from adjuvant therapy.

	NORMAL MUCOSA		TUMOR TISSUE	
miR_ratio	**p-value**	**AUC**	**p-value**	**AUC**
miR-18a/miR-21	0.3084	0.58	0.40	0.51
miR-18a/miR-182	**0.0053**	**0.76**	0.46	0.56
miR-18a/miR-183	**0.0100**	**0.78**	0.46	0.49
miR-18a/miR-139	0.1178	0.60	0.51	0.61
miR-21/miR-182	0.0632	0.69	0.79	0.49
miR-21/miR-183	**0.0011**	**0.83**	0.99	0.53
miR-21/miR-139	0.1794	0.66	0.08	0.67
miR-182/miR-183	0.1752	0.56	0.65	0.62
miR-182/miR-139	0.7342	0.53	0.23	0.62
miR-183/miR-139	0.1919	0.58	0.20	0.63

Table 2. Evaluation of capability of predicting relapse of miRNA ratios in normal mucosa adjacent to tumor and in tumor tissue. A univariate logistic regression model was developed for each miRNA ratio to evaluate its capability to distinguish between patients who were relapsing by 55 months after bowel resection and those who did not, both in normal mucosa adjacent to tumor and in tumor tissue. The corresponding area under the ROC curve was calculated and reported in table as AUC. Three miRNA ratios resulted significant predictors of relapse ($p<0.01$ and $AUC>0.75$) in normal mucosa adjacent to tumor.

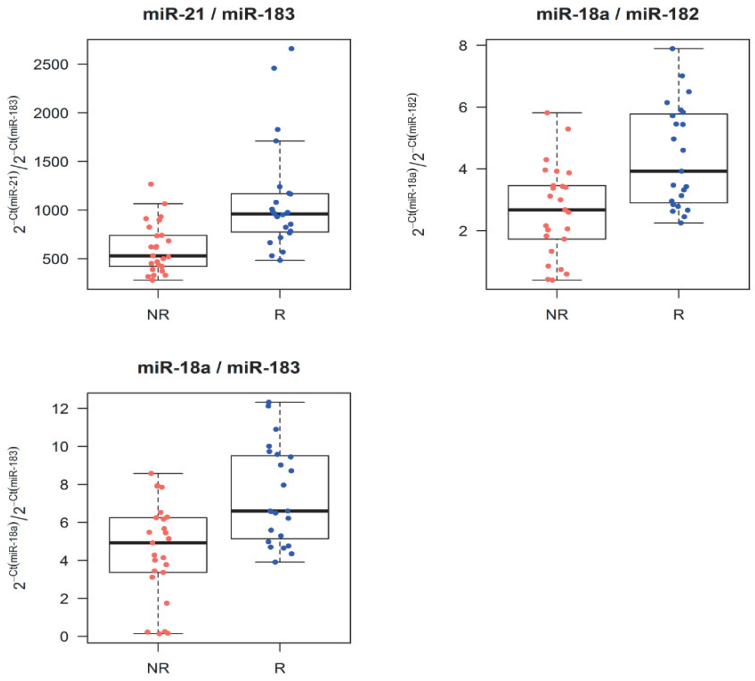

Figure 3: Boxplots of the distribution of miR-21/miR-183, miR-18a/182 and miR-18a/183 ratios. The three miRNA ratios measured in the adjacent, morphologically normal, mucosa were predictive of relapse by 55 months after bowel resection ($p<0.01$, in univariate logistic regression analysis). The panels show the distribution of miRNA ratio relative expression levels, indicated as $2^{-\Delta Ct}$, in CRC patients who relapsed by 55 months after resection (R) and those who did not (NR).

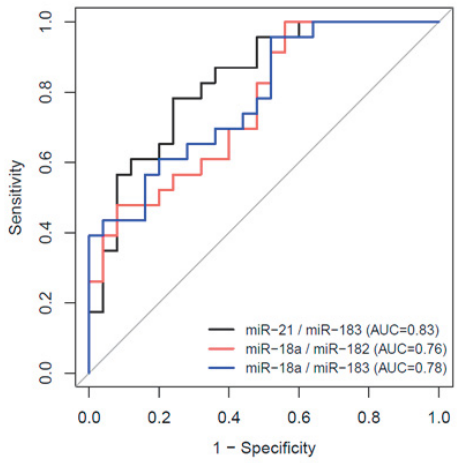

Figure 4: miR-21/miR-183, miR-18a/182 and miR-18a/183 ratios in normal mucosa adjacent to tumor predict the recurrence of colorectal cancer after bowel resection. ROC curves generated from univariate logistic regression models. Corresponding areas under ROC curves (AUC) were: miR-21/miR-183 (AUC=0.83), miR-18a/182 (AUC=0.76) and miR-18a/183 (AUC=0.78).

This part of the PhD project was carried out in collaboration with Dott. A. Grassi (Oncology and Immunology Division, DiSCOG, University of Padova,).

Manuscript submitted.

Task 2: The inhibition of miR-182 increases the apoptosis and reduces tumor growth

miR-182 is expressed at high levels in CRC cell lines

Considering the set of four miRNAs that we have demonstrated to be associated with CRC tumorigenesis, miR-182 seems to be a key player. Indeed, in our previous work (54) we demonstrated that it has a central role in the post-transcriptional regulatory sub-network containing the most up-regulated miRNAs as it support, alone, the largest number of targets. We evaluated the expression level of miR-182 in a panel of CRC cell lines by qRT-PCR, using a pool of normal colon mucosa samples as reference. We observed that miR-182 expression levels are significantly up-regulated, and specially CG-758 and TC22 showed the highest expression levels between the cancer cell lines considered. In particular, the expression level of miR-182 is higher in TC22 compared to MICOL-14$^{h\text{-}tert}$ (**Figure 5**).

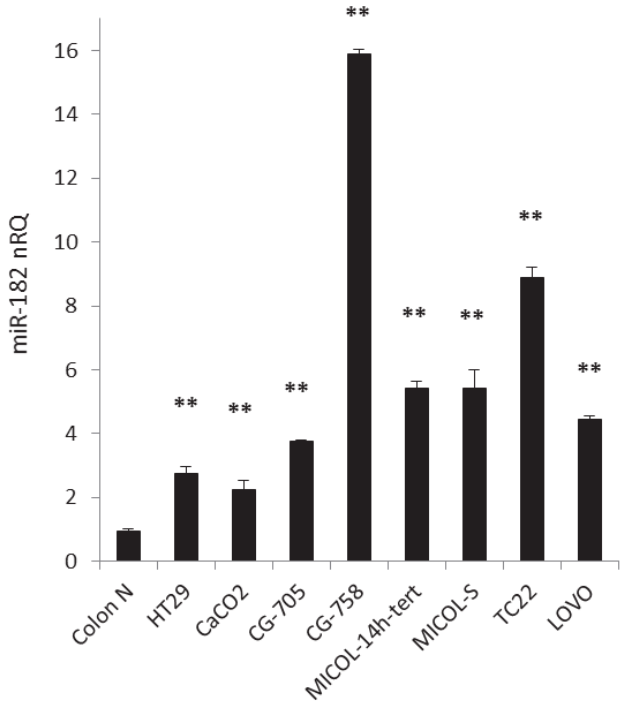

Figure 5: miR-182 expression levels in CRC cell lines compared to normal colon mucosa. Panel of CRC cell lines investigated by qRT-PCR for miR-182 expression level compared to normal colon mucosa. All cell lines show high levels of miR-182. Colon N, pool of normal colon mucosa sample. nRQ, normalized Relative Quantity. ** $p<0.01$.

miR-182 silencing has no impact on Caco2 and HT29 cell lines

In order to explore the functional role of miR-182 we initially chosen the well-known CRC cell lines Caco2 and HT29, and we treated them with the anti- miR-182 or anti-miR-NC. We evaluated the inhibition of miR-182 expression levels by qRT-PCR at different time points after the treatment, and we observed a significant down-regulation of miR-182. In particular, the inhibition of miR-182 expression level in Caco2 was maintained at least until 72h post-transfection, instead in HT29 the effect wears off after 48h, compared to NT and anti-miR-NC treated cells (**Figure 6**).

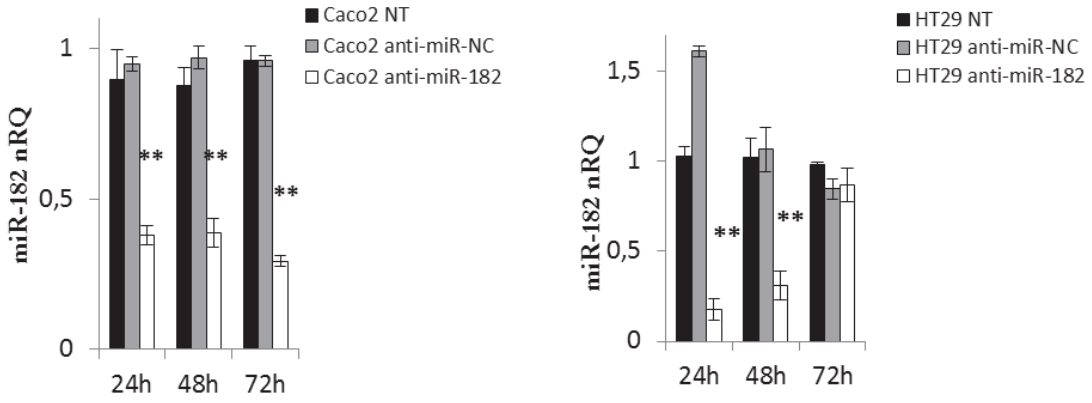

Figure 6: mir-182 inhibition in Caco2 and HT29. The evaluation of the miR-182 expression levels was performed by real-time PCR at different time points after transfection. Data analysis was performed by ΔΔCt method, and the control groups (NT and anti-miR-NC treated cells) were used as sample references at each time point. Data were mean±SD of three independent tests. nRQ, normalized Relative Quantity. **p<0.01.

We carried out *in vitro* cell apoptosis and cell cycle assays at different time points after the treatment. These cell lines did not show significant differences about the percentage of apoptotic cells at 24, 48 and 72h after anti-miR-182 treatment, as demonstrated by Annexin V FITC/PI binding assay (**Figure 7A**). Likewise, also the cell cycle phases were not modify by miR-182 inhibition (**Figure 7B**). Therefore, we concluded that miR-182 did not induce a significant change in apoptotic levels and proliferation state in these cell lines.

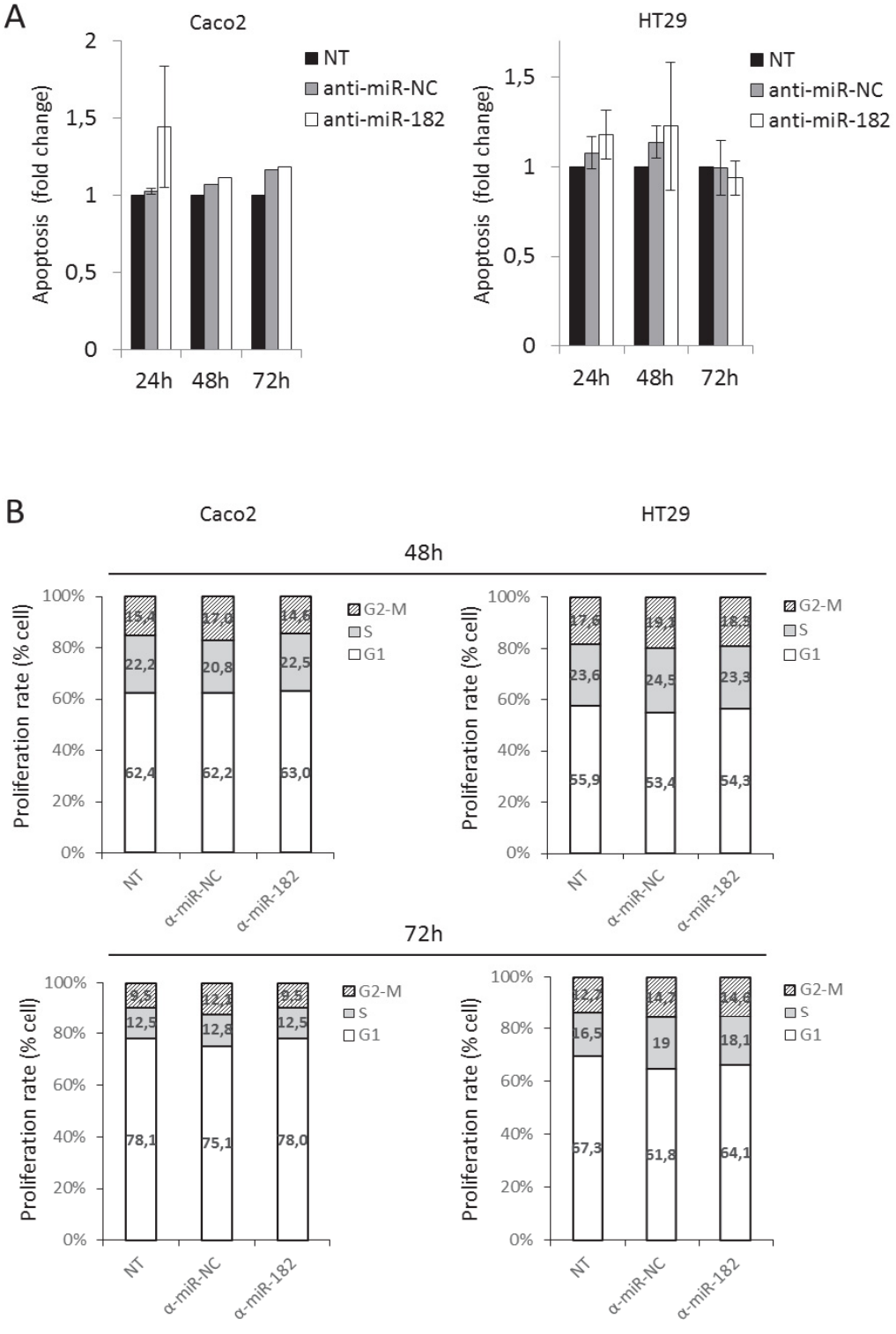

Figure 7: Apoptotic and cell cycle assays in anti-miR-182 treated Caco2 and HT29 cells. A. Anti-miR-182 treatment did not show an apoptotic effect in Caco2 and HT29 cell lines. The percentage of cell population±SD shown is the mean of at least three independent experiments in triplicate. **B.** The cell cycle assay in Caco2 and HT29 cells was performed at 48 and 72h after treatment. The control groups (NT and anti-miR-NC treated cells) were used as references at each time point.

Apoptosis-induced by inhibition of miR-182 in MICOL-14$^{h\text{-}tert}$ and TC22

Based on different *in vivo* behavior we focused our attention on MICOL-14$^{h\text{-}tert}$ and TC22 cell lines as CRC model of tumor dormancy and its tumorigenic variant, respectively. We decided to evaluate in these cell lines the potential impact and functional role of miR-182 on tumor cell growth.

To this aim, we treated the cells with anti-miR-182 or anti-miR-NC and we performed experiments to investigate cell apoptosis, cell cycle progression and cell migration. We evaluated the inhibition of miR-182 expression levels by qRT-PCR at different time points after the treatment, and we observed a significant down-regulation of miR-182 in both cell lines (**Figure 8**).

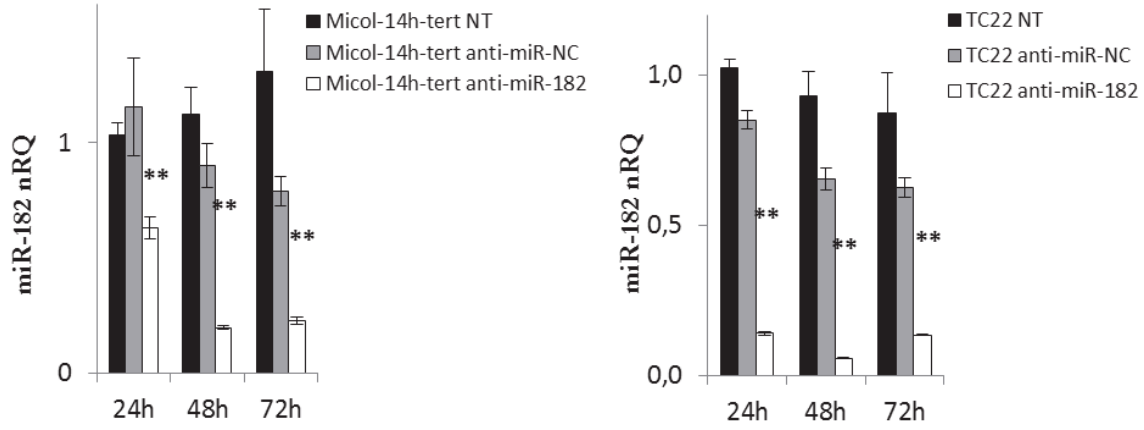

Figure 8: mir-182 inhibition in MICOL-14$^{h\text{-}tert}$ and TC22 cells. The evaluation of the miR-182 level was performed by real-time PCR at 24, 48, and 72 h after transfection. Data analysis was performed by ΔΔCt method, and the control groups (NT and anti-miR-NC treated cells) were used as sample references at each time point. Data were mean±SD of three independent tests. nRQ, normalized Relative Quantity. **p<0.01.

MICOL-14$^{h\text{-}tert}$ showed a significant increase of cell apoptosis at 24h after miR-182 inhibition compared to NT or anti-miR-NC treated cells, which is maintained at least until 72h. TC22 were not affected at 24h post-treatment, and a significant level of cell apoptosis was observed 48h after treatment. In general, we observed that 72h after anti-miR-182 inhibition, a significant increase of cell apoptosis was detectable in both cell lines compared to the

controls. In particular, the cell apoptosis due to inhibition of miR-182 was stronger in TC22 compared to MICOL-14$^{h\text{-}tert}$ (**Figure 9A**).

To strengthen these evidences, we carried out Western blot experiments in whole cell lysates at 48h post-treatment to detect cleaved PARP and Caspase-3 proteins. Caspase-3 is one of the key executioners of apoptosis, as it is partially or totally responsible for the proteolytic cleavage of its main target PARP. This polymerase is important for cells to maintain their viability and its cleavage facilitates cellular disassembly and serves as a marker of cells undergoing apoptosis. We observed an over-expression of cleaved Caspase-3 in both cell lines after anti-miR-182 treatment, although significantly more evident in TC22. In agreement, total PARP decreased and cleaved PARP seems to be higher in tumorigenic variant after anti-miR-182 treatment, compared to MICOL-14$^{h\text{-}tert}$ (**Figure 9B**).

We performed the wound healing assay to evaluate whether miR-182 inhibition could have an effect on cell migration. The scratch assay is a common method to track migration of individual cells at the leading edge of the gap. MICOL-14$^{h\text{-}tert}$ and TC22 were seeded and treated with anti-miR-182 or control, and a scratch was applied after 24h directly on the monolayer with a sterile pipette tip (T0). The cell ability to move and fill again the scratch was evaluated at different time points. As shown in Figure 9C, 18h after the scratch (42h after miR-182 inhibition) MICOL-14$^{h\text{-}tert}$ closed the gap. At the same time point, TC22 cell proliferation was not evaluable because of the strong pro-apoptotic effect of miR-182 inhibition. Indeed, a high amount of cells appear detached from the well plate modifying their morphology and appearing smaller and rounded (**Figure 9C**).

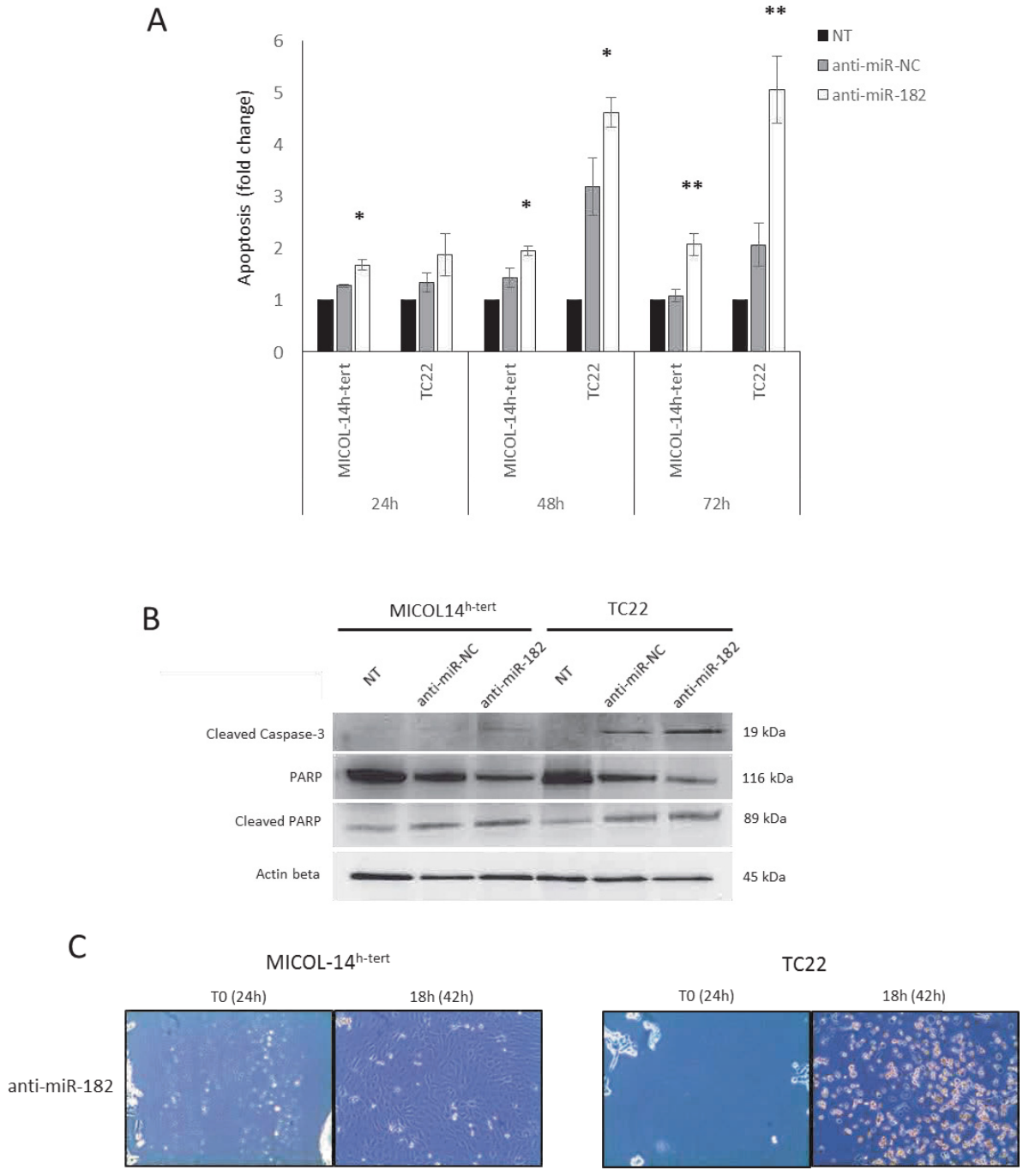

Figure 9. Anti-miR-182 treatment induced apoptosis in MICOL-14h-tert and TC22 cell lines. **A.** Anti-miR-182 increases the sensitivity of cells to apoptosis as determined by Annexin V/PI staining using the Annexin-V-FLUOS kit. The fold change±SD shown is the mean of at least three independent experiments in triplicate. **B.** Western blot analysis of CRC cell lines transfected with miR-182 inhibitor using anti-caspase 3 and anti-PARP antibodies show increased level of marker proteins of apoptosis. B-actin was used as a loading control. Photograph is representative of three independent experiments. **C.** Representative images depicting a cell migration assay performed in anti-miR-182 treated cells. At right MICOL-14$^{h\text{-}tert}$ have restored the monolayer homogeneously after 18h from the scratch (42h post-treatment), instead on the left, TC22 were detached from the plate due to diminished cell vitality. The control groups (NT and anti-miR-NC treated cells) were used as references at each time point. *p<0.05, **p<0.01.

miR-182 partially influences the cell cycle progression in the tumorigenic variant TC22

We also assessed in MICOL-14$^{h\text{-}tert}$ and TC22 whether miR-182 is involved in cell cycle progression. Our findings showed that miR-182 partially influences also the cell cycle progression of TC22. Indeed, 48h after anti-miR-182 treatment, the proportion of cells in G0/G1 phase was weakly increased while the proportion of cells in S and G2 phases was decreased, compared to controls. MICOL-14$^{h\text{-}tert}$, instead, did not present variations of cell cycle phases after anti-miR-182 treatment (**Figure 10**).

Hence, miR-182 inhibition seems not to affect the cell cycle progression in MICOL-14$^{h\text{-}tert}$ and only a weakly decrease of cell proliferation was detectable in the tumorigenic variant TC22.

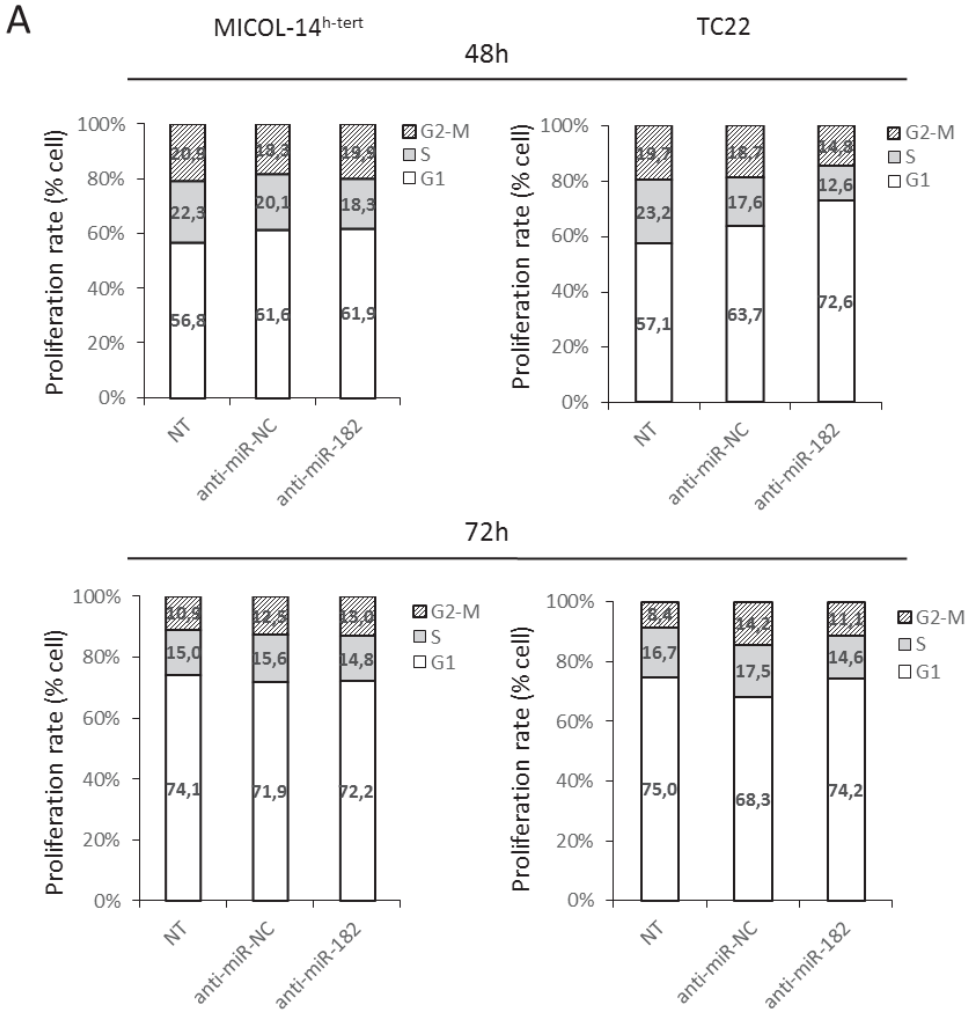

Figura 10. Anti-miR-182 weakly decreased cell cycle progression of TC22 cells. The cell cycle assay in MICOL-14$^{h\text{-}tert}$ and TC22 cells was performed at 48 and 72h after the treatment. The control groups (NT and anti-miR-NC treated cells) were used as references at each time point.

miR-183 is modulated by inhibition of miR-182, instead anti-miR-183 treatment only partially affected the miR-182 expression level and apoptosis

We previously demonstrated that miR-182 is related to other important up-regulated miRNAs in a transcriptional regulatory network. In particular, miR-182 with miR-183 share several common target genes (54). Furthermore, these miRNAs were described as members of the miR-183 family and polycistronic miR-183-96-182 cluster (71). Indeed, they were transcribed in the same direction from physically adjacent miRNA genes, are characterized by sequence homology and could function synergistically. Starting from these premises, we investigated by qRT-PCR whether the inhibition of miR-182 in MICOL-14$^{h\text{-}tert}$ and TC22 cells could affect the expression level of miR-183, and viceversa. We observed that the anti-miR-182 treatment also induced a significant down-regulation of miR-183 expression level compared to controls at each time point considered in both cell lines (**Figure 11A**). Instead, the inhibition of miR-183 also partially influenced the miR-182 expression level. In particular, MICOL-14$^{h\text{-}tert}$ showed a decrease of miR-182 only at 72h after the treatment, while TC22 cells presented a significant miR-182 down-regulation after 24h post-treatment (**Figure 11B**).

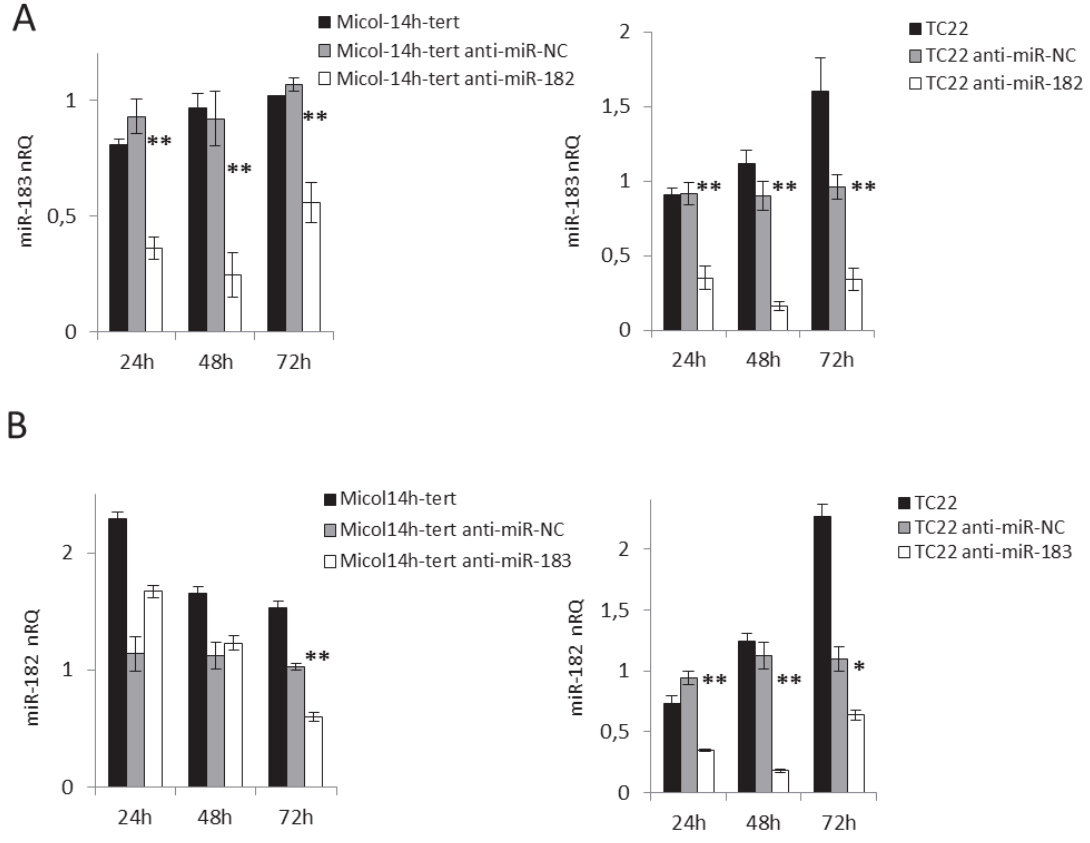

Figure 11. Anti-miR-182 treatment significantly influences the miR-183 expression level, instead miR-183 inhibition partially reduced miR-182 expression level. A. The evaluation of miR-183 expression level following the miR-182 inhibition was performed in MICOL-14$^{h\text{-}tert}$ and TC22 cells by qRT-PCR at 24, 48, and 72h after treatment. **B.** The evaluation of miR-182 expression level after the anti-miR-183 treatment was performed in both cell lines by qRT-PCR at 24, 48, and 72h after treatment. Data were analyzed by ΔΔCt method, and the control groups (NT and anti-miR-NC) were used as references at each time point considered. Data were mean±SD of three independent tests. nRQ, normalized Relative Quantity. *p<0.05, **p<0.01.

In order to clarify whether the pro-apoptotic effects were a direct consequence of miR-182 inhibition or could be also ascribed to miR-183 or both, we evaluated the effect of anti-miR-183 treatment on cell apoptosis. We observed that the anti-miR-183 treatment did not induce significant variation until 48h in both cell lines, compared to controls. Starting from 72h we measured a substantial apoptotic effect in MICOL-14$^{h\text{-}tert}$, and more significant in tumorigenic variant TC22 (**Figure 12**). Interestingly, the cellular apoptosis in MICOL-14$^{h\text{-}tert}$ was enhanced only at 72h after the anti-miR-183 treatment (**Figure 12**), in agreement with the down-regulation of miR-182 due to miR-183 inhibition (**Figure 11B**).

In addition, we investigated the consequence of the co-inhibition of miR-182 and miR-183, and we observed the same results obtained with the inhibition of miR-182 alone (data not shown).

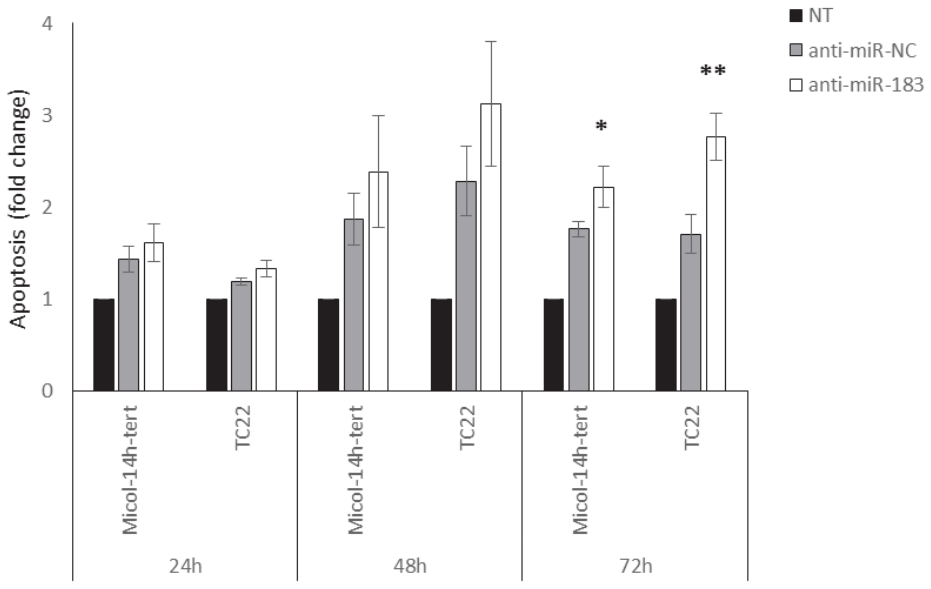

Figure 12: Anti-miR-183 induced apoptosis 72h after the treatment in both cell lines. Inhibition of miR-183 increases the sensitivity of cells to apoptosis only after 72h as determined by Annexin V/PI staining. The percentage cell population±SD shown is the mean of at least three independent experiments in triplicate. The control groups (NT and anti-miR-NC treated cells) were used as references at each time point. *p<0.05, **p<0.01.

miR-182 inhibition in TC22 xenografts reduces the *in vivo* tumor growth

With the aim to evaluate the effect of anti-miR-182 treatment *in vivo*, we injected subcutaneously TC22 cell lines after anti-miR-182 or anti-miR-NC treatment in NOD/SCID mice. Initially, we verified by qRT-PCR how long the transient inhibition of miR-182 was maintained in TC22 cells, and we observed that the miRNA was down-regulated until at least 1 week after transfection (**Figure 13**).

We injected anti-miR-182 treated cells at 24h after *in vitro* transient transfection, and 1 week later we performed also an *in vivo* intra-tumoral anti-miR-182 injection using Invivofectamine. The resulting tumors were inspected periodically and measured by caliper. All of the mice survived until the experimental end point.

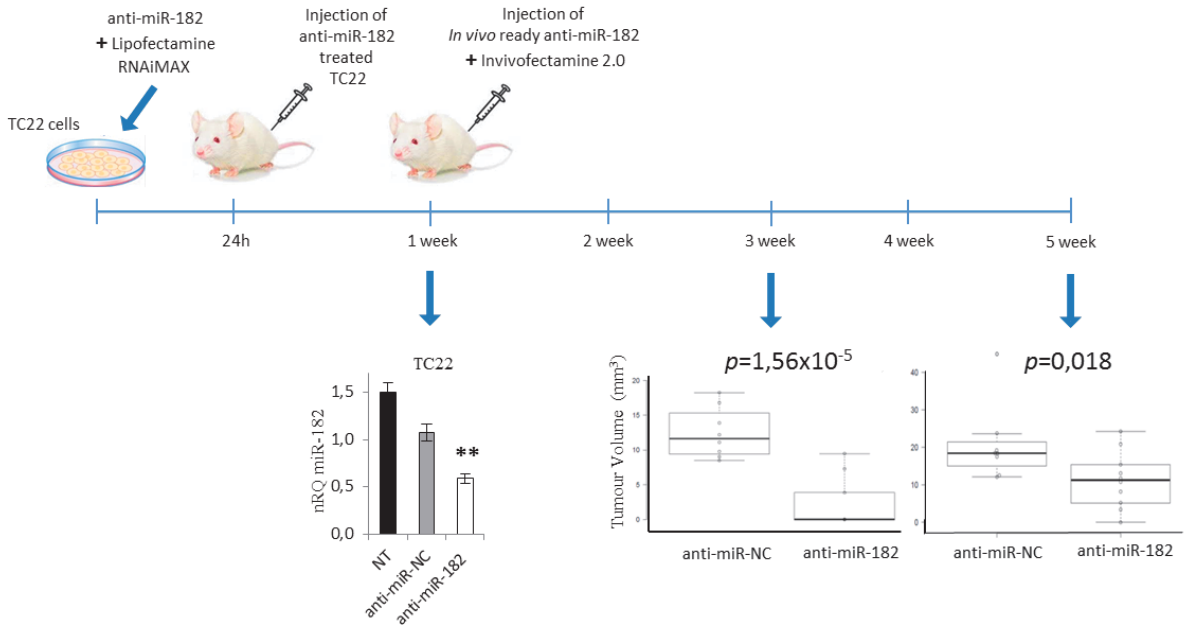

Figure 13. Experimental workflow for injection of TC22 cells with miR-182 inhibition in mice. TC22 cell lines was treated with anti-miR-182 or anti-miR-NC, and after 24h they were s.c. injected in NOD/SCID mice. After a week we performed in mice an intratumoral injection with *in vivo* ready anti-miR-182 and Invivofectamine. We also demonstrated by qRT-PCR that, after a week from transfection, TC22 maintained the *in vitro* miR-182 inhibition. After 3and 5 weeks from the injection of TC22 treated cells the tumor sizes were significantly reduced by miR-182 inhibition. The control group (anti-miR-NC treated cells) was used as references at each time point.

We found that anti-miR-NC controls developed growing tumors invariably higher compared to anti-miR-182 treated cells (**Figure 14**). Interestingly, we observed that miR-182 inhibition significantly reduced tumor size after 3 weeks from the injection (*p*-value=1,56x10^{-5}). 5 weeks after tumor cell injection, the tumor mass were still different, although the differences were less significant (p=0.018) (**Figure 14A**). Subsequently we performed H&E staining on the samples obtained from the tumor mass to analyze the possible histological and morphological changes induced by miR-182 inhibition. In particular, we observed that the tumor mass obtained with both NT and anti-miR-NC treated cells was characterized by the aspect of moderately to poorly differentiated adenocarcinoma, with bulky appearance, trabecular-solid pattern, minimal fibrosis and pushing borders. The anti-miR-182 treated TC22 cells showed to grow mainly as moderately differentiated adenocarcinoma, with mild fibrosis within (**Figure 14B, Table 3**). The histological aspect of anti-miR-182 resulting tumors reminds the one of treated CRC, that is fibrotic and with atrophic features. None presents conspicuous necrosis, but isolated necrotic foci and minimal leukocyte infiltration are detectable in all three groups. Finally, we demonstrated that anti-miR-182 treatment significantly reduced tumor growth and modified the tumor cell morphology *in vivo*.

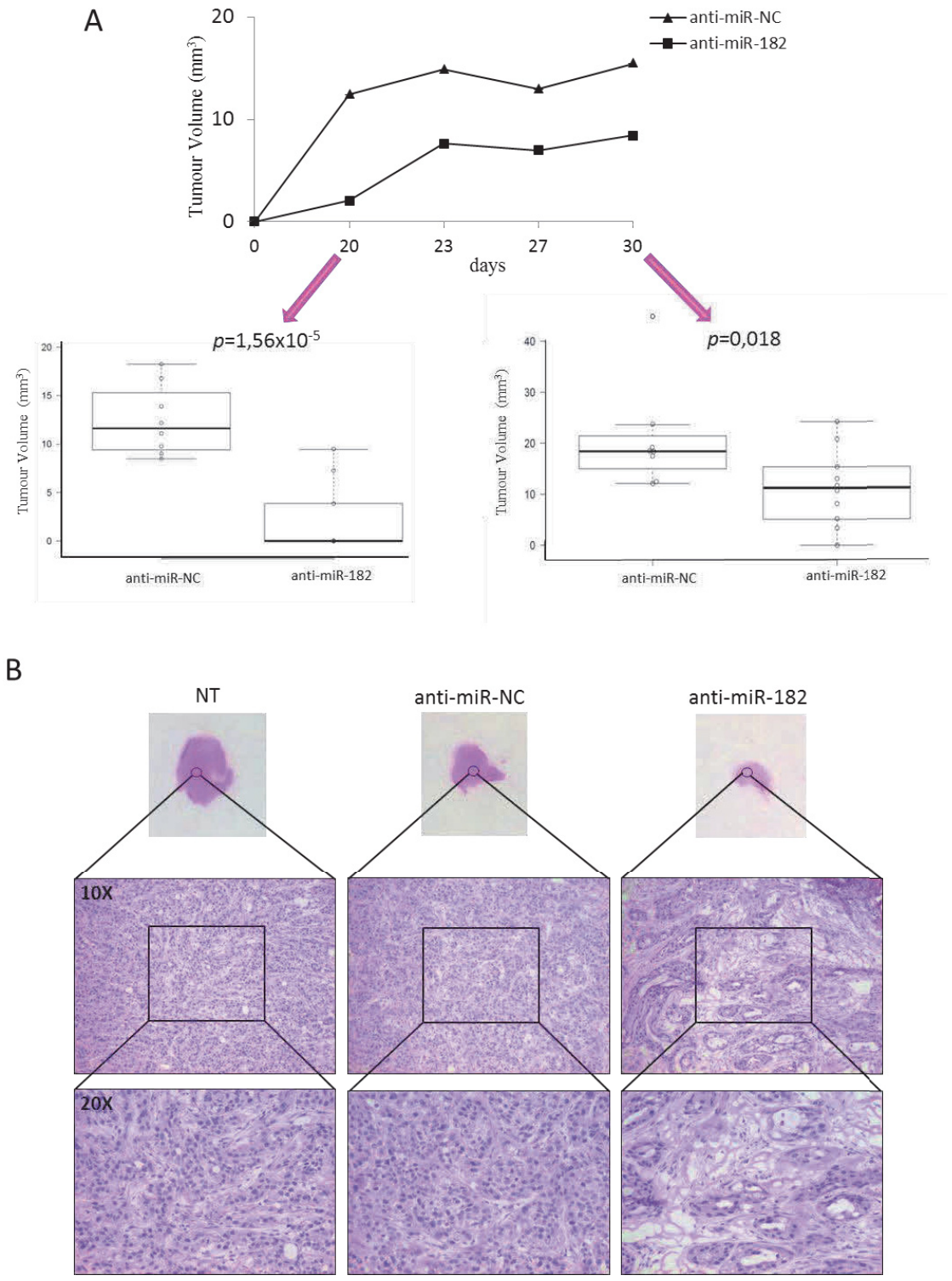

Figure 14. miR-182 inhibition in TC22 xenografts reduced the growth and modified morphological features of the tumor. A. Box plot distribution of tumor mass volume resulting in TC22 xenografts 5 weeks after tumor cell injection with anti-miR-182 or anti-miR-NC. miR-182 silencing leads to observe smaller tumors in treated mice compared to controls. Center lines show the medians; box limits indicate the 25th and 75th percentiles as determined by R software. Data points are plotted as open circles. n = 8, 10 sample points. **B.** H&E staining of tumor sections. NT and anti-miR-NC tumors presented the same histological and morphological pattern compared the anti-miR-182 treated tumor mass *in vivo*, in which the adenocarcinoma was moderately differentiated with mild fibrosis. Magnification 10X and 20X. The control groups (NT and anti-miR-NC treated cells) were used as references at each time point.

One of the main histological and morphological aspects that may be considered in the dynamic development of colorectal carcinoma, besides the grading of de-differentiation and growth pattern, is the mitotic index. This is defined as the ratio between the number of cells in a population undergoing mitosis to the number of cells in a population not undergoing mitosis, thus it measures cellular proliferation. As detailed in Table 3 we evaluated the mitotic index of the tumor mass, and we observed that in controls generally it was higher compared to those from anti-miR-182 treated TC22 cells.

Samples		Mitotic index	G (Grading)
1	Non Treated TC22	42	G3
2		23	G2/G3
3		9	G2/G3
4		20	G2/G3
5		21	G3
6		13	G2/G3
7		11	G3
8		21	G2/G3
9	anti-miR-NC treated TC22	15	G2/G3
10		5	G2/G3
11		26	G2/G3
12		20	G2/G3
13		17	G2/G3
14		21	G2/G3
15		8	G2/G3
16		15	G3
17	anti-miR-182 treated TC22	8	G2/G3
18		15	G2
19		26	G3
20		15	G2/G3
21		4	G2
22		7	G2
23		5	G2
24		15	G2/G3
25		7	G2/G3

Table 3: Mitotic index and grading were lower in tumor mass from anti-miR-182 treated TC22 than controls. Inhibition of miR-182 decrease the mitotic index of the tumor cells. Controls grew as G2/G3 or G3 adenocarcinomas, while anti-miR-182 treated tumor mass grew mainly as moderately differentiated adenocarcinoma (G2 and G2/G3). The control groups (NT and anti-miR-NC treated cells) were used as references.

The *in vivo* experiments were performed in collaboration with Dott. M. Curtarello of the S. Indraccolo's group (Oncology and Immunology Division, DiSCOG, University of Padova).
The morphological and histological evaluations were performed in collaboration with Dott. L. Albertoni of the Professor Rugge's group (Surgical Pathology and Cytopathology Unit, DIMED, University of Padova).

Differentially expressed transcripts modulated by miR-182 in MICOL-14$^{h\text{-}tert}$ and TC22

To investigate the mRNA expression profile and to explain the involvement of miR-182 in molecular pathways relevant to cancer we carried out Primeview Array in MICOL-14$^{h\text{-}tert}$ and TC22 after anti-miR-182 treatment. We analyzed total RNA of the cells after anti-miR-182 and anti-miR-NC treatment and for each condition we obtained four replicates for a total of 16 samples. We acquired expression profiles of 49,293 probesets, corresponding to 41,532 transcripts and to 19,942 genes.

In Figure 15 is described the dataset, providing the box-plots of log-intensity distributions in considered samples after normalization (**Figure 15A**) and descriptive unsupervised analyses, as Principal Component Analysis (PCA; **Figure 15B**) and pairwise sample correlation based on transcript expression profiles (**Figure 15C**). Both PCA and sample correlations showed that, as expected, samples separated first for cell line and then by treatment underlying the effect on expression profiles of miR-182 inhibition.

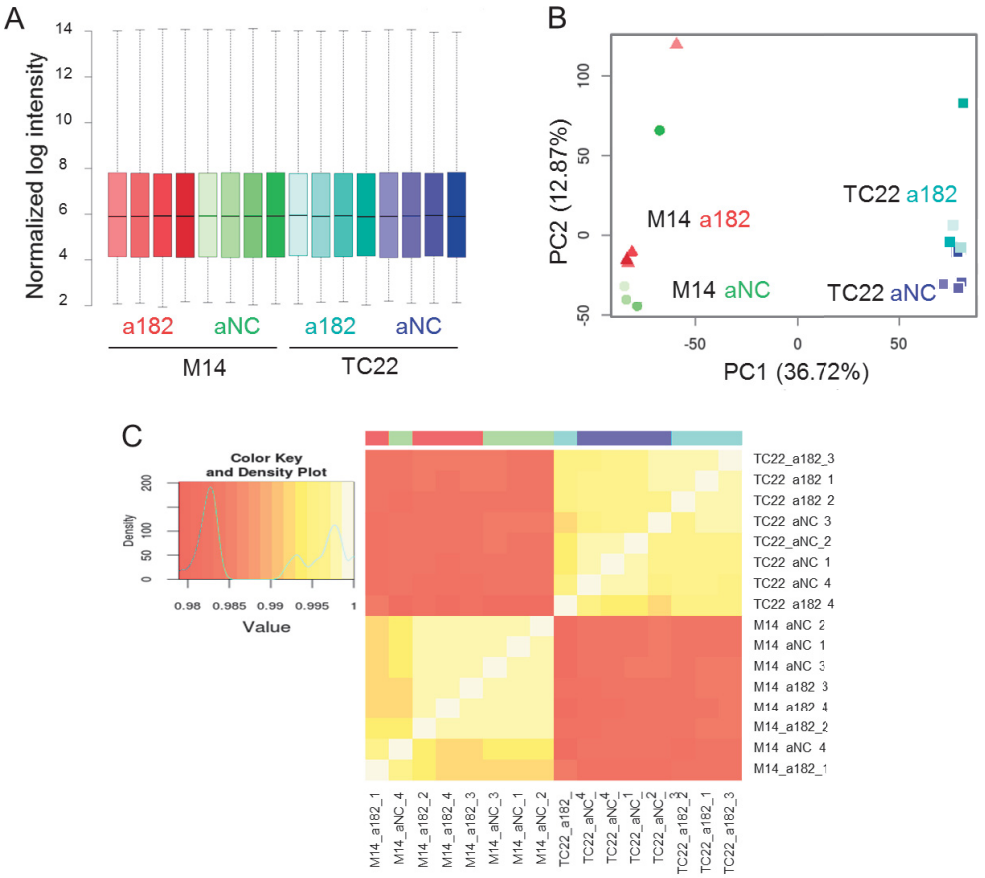

Figure 15. Descriptive analyses of gene expression profiles in MICOL-14$^{h\text{-}tert}$ and TC22 after anti-miR-182 or anti-miR-NC treatment. A. Boxplot of intensity values distribution per samples after RMA normalization; unsupervised analyses depicting sample relationships, considering expression profiles of all probesets and transcripts represented in Primeview arrays, are reported in **B.** PCA analysis and **C.** pair-wise sample correlation plot. M14, MICOL-14$^{h\text{-}tert}$; a182, anti-miR-182; aNC, anti-miR-NC.

The heatmap in **Supplementary Figure 1** shows the cluster analysis and the expression profiles of a subset of 12,323 transcripts (25% of the total) selected according to expression level and variability across the total of samples. Differentially expressed probesets with significantly variable expression after miR-182 inhibition were detected in both cell lines (**Table 4**). The impact of anti-miR-182 on gene expression was more important in the TC22 cells, where 1,878 probesets, corresponding to 3,472 transcripts and 1,382 genes, resulted significantly modulated. In MICOL-14$^{h\text{-}tert}$ cells we detected 312 differentially expressed probests (669 and 243 transcripts and genes, respectively). The anti-miR-NC treated cells were used as references.

Contrast		Differentially expressed		
		Probesets	**Transcripts**	**Genes**
MICOL-14$^{h\text{-}tert}$ a182 vs aNC	Up-regulated	228	487	172
	Down-regulated	84	182	70
	Total	**312**	**669**	**243**
TC22 a182 vs aNC	Up-regulated	772	1342	574
	Down-regulated	1106	2130	816
	Total	**1878**	**3472**	**1382**

Table 4: Differential expression after miR-182 inhibition in MICOL-14$^{h\text{-}tert}$ and TC22 cell lines. For each cell type, the total number of significantly differentially expressed probesets (adjusted p-value < 0.05) and the corresponding number of unique transcripts and genes is indicated; counts of up- and down-regulated elements are also indicated separately. a182, anti-miR-182; aNC, anti-miR-NC.

The **Figure 16A** shows the heatmap of differentially expressed probesets in MICOL-14$^{h\text{-}tert}$ cells, corresponding to 487 and 182 transcripts after miR-182 inhibition. Symmetrically, the heatmap in **Figure 16B** displays the expression profile variations in TC22 cells after miR-182 treatment, showing also that a higher number of down- than up-regulated probesets were detected, corresponding to 2,130 down- and 1,342 up-regulated transcripts.

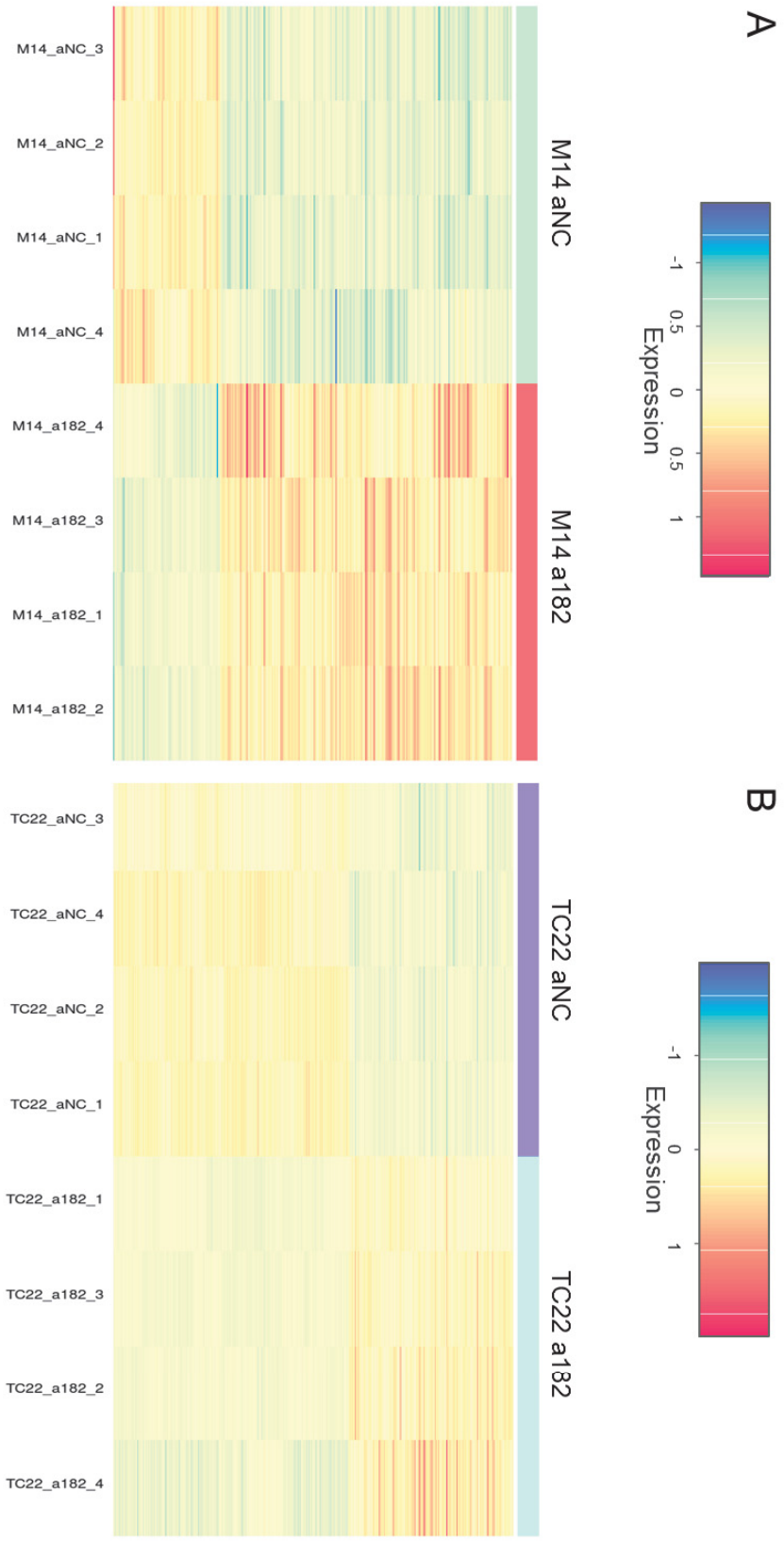

Figure 16. Heatmaps of expression profiles of probesets differentially expressed after miR-182 inhibition. A. and **B.** showed 3,472 and 669 differentially expressed probesets detected in TC22 and MICOL-14$^{h\text{-}tert}$ cell lines, respectively. a182, anti-miR-182; aNC, anti-miR-NC.

Notably, 158 genes were associated to probesets and transcripts differentially expressed after miR-182 inhibition in both cell lines. The large majority (153) of common genes deregulated after the treatment changed in the same direction in the two cell lines, with 103 and 50 that were respectively up- and down-regulated.

Functional Gene Ontology (GO) terms and KEGG and Reactome pathways significantly enriched among differentially expressed genes were reported in **Supplementary Table 2**.

According to TarBase data, 12 genes (ATF1, ANKRD36, BRWD1, DDAH1, FAM193A, FLOT1, NR3C1, PNISR, QSER1, RBM12, SESN2, and TNRC6A) that we found significantly up-regulated after miR-182 inhibition were already validated as miR-182 target genes. Among them, ATF1 and FLOT1 were the first target validated with strong evidence based on luciferase reported assays and other methods. In our data, ATF1 was up-regulated in both cell lines with a fold change of at most 0.41. FLOT1 resulted up-regulated only in TC22 cells with a fold change at most 0.40. (**Supplementary Table 3**).

Next, we aimed to identify new putative direct miR-182 targets, which were expected to be up-regulated after the miRNA inhibition. To this purpose, we selected 1,086 probesets showing more marked expression variation in terms of average expression and fold change (see Methods), corresponding to 1,825 transcripts from 759 genes. We then focused on 492 of these selected up-regulated transcripts (from 218 genes, corresponding to 323 probesets) that were putative miR-182 targets, since they carried one or more miR-182 target sites according to TargetScan predictions and passed our score- and expression-based filtering (**Supplementary Table 4**). Based on these criteria of selection, the availability of transcript assays and the biological role we validated by qRT-PCR four putative targets (HIST1HBH, NABP1, RND3, TRIO) (**Figure 17**).

The bioinformatics analysis of gene expression were performed in collaboration with Professor Bortoluzzi's group (Department of Molecular Medicine, University of Padova).

A

GENE	Probeset ID	LogFC MICOL14$^{h\text{-}tert}$	LogFC TC22
HIST1H2BH	11759111_x_at	1,06	0,65
NABP1	11726725_a_at	0,75	0,81
	11726726_a_at	0,71	0,76
	11726727_a_at	0,75	0,72
	11726728_a_at	0,48	0,50
RND3	11753427_a_at	0,35	0,43
TRIO	11724261_a_at	0,74	1,30
	11744590_a_at	0,14	0,40

B

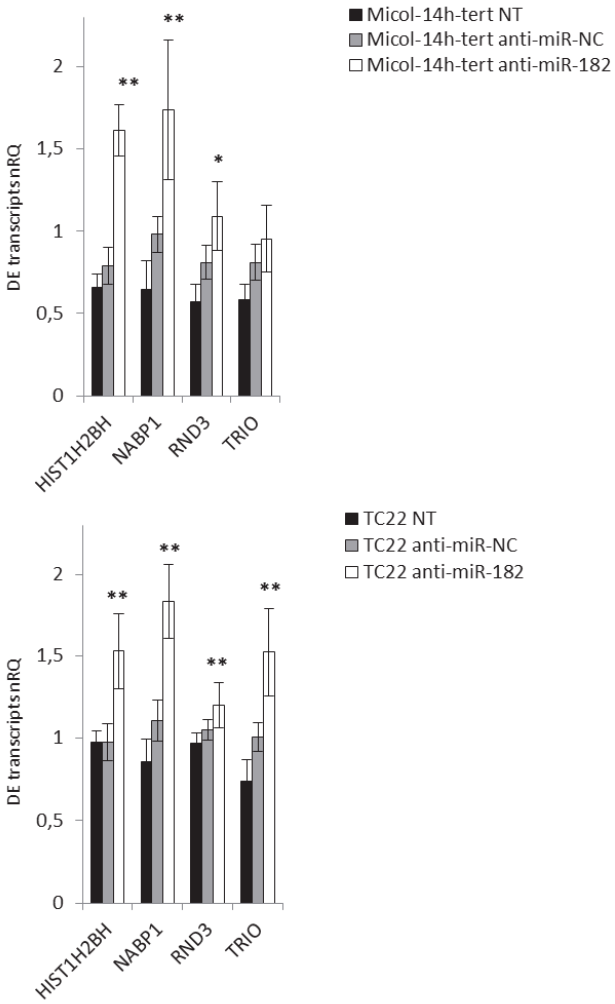

Figure 17. miR-182 transcript targets validation. A. Description of validated target gene transcripts and logFC up-regulation in MICOL-14$^{h\text{-}tert}$ and TC22 cell lines after miR-182 inhibition. **B.** The evaluation of the transcript expression levels was performed by real-time PCR in cell lines and, for NABP1 also in sample tissues. Data analysis was performed by ΔΔCt method, and the control groups (NT and anti-miR-NC treated cells) were used as sample references in cell lines. Normal colon mucosa (N) was used as reference for primary tumor tissue (T). Data were mean±SD of three independent tests. nRQ, normalized Relative Quantity. *p<0.05 **p<0.01.

Manuscript in preparation.

DISCUSSION

Colorectal cancer is the third most common cancer and the third leading cause of cancer death in men and women (1). Adjuvant chemotherapy is usually reserved to node-positive (TNM stage III) patients, whereas no further treatment is recommended for node-negative (TNM stage I and II) patients after surgical resection. Actually, within five years from surgery, up to 20% of node-negative patients develop recurrence and the identification of biomarkers able to characterize a node-negative population at highest risk of recurrence, who could benefit more of adjuvant chemotherapy, is still elusive.

However, metastatic spread remains the ultimate cause of cancer-related death in most CRC cases, and 20-25% of patients present metastatic disease at diagnosis. Only about 70% of stage III CRC cases with regional lymph node metastasis are curable by surgery combined with adjuvant chemotherapy. Metastatic disease (stage IV), despite improved survival due to recent advances in chemotherapy, is usually incurable (74, 75). Therefore, it is of critical importance to understand the molecular alterations involved in CRC development and progression, and identify diagnostic and prognostic biomarkers for improving CRC patients' survival (23, 76).

Using a large dataset of CRC miRNA and gene expression profiles, we previously described (54) the interplay of miRNA groups in regulating gene expression, which in turn affects modulated pathways that are important for tumor development. The data we obtained demonstrate that miR-182 could contribute to colorectal cancer tumorigenesis and progression.

In the attached paper published in my first year of PhD (68, Appendix 1) we confirmed that miR-182 is significantly up-regulated during colon carcinogenesis cascade and metastasis, and is associated to prognosis of CRC patients. The miR-182 prognostic impact is also supported by our elaboration of data from TCGA CRC cohort showing higher miR-182 expression in more advanced stages of CRC, and shorter survival in patients with high miR-182 expression levels. Due to the stability of circulating miRNAs as well as the role of miRNA dysregulation at different stages of carcinogenesis, they have the potential to serve as very promising non-invasive biomarkers for different types of human cancers (72). Therefore, we demonstrated that also plasma miR-182 levels are significantly higher in CRC patients than in healthy controls and were significantly reduced in post-operative samples after radical hepatic metastasectomy, compared to pre-operative samples. These results showed that miR-

182 up-regulation starts at the beginning of colon carcinogenesis and is maintained in the metastatic process. Our findings also indicated that the evaluation of circulating miR-182 levels could be a promising approach to improve the repertoire of non-invasive blood based biomarkers for CRC monitoring and screening.

In the following submitted manuscript, we then analyzed an independent series of patients with localized CRC (stage I/II, N0 M0) subdivided in Recurrent group and Non-Recurrent group. In particular, we explored the efficacy of a set of 5 miRNAs, already known to be involved in CRC progression, as biomarkers of relapse after bowel resection. Our analysis confirmed that the panel of selected miRNAs were strongly differentially expressed also in the early phases of the CRC tumor process, suggesting a promoting role already in the initial steps of colon carcinogenesis. Specifically, miR-18a, miR-21, miR-182 and miR-183 were strongly up-regulated in cancer tissue *vs*. normal colon mucosa, whereas miR-139 was strongly down-regulated. This finding extended to stage I-II CRC the results obtained in our previous work in stage IV CRC (54), showing that these five miRNAs accompany the CRC tumor process, from initial stages to advanced tumorigenesis. Moreover, our data indicated that the modulations of miR-182, miR-183 and miR-139 are more specific of the tumor process. MiR-18a and miR-21, instead, appear weakly up-regulated also in inflamed bowel tissue, thus suggesting that the strong up-regulation of these two miRNAs in the tumor could be partially related to inflammation. We thus hypothesized that these miRNAs, that accompany the tumorigenesis process, were present also in the pre-neoplastic, morphologically normal, mucosa adjacent to the tumor and that could be tested as possible predictors of relapse. Our results suggested that not a single miRNA, but rather a coordinated alteration of four miRNAs (i.e. miR-21, miR-18a, miR-182 and miR-183) from the same post-transcriptional network, may be useful to predict recurrence after resection, when evaluate in the normal mucosa adjacent to tumor. Furthermore, the miRNA ratio approach described in the present study may be transported for the evaluation of these modulated miRNAs into the plasma tissue and applied on a large-scale, as it requires measuring only four miRNAs and overcomes the need for a normalizer RNA. Interestingly, the miRNA ratios resulted to be predictive markers when evaluated in the adjacent, morphologically normal, mucosa and not in the tumor tissue. This result, apparently counterintuitive, is in line with previous findings reported in CRC (69) and also in other tumors (70, 77). Indeed, it is emerging with increasing evidence that the crosstalk between tumor and microenvironment could affect the adjacent mucosa and that also this tissue may be informative. In a recent

study, Sanz-Pamplona *et al.* (69) demonstrated that a number of genes related to the presence of the tumor were activated in adjacent mucosa of CRC patients. Moreover, these activated genes were enriched in transcription factors (TFs), indicating the existence of a transcriptional program driving the observed altered expression pattern in normal mucosa. At a higher level, we expected that also miRNAs are involved in regulating TFs and, in cascade, the genes activated in adjacent mucosa. MiRNA expression in adjacent mucosa could be modulated in response to signals produced by the tumor to establish a tumor-microenvironment crosstalk advantageous for neoplastic transformation process, or it could be an indicator of microenvironment remodeling associated with the local progression of cancer. In this study we highlighted the importance of its investigation also for the presence of potential biomarkers of tumor relapse.

The main limitation of our analyses is the restricted samples size, which could affects the statistical evaluation of miRNA expression levels and their relationships to clinicopathological variables. Nevertheless, this first part of the study has several important clinical implications. First, the specific involvement of miR-182 in CRCs indicates its potential to be developed into a potential non-invasive marker for these patients. Secondly, miR-182 in combination with other miRNAs could be a possible prognostic biomarker for the monitoring of relapse in localized CRC patients. These results, if confirmed in an ample cohort of patients, may help to identify patients at high-risk of recurrence who would benefit most from adjuvant therapy.

To gain insights in the functional role played by miR-182 in the tumorigenesis, in a parallel set of experiments we investigated the effects of miR-182 inhibition in CRC cell lines. We first evaluated Caco2 and HT29 cell lines, in which we did not observe an impact on cell apoptosis. Probably in these CRC cell lines, miR-182 acts exploiting other molecular mechanisms that we have not investigated and highlighted. However, these cell lines as well-known cancer cell lines are easy to culture and have limitless growth potential. So, they could be maintained *in vitro* for prolonged periods, and consequently can change genetically over multiple passages partially losing the feature to be representatives of the cancers from which they were derived (78). Thereafter, we focused on other two colorectal cancer cell lines as *in vitro* models: MICOL-14$^{h\text{-}tert}$ (an *in vivo* non-tumorigenic cell line derived from a lymph node metastasis of rectal cancer) and its *in vivo* tumorigenic variant TC22. Interestingly, as reported by Dalerba P. *et al* (55), in MICOL-14$^{h\text{-}tert}$ the set of detected mutations

corresponded to that of the original tumor tissue proving that the cell culture was representative of the tumor *in vivo* cell population.

By analyzing the expression levels of miR-182, we observed that it was higher in TC22 compared to MICOL-14$^{h\text{-}tert}$, suggesting a role of this miRNA in tumor aggressiveness. We demonstrated that, a significant increase of cell apoptosis was stronger in TC22 compared to MICOL-14$^{h\text{-}tert}$ after miR-182 inhibition. Furthermore, a partially modulation of cell cycle progression in TC22 due to anti-miR-182 treatment, was detectable. We observed also a down-regulation of miR-183 after the inhibition of miR-182, in both cell lines. To further deepen whether the pro-apoptotic effects were a direct consequence of miR-182 inhibition or could be also ascribed to miR-183 or both, we also evaluated the effect of miR-183 inhibition on miR-182 expression level and cell apoptosis. We concluded that in both cell lines the effect of miR-183 inhibition was lower and delayed compared to that induced by anti-miR-182 treatment, and that miR-183 only partially affected the miR-182 expression level and apoptosis. We also investigated the consequence of the co-inhibition of miR-182 and miR-183 together, and we observed the same results obtained with the inhibition of miR-182 alone. These results highlighted the hypothesis that the main regulator of cell viability in these cancer cell lines is miR-182 rather than miR-183.

Interestingly, the *in vivo* injection of anti-miR-182 treated TC22 cells showed a significant reduction of tumor growth and a modified morphology features, that appeared with less aggressive properties. These data showed that regulation of miR-182 expression levels in TC22 xenografts markedly contributed to modulate CRC cell proliferation and tumorigenic potential.

The cancer is a limited number of "mission critical" events that propel the tumor cell into expansion and uncontrolled invasion. One of these is cell proliferation, which, together with the compensatory suppression of apoptosis, provides a minimal 'platform' necessary to support neoplastic progression (79). The evasion of apoptosis, which is critical for tumor growth and progression (80), could be a mechanism central to oncogenesis in colon cancer exhibiting increase of miR-182 expression level, permitting survival of cells with damaged DNA. Indeed, miR-182 inhibition caused a significant increase in the level of both activated caspase-3 and PARP, indicators of irreversible damage to the integrity of cell and genome, with a resultant increase in apoptotic activity (81). The results were also confirmed by bioinformatics analysis, in which the “positive regulation of apoptotic process” emerged as one of the most GO BP (Biological Process) significantly modulated from miR-182 inhibition

in both cell lines (**Supplementary Table 2**). In order to identify the regulatory molecular pathways by which this miRNA could act we also investigated the predicted target genes of miR-182. We partially validated several putative target transcripts, and in particular HIST1H2BH, NABP1, RND3 and TRIO, based on the availability of the experimentally assays and biological role. The HIST1H2BH gene is part of the histone family that are responsible for the nucleosome structure of the chromosomal fiber, and play a central role in DNA repair and chromosomal stability. Other components of core histones resulted modulated by miR-182 inhibition. Likewise, NABP1, an important paralog of NABP2, is a single-stranded DNA-binding protein (SSB) that promote the repair of DNA damage and G2/M checkpoint, and it is involved in the maintenance of genomic stability (82). Recently, Zhang F. *et al*. identified also INTS6, a gene modulated by miR-182 inhibition, as a major subunit of the core human SSB complex, and they demonstrated that INTS6 relocates to the DNA damage sites (83). The function of RND3, an atypical member of Rho family, is complex. It has been demonstrated to induce apoptosis in prostate cancer, esophageal squamous carcinoma and glioblastoma cell lines (84). TRIO encodes a large protein that functions as GDP to GTP exchange factor and that promotes the reorganization of the actin cytoskeleton, thereby playing a role in cell migration and growth (85).

To further deepen and confirm the role of miR-182 in CRC we are now testing the direct interaction of miR-182 with selected target genes using: the 3'UTR Lenti-reporter-Luc Vector in the Luciferase assay; *in vitro* over-expression of target gene by plasmid transfection and evaluation of functional effects; evaluation of protein expression levels of putative miR-182 target genes involved in functional networks.

REFERENCES

1. Siegel RL, Miller KD, Jemal A. Cancer Statistics, 2017. CA Cancer J Clin. 2017 Jan;67(1):7-30.
2. American Cancer Society: Cancer Facts and Figures 2017-2019. Atlanta.
3. Constance M. Johnson, Caimiao Wei, Joe E. Ensor, Derek J. Smolenski, Christopher I. Amos, Bernard Levin, and Donald A. Berry. Meta-analyses of Colorectal Cancer Risk Factors. Cancer Causes Control. 2013 Jun; 24(6): 1207–1222.
4. Gustavsson, B., G. Carlsson, David Machover, Nicholas Petrelli, Arnaud Roth, Hans-Joachim Schmoll, Kjell-Magne Tveit, Fernando Gibson. A Review of the Evolution of Systemic Chemotherapy in the Management of Colorectal Cancer. Clinical Colorectal Cancer. 2015 Mar;14(1):1-10.
5. Greene, F.L., Stewart, A.K. and Norton, H.J. A new TNM staging strategy for nodepositive (stage III) colon cancer: an analysis of 50,042 patients. Ann. Surg. 2002; 236, 416-421.
6. O'Connell, J.B., Maggard, M.A. and Ko, C.Y. Colon cancer survival rates with the new American Joint Committee on Cancer sixth edition staging. J. Natl. Cancer Inst 2004; 96, 1420-1425.
7. Compton, C.C. and Greene, F.L. The staging of colorectal cancer: 2004 and beyond. CA Cancer J. Clin. 2004; 54, 295-308.
8. UICC (Union for International Cancer Control). The TNM classification of Malignant Tumors 7th edition. 2009. 7 ed. Wiley-Blackwell.
9. IARC (International Agency for Research on Cancer). World Health Organization Classification of Tumours: Pathology and Genetics of Tumours of the Digestive System. 2000. IARC press, Lyon, France.
10. Chung, C.K., Zaino, R.J. and Stryker, J.A. Colorectal carcinoma: evaluation of histologic grade and factors influencing prognosis. J. Surg. Oncol 1982; 21, 143-148.
11. Derwinger, K., Kodeda, K., Bexe-Lindskog, E. and Taflin, H. Tumour differentiation grade is associated with TNM staging and the risk of node metastasis in colorectal cancer. Acta Oncol., 2010;49, 57-62.
12. Ewing I, Hurley JJ, Josephides E and Millar A. The molecular genetics of colorectal cancer. Frontline Gastroenterol 2014;5: 26-30.
13. Vogelstein B, Fearon ER , Hamilton SR , Kern SE , Preisinger AC,Leppert M, Nakamura Y, White R, Smits AM and Bos JL:Genetic alterations during colorectal-tumor development. N EnglJ Med 1988;319: 525-532.
14. Adam Humphries & Nicholas A. Wright. Colonic crypt organization and tumorigenesis. Nature Reviews Cancer 2008;8, 415-424.
15. Kosinski C, Li VS, Chan AS, Zhang J, Ho C, Tsui WY, Chan TL , Mifflin RC , Powell DW, Yuen ST , et al: Gene expression patterns of human colon tops and basal crypts and BMP antagonists as intestinal stem cell niche factors. Proc Natl Acad Sci USA 2007;104: 15418-15423.
16. Medema JP and Vermeulen L: Microenvironmental regulation of stem cells in intestina omeostasis and cancer (Review). Nature 2011;474: 318-326.

17. Goel A, Nagasaka T, Arnold CN , Inoue T, Hamilton C , Niedzwiecki D, Compton C, Mayer RJ, Goldberg R, Bertagnolli MM, et al: The CpG island methylator phenotype and chromosomal instability are inversely correlated in sporadic colorectal cancer. Gastroenterology 2007;132: 127-138.
18. Alfred G. Knudson. Two genetic hits (more or less) to cancer. Nature Reviews Cancer 2001;1, 157-162.
19. Aghagolzadeh P, Radpour R. New trends in molecular and cellular biomarker discovery for colorectal cancer. 2016. World J Gastroenterol; 22(25): 5678-5693.
20. Pino MS and Chung DC: The chromosomal instability pathway in colon cancer. Gastroenterology 2010;138: 2059-2072.
21. Boland CR and Goel A: Microsatellite instability in colorectal cancer (Review). Gastroenterology 2010;138: 2073-2087.e3.
22. Colussi D, Brandi G, Bazzoli F and Ricciardiello L: Molecular pathways involved in colorectal cancer: implications for disease behavior and prevention.. Int J Mol Sci 2013;14: 16365-16385.
23. Markowitz SD and Bertagnolli MM: Molecular origins of cancer: molecular basis of colorectal cancer.. N Engl J Med 2009; 361: 2449-2460.
24. Guinney J, Dienstmann R, Wang X, de Reyniès A, Schlicker A, Soneson C, Marisa L, Roepman P, Nyamundanda G, Angelino P, Bot BM, Morris JS, Simon IM, Gerster S, Fessler E, De Sousa E Melo F, Missiaglia E, Ramay H, Barras D, Homicsko K, Maru D, Manyam GC, Broom B, Boige V, Perez-Villamil B, Laderas T, Salazar R, Gray JW, Hanahan D, Tabernero J, Bernards R, Friend SH, Laurent-Puig P, Medema JP, Sadanandam A, Wessels L, Delorenzi M, Kopetz S, Vermeulen L, Tejpar S. The consensus molecular subtypes of colorectal cancer. Nature Medicine 2015.
25. Wang, R.F., Song, B.R., Peng, J.J., Cai, G.X., Liu, F.Q., Wang, M.H., Cai, S.J. and Ye, X. The Prognostic Value of Preoperative Serum CEA and CA19-9 Values in Stage I-III.. Colorectal Cancer. Hepatogastroenterology 2014; 61, 994-999.
26. Fletcher, R.H. Carcinoembryonic antigen. Ann. Intern. Med. 1986; 104, 66-73.
27. Chevinsky, A.H. CEA in tumors of other than colorectal origin. Semin. Surg. Oncol. 1991; 7, 162-166.
28. Ruibal Morell, A. CEA serum levels in non-neoplastic disease. Int. J. Biol. Markers 1992; 7, 160-166.
29. Fukuda, I., Yamakado, M. and Kiyose, H. Influence of smoking on serum carcinoembryonic antigen levels in subjects who underwent multiphasic health testing and services. J. Med. Syst., 1998;22, 89-93.
30. Duffy MJ. Personalized treatment for patients with colorectal cancer: role of biomarkers. Biomark Med. 2015;9(4):337-47.
31. Leigh-Ann MacFarlane and Paul R. Murphy. MicroRNA: Biogenesis, Function and Role in Cancer. Curr Genomics. 2010 Nov;11(7):537-61.
32. Esquela-Kerscher A1, Slack FJ. Oncomirs - microRNAs with a role in cancer. Nat Rev Cancer. 2006 Apr;6(4):259-69.

33. Minju Ha & V. Narry Kim. Regulation of microRNA biogenesis. Nature Reviews Molecular Cell Biology 2014;15, 509–524.
34. Shuibin Lin and Richard I. Gregory. MicroRNA biogenesis pathways in cancer. Nature Reviews Cancer 2015;15, 321–333.
35. Michael MZ1, O' Connor SM, van Holst Pellekaan NG, Young GP, James RJ. Reduced accumulation of specific microRNAs in colorectal neoplasia. Mol Cancer Res. 2003 Oct;1(12):882-91.
36. Sonja Hrašovec and Damjan Glavač. MicroRNAs as novel biomarkers in colorectal cancer. Front. Genet., 19 October 2012.
37. Chivukula, Raghu R. et al. An Essential Mesenchymal Function for miR-143/145 in Intestinal Epithelial Regeneration. Cell , Volume 157 , Issue 5 , 1104 – 1116.
38. Strubberg AM, Madison BB. MicroRNAs in the etiology of colorectal cancer: pathways and clinical implications. Dis Model Mech. 2017 Mar 1;10(3):197-214.
39. Nielsen BS1, Jørgensen S, Fog JU, Søkilde R, Christensen IJ, Hansen U, Brünner N, Baker A, Møller S, Nielsen HJ. High levels of microRNA-21 in the stroma of colorectal cancers predict short disease-free survival in stage II colon cancer patients. Clin Exp Metastasis. 2011 Jan;28(1):27-38.
40. Jane V Carter, Norman J Galbraith, Dongyan Yang, James F Burton, Samuel P Walker and Susan Galandiuk. Blood-based microRNAs as biomarkers for the diagnosis of colorectal cancer: a systematic review and meta-analysis. British Journal of Cancer (2017) 116, 762–774.
41. Akçakaya P1, Ekelund S, Kolosenko I, Caramuta S, Ozata DM, Xie H, Lindforss U, Olivecrona H, Lui WO. miR-185 and miR-133b deregulation is associated with overall survival and metastasis in colorectal cancer. Int J Oncol. 2011 Aug;39(2):311-8.
42. Sinéad T Aherne, Stephen F Madden, David J Hughes, Barbara Pardini, Alessio Naccarati, Miroslav Levy, Pavel Vodicka, Paul Neary, Paul Dowling, and Martin Clynes. Circulating miRNAs miR-34a and miR-150 associated with colorectal cancer progression. BMC Cancer. 2015; 15: 329.
43. Zhang GJ, Zhou H, Xiao HX, Li Y, Zhou T. MiR-378 is an independent prognostic factor and inhibits cell growth and invasion in colorectal cancer. BMC Cancer. 2014 Feb 20;14:109.
44. Pu XX, Huang GL, Guo HQ, Guo CC, Li H, Ye S, Ling S, Jiang L, Tian Y, Lin TY. Circulating miR-221 directly amplified from plasma is a potential diagnostic and prognostic marker of colorectal cancer and is correlated with p53 expression. J Gastroenterol Hepatol. 2010 Oct; 25(10):1674-80.
45. Rapti SM, Kontos CK, Papadopoulos IN, Scorilas A. Enhanced miR-182 transcription is a predictor of poor overall survival in colorectal adenocarcinoma patients. Clin Chem Lab Med. 2014 Aug;52(8):1217-27.
46. Yuan D1, Li K, Zhu K, Yan R, Dang C. Plasma miR-183 predicts recurrence and prognosis in patients with colorectal cancer. Cancer Biol Ther. 2015;16(2):268-75.
47. Li J, Liu Y, Wang C, et al. Serum miRNA expression profile as a prognostic biomarker of stage II/III colorectal adenocarcinoma. *Scientific Reports*. 2015;5:12921.

48. Keun Hur, Yuji Toiyama, Aaron J. Schetter, Yoshinaga Okugawa, Curtis C. Harris, C. Richard Boland, and Ajay Goel. Identification of a Metastasis-Specific MicroRNA Signature in Human Colorectal Cancer. J Natl Cancer Inst. 2015 Mar; 107(3): dju492.
49. Chen J, Wang W, Zhang Y, Chen Y, Hu T. Predicting distant metastasis and chemoresistance using plasma miRNAs. Med Oncol. 2014 Jan;31(1):799.
50. Liu K1, Li G, Fan C, Zhou X, Wu B, Li J. Increased expression of microRNA-21and its association with chemotherapeutic response in human colorectal cancer. J Int Med Res. 2011;39(6):2288-95.
51. L Perez-Carbonell, F A Sinicrope, S R Alberts, A L Oberg, F Balaguer, A Castells, C R Boland, and A Goel. MiR-320e is a novel prognostic biomarker in colorectal cancer. Br J Cancer. 2015 Jun 30; 113(1): 83–90.
52. Ma Y, Zhang P, Wang F, Zhang H, Yang J, Peng J, Liu W, Qin H. miR-150 as a potential biomarker associated with prognosis and therapeutic outcome in colorectal cancer. Gut. 2012 Oct;61(10):1447-53.
53. M Karaayvaz, H Zhai, and J Ju. miR-129 promotes apoptosis and enhances chemosensitivity to 5-fluorouracil in colorectal cancer. Cell Death Dis. 2013 Jun; 4(6): e659.
54. Pizzini S, Bisognin A, Mandruzzato S, Biasiolo M, Facciolli A, Perilli L, Rossi E, Esposito G, Rugge M, Pilati P, Mocellin S, Nitti D, Bortoluzzi S, Zanovello P. Impact of microRNAs on regulatory networks and pathways in human colorectal carcinogenesis and development of metastasis. BMC Genomics. 2013 Aug 29;14:589.
55. Dalerba, P, Guiducci, C, Poliani, PL, Cifola, I, Parenza, M, Frattini, M, Gallino, G, Carnevali, I, Di Giulio, I, Andreola, S, Lombardo, C, Rivoltini, L, Schweighoffer, T, Belli, F, Colombo, MP, Parmiani, G & Castelli, C. Reconstitution of human telomerase reverse transcriptase expression rescues colorectal carcinoma cells from in vitro senescence: Evidence against immortality as a constitutive trait of tumor cells. Cancer Research, 2005. vol 65, no. 6, pp. 2321-2329.
56. Indraccolo S, Minuzzo S, Masiero M, Pusceddu I, Persano L, Moserle L e altri. Cross-talk between tumor and endothelial cells involving the Notch3-DII4 interaction marks escape from tumor dormancy. Cancer Research. 2009 feb 15;69(4):1314-1323.
57. Serafin, V., Persano, L., Moserle, L., Esposito, G., Ghisi, M., Curtarello, M., Bonanno, L., Masiero, M., Ribatti, D., Stürzl, M., Naschberger, E., Croner, R. S., Jubb, A. M., Harris, A. L., Koeppen, H., Amadori, A. and Indraccolo, S. Notch3 signalling promotes tumour growth in colorectal cancer. J. Pathol. 2011, 224: 448–460.
58. Masters JR. Human cancer cell lines: fact and fantasy. Nat Rev Mol Cell Biol. 2000 Dec;1(3):233-6.
59. American Type Culture Collection Standards Development Organization Workgroup. Cell line misidentification: the beginning of the end. Nature Reviews Cancer 10, June 2010
60. Boeri M, Verri C, Conte D, Roz L, Modena P, Facchinetti F, Calabro E, Croce CM, Pastorino U, Sozzi G. MicroRNA signatures in tissues and plasma predict development and prognosis of computed tomography detected lung cancer.

Proceedings of the National Academy of Sciences of the United States of America. 2011; 108: 3713-3718.
61. Sharova E, Grassi A, Marcer A, Ruggero K, Pinto F, Bassi P, Zanovello P, Zattoni F, D'Agostino DM, Iafrate M, Ciminale V. A circulating miRNA assay as a first-line test for prostate cancer screening. British journal of cancer. 2016; 114: 1362-1366.
62. Parman C., Halling C., and Gentleman R. affyQCReport: QC Report Generation for affyBatch objects. 2005. R package version 1.48.0.
63. Gautier L, Cope L, Bolstad BM, Irizarry RA. affy--analysis of Affymetrix GeneChip data at the probe level. Bioinformatics. 2004, 12;20(3):307-15.
64. Ritchie ME, Phipson B, Wu D, Hu Y, Law CW, Shi W, Smyth GK. limma powers differential expression analyses for RNA-sequencing and microarray studies. Nucleic Acids Res. 2015, 20;43(7):e47.
65. Huang da W, Sherman BT, Lempicki RA. Systematic and integrative analysis of large gene lists using DAVID bioinformatics resources. Nat Protoc. 2009, 4(1):44-57.
66. Agarwal V, Bell GW, Nam JW, Bartel DP. Predicting effective microRNA target sites in mammalian mRNAs. Elife. 2015, 12;4.
67. Chou CH, Chang NW, Shrestha S, Hsu SD, Lin YL, Lee WH, Yang CD, Hong HC, Wei TY, Tu SJ, Tsai TR, Ho SY, Jian TY, Wu HY, Chen PR, Lin NC, Huang HT, Yang TL, Pai CY, Tai CS, Chen WL, Huang CY, Liu CC, Weng SL, Liao KW, Hsu WL, Huang HD. miRTarBase 2016: updates to the experimentally validated miRNA-target interactions database. Nucleic Acids Res. 2016, 4;44.
68. Perilli L, Vicentini C, Agostini M, Pizzini S, Pizzi M, D'Angelo E, Bortoluzzi S, Mandruzzato S, Mammano E, Rugge M, Nitti D, Scarpa A, Fassan M, Zanovello P. Circulating miR-182 is a biomarker of colorectal adenocarcinoma progression. Oncotarget. 2014;5(16):6611-9.
69. Sanz-Pamplona R, Berenguer A, Cordero D, Mollevi DG, Crous-Bou M, Sole X, Pare-Brunet L, Guino E, Salazar R, Santos C, de Oca J, Sanjuan X, Rodriguez-Moranta F, et al. Aberrant gene expression in mucosa adjacent to tumor reveals a molecular crosstalk in colon cancer. Molecular cancer. 2014; 13: 46-4598-13-46.
70. Raudenska M, Sztalmachova M, Gumulec J, Fojtu M, Polanska H, Balvan J, Feith M, Binkova H, Horakova Z, Kostrica R, Kizek R, Masarik M. Prognostic significance of the tumour-adjacent tissue in head and neck cancers. Tumour biology : the journal of the International Society for Oncodevelopmental Biology and Medicine. 2015; 36: 9929-9939.
71. Dambal S, Shah M, Mihelich B, Nonn L. The microRNA-183 cluster: the family that plays together stays together. Nucleic Acids Research. 2015;43(15):7173-7188. doi:10.1093/nar/gkv703.
72. Hayes J, Peruzzi PP, Lawler S. MicroRNAs in cancer: biomarkers, functions and therapy. Trends in molecular medicine, 2014; 20(8):460–469.
73. Cunningham D, Atkin W, Lenz HJ, Lynch HT, Minsky B, Nordlinger B and Starling N. Colorectal cancer. Lancet. 2010; 375(9719):1030-1047.
74. Price TJ, Segelov E, Burge M, Haller DG, Ackland SP, Tebbutt NC, Karapetis CS, Pavlakis N, Sobrero AF, Cunningham D and Shapiro JD. Current opinion on optimal

75. treatment for colorectal cancer. Expert Rev Anticancer Ther. 2013; 13(5):597-611.
76. Cancer Genome Atlas Network. Comprehensive molecular characterization of human colon and rectal cancer. Nature. 2012; 487(7407):330-337.
77. Tian F, Li R, Chen Z, et al. Differentially Expressed miRNAs in Tumor, Adjacent, and Normal Tissues of Lung Adenocarcinoma. *BioMed Research International*. 2016;2016:1428271.
78. Masters JR. Human cancer cell lines: fact and fantasy. Nat Rev Mol Cell Biol. 2000 Dec;1(3):233-6. Review.
79. Gerard I. Evan & Karen H. Vousden. Proliferation, cell cycle and apoptosis in cancer. Nature, 2001; 411, 342-348.
80. Hanahan D., Weinberg RA. The Hallmarks of cancer: the next generation. Cell, 2011; 144: 646-674.
81. Imam JS, Plyler JR, Bansal H, Prajapati S, Bansal S, Rebeles J, et al. Genomic Loss of Tumor Suppressor miRNA-204 Promotes Cancer Cell Migration and Invasion by Activating AKT/mTOR/Rac1 Signaling and Actin Reorganization. PLoS ONE, 2012; 7(12): e52397.
82. Huang J, Gong Z, Ghosal G, Chen J. SOSS Complexes Participate in the Maintenance of Genomic Stability. Molecular Cell, 2009; 35(3):384-393.
83. Zhang F, Ma T, Yu X. A core hSSB1–INTS complex participates in the DNA damage response. J Cell Sci 2013 126: 4850-4855.
84. Paysan L, Piquet L, Saltel F, Moreau V. Rnd3 in Cancer: A Review of the Evidence for Tumor Promoter or Suppressor. Mol Cancer Res November 1 2016 (14) (11) 1033-1044.
85. Bellanger JM, Astier C, Sardet C, Ohta Y, Stosse TP, Debant A. The Rac1- and RhoG-specific GEF domain of Trio targets filamin to remodel cytoskeletal actin. Nature Cell Biology 2000; 2, 888-892.

SUPPLEMENTARY

Supplementary Table 1: STR profiling of CRC cell lines. Description and comparation of CRC cell lines using a set of 16 STR markers. In the right, MICOL14$^{h\text{-}tert}$ and TC22 show the same STR profile. NA, not analyzed markers

	Caco2	HT29	MICOL14$^{h\text{-}tert}$	TC22
D3S1358	NA	NA	15	15
TH01	6	6-9	6-7	6-7
D21S11	30	29-30	29	29
D18S51	12	13-9.2	14	14
Penta E	NA	NA	9	9
D5S818	12-13	11-12	13	13
D13S317	13	11-12	12	12
D7S820	11-12	10	8-10	8-10
D16S539	12-13	11-12	9-13	9-13
CSF1PO	11	11-12	11	11
Penta D	NA	NA	13	13
AMEL	X	X	X	X
vWA	16-18	17-19	15-16	15-16
D8S1179	12	10-16	11	11
TPOX	9-11	8-9	8-13	8-13
FGA	19	20-22	20-23	20-23

Supplementary Figure 1. Unsupervised cluster analysis and expression profiles. The heatmap showed sample clustering and expression profiles of a subset of 12,323 transcripts selected according to expression level and variability across the 16 considered total samples (average expression value and coefficient of variation > median). M14, MICOL-14$^{h\text{-}tert}$; a182, anti-miR-182; aNC, anti-miR-NC.

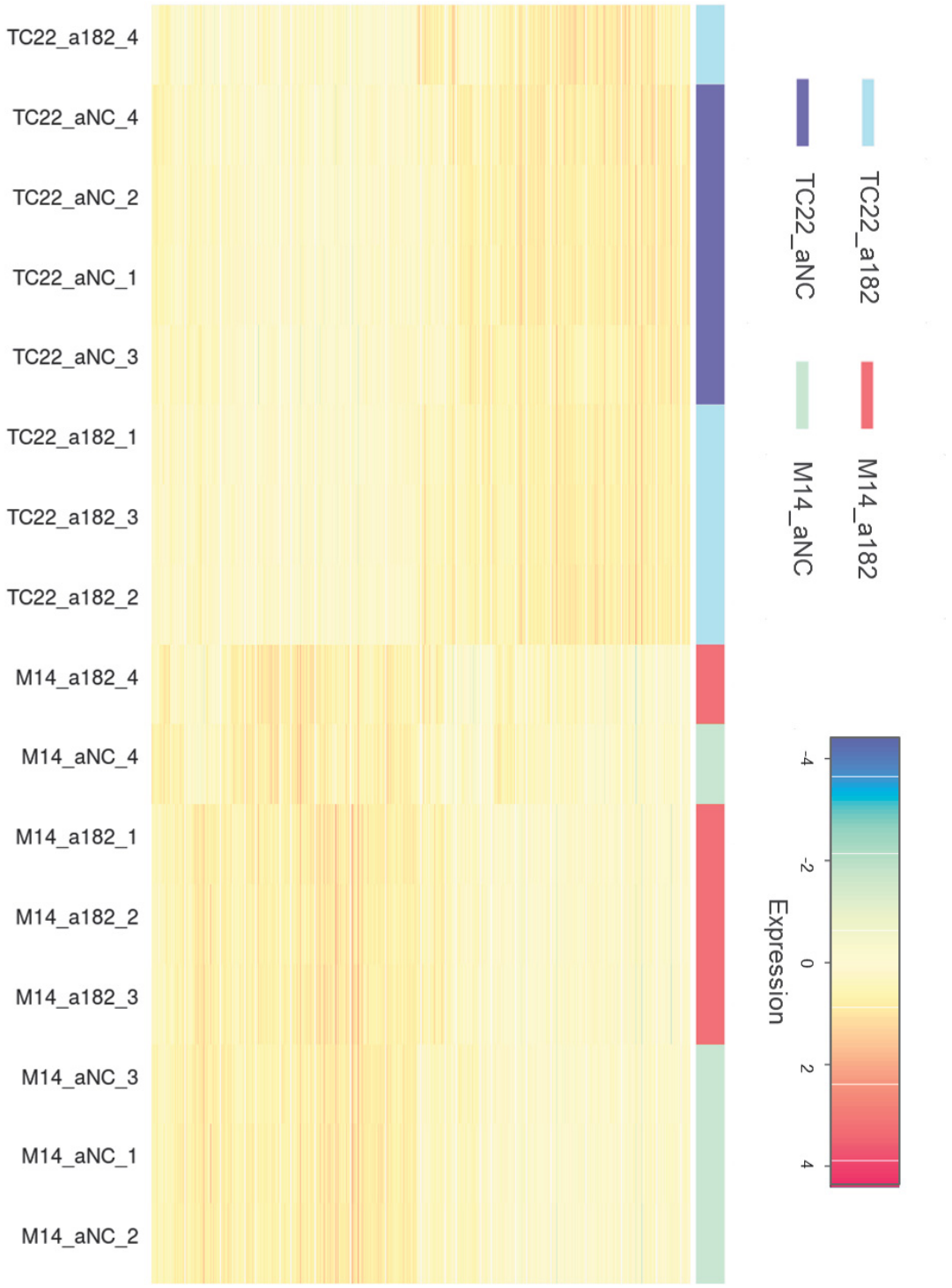

Supplementary Table 2. Gene Ontology (GO) functional terms, KEGG and Reactome pathways significantly enriched considering genes differentially expressed after miR-182 inhibition. Enriched terms, involved genes and fold-enrichment are showed separately for each cell line and considering only genes resulting differentially expressed after miR-182 inhibition in both cell line. BP, Biological Process; CC, Cellular Component; MF, Molecular Function.

DEG group	Functional category	Term/Pathway	Gene symbol	Genes	Fold Enrichment	Adjusted p-value
common (158)	GO BP	GO:0006355~ regulation of transcription, DNA-templated	ITGB3BP, EID3, SRSF10, EID2B, PPHLN1, ZNF557, SPTY2D1, NR3C1, ZNF638, ZNF655, ZNF165, ZFP36L1, SRRT, SFSWAP, ZNF181, ZNF226, HIF1A, PNRC2, THAP1, TCF3, NFIA, ZNF267, ZNF101	23	2.52	0.0270
		GO:0043065~ positive regulation of apoptotic process	ITGB3BP, HIF1A, SQSTM1, TRIO, GADD45B, VAV2, GADD45A, LATS1, BCL2L11, IP6K2, PHLDA1	11	5.21	0.0333
	GO CC	GO:0005634~ nucleus	ITGB3BP, TUBB2A, EID2B, CLK1, HIST2H4A, TCEAL1, CAMKK2, NFATC2IP, FUBP1, SFSWAP, CCNE1, ZNF181, BLZF1, CLK4, ANKRD11, NSMCE2, AKIRIN1, IP6K2, ZNF101, TIGD1, RELB, CCNL1, NABP1, HIF1A, MSANTD4, CUX1, GADD45B, GADD45A, SRSF10, SLF2, ZNF557, NR3C1, ZNF655, PXK, SESN2, TSPYL4, ZFP36L1, SFR1, VRK2, ZNF226, HIST1H4E, THAP1, TCF3, ZNF267, FKTN, TKT, ZNF165, RERG, CDKN1A, ATF3, ZBED4, PNRC2, RNPC3, PDCD6, PPP2R3C, NFIA	56	1.53	0.0202
		GO:0005654~ nucleoplasm	ITGB3BP, EID3, SRSF10, NR3C1, ZNF638, HIST2H4A, TCEAL1, FUBP1, CCNE1, SRRT, BLZF1, SQSTM1, ANKRD11, HIST1H4E, NSMCE2, AKIRIN1, TCF3, AKT3, IP6K2, NQO2, PPP4R3B, PPHLN1, RELB, TKT, TRNT1, NABP1, CDKN1A, ATF3, HIF1A, SMARCC1, MAPK9, RNPC3, SCAF8, CUX1, GADD45A, NFIA	36	1.94	0.0127
	GO MF	GO:0005515~ protein binding	ITGB3BP, TUBB2A, CLK1, HIST2H4A, LATS1, RSRC2, FUBP1, SFSWAP, CCNE1, BLZF1, CLK4, ARL14, RABGEF1, NSMCE2, AKIRIN1, AKT3, ZNF101, NQO2, IP6K2, RAP2A, TTC32, RELB, CCNL1, RBKS, CCT6A, C8ORF44-SGK3, MRM1, BCL2L11, NABP1, HIF1A, NUCB2, USO1, MAPK9, G0S2, MAPRE2, GADD45B, SCAF8, GADD45A, EID3, SRSF10, SLC38A9, SNX5, CALD1, SLF2, RPS15A, FAM122A, FKBP1A, NR3C1, C6ORF226, ZNF655, TSPYL4, PPCDC, SESN2, ZFC3H1, ZFP36L1, SRRT, SFR1, VRK2, C1ORF50, KLC1, SQSTM1, HIST1H4E, LETMD1, THAP1, TCF3, INPP5A, PHLDA1, CCNB1IP1, RBM12B, PPHLN1, ASXL1, TRIO, TKT, RCAN3, VAV2, SGTB, ATG3, RPL28, ZNF165, PPIF, CDKN1A, C1ORF116, ATF3, SMARCC1, PNRC2, ZBED4, RIT1, AGR2, PDCD6, ALG13, PPP2R3C	91	1.46	1.05E-05
	KEGG	hsa04068:FoxO signaling	CDKN1A, MAPK9, GADD45B, C8ORF44-SGK3, GADD45A, AKT3, BCL2L11	7	8.31	0.0185

		pathway				
		hsa04115:p53 signaling pathway	CCNE1, CDKN1A, GADD45B, SESN2, GADD45A	5	11.86	0.0434
MICOL-14$^{h\text{-}tert}$ (242)	GO BP	GO:0006355~ regulation of transcription, DNA-templated	ITGB3BP, EID3, SRSF10, EID2B, ZNF558, ZNF557, NR3C1, ZNF638, ZNF655, NOCT, ZFP36L1, SRRT, SFSWAP, ZNF181, ZNF226, THAP1, TCF3, ZNF267, ZNF101, L3MBTL4, ZBTB21, PPHLN1, SPTY2D1, ARNTL, DDIT3, ZNF165, HIF1A, PNRC2, NFIA	29	1.99	0.0453
	GO BP	GO:0043065~ positive regulation of apoptotic process	ITGB3BP, ABR, HIF1A, SQSTM1, MTCH1, TRIO, GADD45B, VAV2, GADD45A, LATS1, BCL2L11, IP6K2, PHLDA1	13	3.84	0.0141
	GO BP	GO:0006334~ nucleosome assembly	ITGB3BP, HIST4H4, HIST2H2BF, HIST1H3A, HIST1H4E, SPTY2D1, HIST2H4A, TSPYL4, HIST1H4I, HIST1H4J	10	6.58	9.85E-03
	GO BP	GO:0045815~ positive regulation of gene expression, epigenetic	HIST4H4, HIST1H3A, HIST1H4E, HIST2H4A, HIST1H4I, HIST1H4J	6	8.54	0.0469
	GO BP	GO:0006303~ double-strand break repair via nonhomologous end joining	HIST4H4, HIST1H4E, NSMCE2, HIST2H4A, HIST1H4I, HIST1H4J	6	8.4	0.0469
	GO BP	GO:0000183~ chromatin silencing at rDNA	HIST4H4, HIST1H3A, HIST1H4E, HIST2H4A, HIST1H4I, HIST1H4J	6	12.91	0.0109
	GO BP	GO:0034080~ CENP-A containing nucleosome assembly	ITGB3BP, HIST4H4, HIST1H4E, HIST2H4A, HIST1H4I, HIST1H4J	6	12.61	0.0109
	GO BP	GO:0032200~ telomere organization	HIST4H4, HIST1H3A, HIST1H4E, HIST2H4A, HIST1H4I, HIST1H4J	6	19.61	0.0107
	GO BP	GO:0051290~ protein heterotetramerization	HIST4H4, HIST1H3A, HIST1H4E, HIST2H4A, HIST1H4I, HIST1H4J	6	13.93	8.57E-03
	GO BP	GO:0032776~ DNA	HIST4H4, HIST1H3A, HIST1H4E, HIST2H4A, HIST1H4I, HIST1H4J	6	15.57	6.90E-03

	methylation on cytosine				
GO BP	GO:0006335~ DNA replication-dependent nucleosome assembly	HIST4H4, HIST1H3A, HIST1H4E, HIST2H4A, HIST1H4I, HIST1H4J	6	16.54	6.36E-03
GO BP	GO:0006336~ DNA replication-independent nucleosome assembly	HIST4H4, HIST1H4E, HIST2H4A, HIST1H4I, HIST1H4J	5	16.97	0.0163
GO BP	GO:0035574~ histone H4-K20 demethylation	HIST4H4, HIST1H4E, HIST2H4A, HIST1H4I, HIST1H4J	5	27.57	7.99E-03
GO BP	GO:0045653~ negative regulation of megakaryocyte differentiation	HIST4H4, HIST1H4E, HIST2H4A, HIST1H4I, HIST1H4J	5	24.51	6.61E-03
GO CC	GO:0005634~ nucleus	ITGB3BP, CYP24A1, HIST4H4, EID2B, TUBB2A, RBM3, CLK1, HIST2H4A, TCEAL1, DGCR14, NOCT, CAMKK2, FUBP1, NFATC2IP, SFSWAP, CCNE1, ZNF181, BLZF1, CLK4, ANKRD11, C8ORF4, NSMCE2, SMOX, NFIL3, AKIRIN1, ZNF101, IP6K2, L3MBTL4, ZBTB21, TIGD1, RELB, CCNL1, ARNTL, MXD3, DDIT3, NABP1, HIF1A, HIST2H2BF, MSANTD4, GADD45B, CUX1, GADD45A, CAMTA2, ZNF552, SRSF10, ZNF558, ZNF557, SLF2, TRA2A, TRIB3, NR3C1, ZNF655, PXK, TSPYL4, ZNF177, SESN2, CCNG1, ZFP36L1, SFR1, VRK2, ZNF226, HNRNPF, HIST1H4E, NDRG1, THAP1, HIST1H4I, HIST1H4J, TCF3, ZNF267, FKTN, RECQL5, KLF10, ZMYM5, JRKL, TKT, TRIM23, SNAI2, ZNF165, RERG, CDKN1A, ATF3, PNRC2, ZBED4, HIST1H3A, IRF1, RNPC3, PDCD6, CARNMT1, NFIA, PPP2R3C	90	1.57	1.62E-04
GO CC	GO:0005654~ nucleoplasm	ITGB3BP, CYP24A1, HIST4H4, RBM3, ZNF638, HIST2H4A, TCEAL1, NOCT, FUBP1, CCNE1, BLZF1, INTS6, ANKRD11, NSMCE2, AKIRIN1, AKT3, IP6K2, NQO2, RELB, ARNTL, DDIT3, NABP1, HIF1A, HIST2H2BF, MAPK9, CCDC174, CUX1, SCAF8, GADD45A, EID3, SRSF10, TRIB3, PPP6R3, NR3C1, SRRT, SQSTM1, HNRNPF, HIST1H4E, HIST1H4I, TCF3, HIST1H4J, PPP4R3B, RECQL5, PPHLN1, TKT, TRNT1, CDKN1A, ATF3, CHML, SMARCC1, HIST1H3A, IRF1, RNPC3, EAF2, RBM14, NFIA	56	1.94	8.36E-05
GO CC	GO:0000786~	HIST4H4, HIST1H3A, HIST1H4E, H2AFJ,	7	7.04	0.0209

	nucleosome	HIST2H4A, HIST1H4I, HIST1H4J			
GO CC	GO:0000228~nuclear chromosome	HIST4H4, HIST1H3A, HIST1H4E, HIST2H4A, HIST1H4I, HIST1H4J	6	10.84	0.0129
GO MF	GO:0005515~protein binding	ITGB3BP, TUBB2A, RBM3, CLK1, MAGEC1, SFSWAP, CLK4, ARL14, INTS6, C8ORF4, RABGEF1, C9ORF43, AKIRIN1, FNDC3B, NQO2, ZNF101, L3MBTL4, RELB, SOCS4, RBKS, ARNTL, MRM1, DDIT3, BCL2L11, NABP1, HIF1A, USO1, MAPK9, SCAF8, TRAF1, CAMTA2, EID3, SRSF10, CACUL1, SLC38A9, SNX5, NFKBIE, SLF2, FAM122A, C6ORF226, PPCDC, TIMP2, SESN2, CCNG1, ZFC3H1, GFM2, VRK2, C1ORF50, HNRNPF, MTCH1, HIST1H4E, NDRG1, LETMD1, HIST1H4I, HIST1H4J, TCF3, RBM12B, KLF10, ASXL1, ZMYM5, TRIO, TKT, VAV2, ATG3, PPIF, CDKN1A, C1ORF116, ATF3, PNRC2, SMARCC1, HIST1H3A, MAP4, RIT1, EAF2, AGR2, PDCD6, ALG13, PPP2R3C, HIST4H4, ANKRD10, HIST2H4A, LATS1, DGCR14, RSRC2, FUBP1, CCNE1, BLZF1, NSMCE2, NFIL3, AKT3, IP6K2, RAP2A, TTC32, ZBTB21, CCNL1, CCT6A, C8ORF44-SGK3, MXD3, NUCB2, G0S2, MAPRE2, GADD45B, GADD45A, MAP3K13, CALD1, RPS15A, TRIB3, C1R, PPP6R3, FKBP1A, NR3C1, ZNF655, SPRR2E, TSPYL4, ZNF177, FAM46B, ZFP36L1, SRRT, SFR1, KLC1, SQSTM1, THAP1, INPP5A, PHLDA1, CCNB1IP1, PPHLN1, TECPR2, TRIM23, SNAI2, RCAN3, SGTB, TAB2, RPL28, ZNF165, ZBED4, IRF1, RBM14	137	1.36	2.04E-05
GO MF	GO:0003677~DNA binding	HIST4H4, ZNF558, ZNF557, ZNF655, HIST2H4A, ZNF177, ZFP36L1, SRRT, BLZF1, ZNF181, ZNF226, RABGEF1, HIST1H4E, NFIL3, HIST1H4I, TCF3, HIST1H4J, ZNF267, ZNF101, TIGD1, ASXL1, SPTY2D1, JRKL, H2AFJ, ARNTL, MXD3, DDIT3, HIST2H2BF, ZBED4, HIST1H3A, NUCB2, IRF1	32	1.9	0.0472
GO MF	GO:0046982~protein heterodimerization activity	HIST4H4, SNX5, ARNTL, H2AFJ, HIST2H4A, DDIT3, ATF3, HIF1A, HIST2H2BF, HIST1H3A, HIST1H4E, ENO3, HIST1H4I, HIST1H4J, TCF3	15	2.73	0.0488
GO MF	GO:0035575~histone demethylase activity (H4-K20 specific)	HIST4H4, HIST1H4E, HIST2H4A, HIST1H4I, HIST1H4J	5	26.97	3.43E-03
KEGG	hsa05203:Viral carcinogenesis	TRAF1, CCNE1, NRAS, CDKN1A, HIST4H4, HIST2H2BF, HIST1H4E, HIST2H4A, HIST1H4I, HIST1H4J	10	4.8	8.64E-03
KEGG	hsa05034:Alcoholism	NRAS, HIST4H4, HIST2H2BF, HIST1H3A, HIST1H4E, H2AFJ, HIST2H4A, HIST1H4I, HIST1H4J, CAMKK2	10	5.56	4.20E-03
KEGG	hsa05322:Sy	HIST4H4, HIST2H2BF, HIST1H3A, HIST1H4E,	9	6.61	7.18E-03

	stemic lupus erythematosus	C1R, H2AFJ, HIST2H4A, HIST1H4I, HIST1H4J			
KEGG	hsa04068:FoxO signaling pathway	NRAS, CDKN1A, MAPK9, GADD45B, C8ORF44-SGK3, GADD45A, AKT3, BCL2L11	8	5.97	0.0114
KEGG	hsa04115:p53 signaling pathway	CCNE1, CDKN1A, GADD45B, CCNG1, SESN2, GADD45A	6	8.95	0.0136
REACTOME	R-HSA-3214847: HATs acetylate histones	HIST4H4, HIST2H2BF, HIST1H3A, HIST1H4E, HIST2H4A, HIST1H4I, HIST1H4J	7	4.64	0.0457
REACTOME	R-HSA-2559580: Oxidative Stress Induced Senescence	HIST4H4, HIST1H3A, HIST1H4E, MAPK9, HIST2H4A, HIST1H4I, HIST1H4J	7	5.35	0.0327
REACTOME	R-HSA-3214815	HIST4H4, HIST2H2BF, HIST1H3A, HIST1H4E, HIST2H4A, HIST1H4I, HIST1H4J	7	7	0.0260
REACTOME	R-HSA-2559582: Senescence-Associated Secretory Phenotype (SASP)	CDKN1A, HIST4H4, HIST1H3A, HIST1H4E, HIST2H4A, HIST1H4I, HIST1H4J	7	5.98	0.0218
REACTOME	R-HSA-3214858	HIST4H4, SMARCC1, HIST1H3A, HIST1H4E, HIST2H4A, HIST1H4I, HIST1H4J	7	8.78	0.0152
REACTOME	R-HSA-2559586: DNA Damage/Telomere Stress Induced Senescence	CCNE1, CDKN1A, HIST4H4, HIST1H4E, HIST2H4A, HIST1H4I, HIST1H4J	7	9.97	0.0148
REACTOME	R-HSA-977225	HIST4H4, HIST1H3A, HIST1H4E, HIST2H4A, HIST1H4I, HIST1H4J	6	5.88	0.0430
REACTOME	R-HSA-5250924	HIST4H4, HIST1H3A, HIST1H4E, HIST2H4A, HIST1H4I, HIST1H4J	6	6.2	0.0362
REACTOME	R-HSA-73777	HIST4H4, HIST1H3A, HIST1H4E, HIST2H4A, HIST1H4I, HIST1H4J	6	6.2	0.0362
REACTOME	R-HSA-912446	HIST4H4, HIST1H3A, HIST1H4E, HIST2H4A, HIST1H4I, HIST1H4J	6	6.49	0.0337

	REACTOME	R-HSA-201722	HIST4H4, HIST1H3A, HIST1H4E, HIST2H4A, HIST1H4I, HIST1H4J	6	6.41	0.0332
	REACTOME	R-HSA-73728	HIST4H4, HIST1H3A, HIST1H4E, HIST2H4A, HIST1H4I, HIST1H4J	6	8.96	0.0235
	REACTOME	R-HSA-212300	HIST4H4, HIST1H3A, HIST1H4E, HIST2H4A, HIST1H4I, HIST1H4J	6	7.73	0.0232
	REACTOME	R-HSA-3214841	HIST4H4, HIST1H3A, HIST1H4E, HIST2H4A, HIST1H4I, HIST1H4J	6	8.82	0.0211
	REACTOME	R-HSA-606279	ITGB3BP, HIST4H4, HIST1H4E, HIST2H4A, HIST1H4I, HIST1H4J	6	7.63	0.0206
	REACTOME	R-HSA-2299718	HIST4H4, HIST1H3A, HIST1H4E, HIST2H4A, HIST1H4I, HIST1H4J	6	7.63	0.0206
	REACTOME	R-HSA-5625886	HIST4H4, HIST1H3A, HIST1H4E, HIST2H4A, HIST1H4I, HIST1H4J	6	8.42	0.0196
	REACTOME	R-HSA-5334118	HIST4H4, HIST1H3A, HIST1H4E, HIST2H4A, HIST1H4I, HIST1H4J	6	8.68	0.0195
	REACTOME	R-HSA-427359	HIST4H4, HIST1H3A, HIST1H4E, HIST2H4A, HIST1H4I, HIST1H4J	6	8.3	0.0187
	REACTOME	R-HSA-3214842	HIST4H4, HIST1H3A, HIST1H4E, HIST2H4A, HIST1H4I, HIST1H4J	6	11.76	0.0109
	REACTOME	R-HSA-69473	HIST4H4, HIST1H4E, HIST2H4A, HIST1H4I, HIST1H4J	5	7.71	0.0441
	REACTOME	R-HSA-171306	HIST4H4, HIST1H4E, HIST2H4A, HIST1H4I, HIST1H4J	5	9.04	0.0352
TC22 (1383)	GO BP	GO:0000278~mitotic cell cycle	ITGB3BP, CEP72, E2F3, CEP78, NUP188, FER, HIST2H4A, MCM10, CCNE2, CCNE1, BLZF1, RAE1, CDKN2C, ORC5, MASTL, TPR, TOP2A, CCNA2, ORC3, CDK1, DSN1, ESPL1, OPTN, NUPL2, ESCO2, CDK2, RFC5, FGFR1OP, NSL1, RRM2, USO1, BUB1B, NUP43, ANAPC16, USP3, POLA1, AZI2, NDC1, TYMS, TUBGCP3, TUBGCP5, POLE2, NCAPG, HIST1H4E, FBXO5, FBXW11, FEN1, ERCC6L, CENPO, RAB2A, GINS1, CENPN, PDS5B, KIF18A, CDC23, CASC5, NDC80, CENPE, BIRC5, SMC2, CENPI, CDC25A, SMC3, SMC4, PLK4, CDKN1A, PSMC4, PSMD12, CENPU, SMC1A	70	2.33	2.03E-07
	GO BP	GO:0006281~DNA repair	COPS2, CLSPN, RAD51C, NBN, HIST2H4A, BOD1L1, FANCI, H2AFX, CDK1, DTL, UFD1L, USP1, LIG3, TOPBP1, MBD4, POLB, RAD52, RMI1, CDK2, RFC5, UBE2N, NABP1, XPC, FANCD2, UBE2W, GADD45A, PPP4R2, EID3, BLM, USP3, POLR2K, SLF2, SLF1, KIAA0101, POLA1, CHEK1, FAAP20, SUMO3, ERCC8, POLE2, HIST1H4E, TCEA1, ACTL6A, RCHY1, FEN1, ERCC2, EXO1, RAD51AP1, MSH2, BRIP1, WHSC1, RAD54L, BRCA1, SMC3, ATRX, PARPBP, BRE, ZRANB3, CUL4B, SMC1A,	61	2.28	2.82E-06

			ALKBH3			
	GO BP	GO:0051301~ cell division	ITGB3BP, SENP5, LATS1, CCNE2, CCNE1, CCSAP, NSMCE2, MASTL, TPR, CCNA2, KIF14, CDK1, KIF11, DSN1, LIG3, HMGA2, CDK2, TACC1, CHMP1B, SYCP3, NSL1, MCMBP, BUB1B, MAPRE2, ARL8B, NUP43, SEPT9, ANAPC16, HAUS6, MPLKIP, USP9X, NCAPG, FBXO5, TNKS, NSUN2, HELLS, ERCC6L, CSNK1A1, PARD6B, PDS5B, CDC23, CASC5, NDC80, BIRC5, CENPE, SMC2, CDC25A, SMC3, SMC4, ANXA11, CENPV, KIF20B, BRE, MIS18BP1, SMC1A	55	2.41	4.23E-06
	GO BP	GO:0007067~ mitotic nuclear division	ITGB3BP, ANAPC16, HAUS6, MPLKIP, USP9X, LATS1, CCSAP, NSMCE2, TNKS, MASTL, TPR, NSUN2, CCNA2, HELLS, ASPM, ERCC6L, CSNK1A1, CDK1, CENPN, KIF11, DSN1, KIF15, CDC23, CASC5, NDC80, BIRC5, GEM, HMGA2, CDK2, CDC25A, SMC3, SYCP3, NSL1, MCMBP, BRE, KIF20B, CENPV, BUB1B, MAPRE2, MIS18BP1, NUP43	41	2.41	2.30E-04
	GO BP	GO:0000724~ double-strand break repair via homologous recombination	CLSPN, RAD51C, NBN, PPP4R2, BLM, CHEK1, HIST2H4A, SFR1, HIST1H4E, NSMCE2, H2AFX, FEN1, EXO1, RAD51AP1, YY1, LIG3, ZSWIM7, BRIP1, WHSC1, TOPBP1, RAD52, RAD54L, RMI1, BRCA1, CDK2, UBE2N, RFC5, NABP1, SFPQ, BRE	30	3.03	1.12E-04
	GO BP	GO:0006302~ double-strand break repair	CLSPN, RAD51C, NBN, PPP4R2, BLM, KIAA0430, CHEK1, HIST2H4A, HIST1H4E, H2AFX, FEN1, TRIP13, EXO1, RAD51AP1, MSH2, LIG3, BRIP1, WHSC1, TOPBP1, RAD52, RMI1, ESCO2, BRCA1, CDK2, UBE2N, RFC5, BRE	27	2.54	7.58E-03
	GO BP	GO:0006260~ DNA replication	CLSPN, KIAA0101, NAP1L1, POLA1, CHEK1, MCM10, TOP1, POLE2, ORC5, FEN1, RBMS1, ORC3, CDK1, DTL, RMI1, RBBP6, CDK2, BRCA1, CDC25A, RFC5, RRM2, TBRG1, NFIC, NFIA, DUT	25	2.71	6.20E-03
	GO BP	GO:0016925~ protein sumoylation	EID3, BLM, ZNF451, SAE1, BIRC5, NUP188, RAD52, SENP5, NUPL2, SMC3, BRCA1, NFATC2IP, NDC1, SUMO3, PHC3, TOP1, XPC, RAE1, NSMCE2, TPR, SMC1A, TOP2A, NUP43	23	2.87	7.01E-03
	GO BP	GO:0007059~ chromosome segregation	CENPN, KIF11, DSN1, USP9X, NDC80, BIRC5, CENPE, BRCA1, ESCO2, CIAO1, TOP1, NSL1, ARL8B, BRD4, TOP2A, NUP43, ERCC2	17	3.31	0.0139
	GO BP	GO:0007095~ mitotic G2 DNA damage checkpoint	CDK1, NBN, BLM, FANCI, SYF2, HMGA2, CCNA2	7	7.66	0.0444

	GO CC	GO:0005737~ cytoplasm	TUBB2A, NAA15, NAA16, STRN, PNISR, CLK1, ZNF638, SART3, CDCA7, HIST1H2BN, RAE1, CCNA2, PLS3, KRR1, IKBKAP, MAGI2, ZHX2, ESPL1, MECOM, RPTOR, ERGIC2, DCAF7, PTRF, MAPK6, KIAA1524, ARL8B, CRTC2, ACP6, NTAN1, UBA5, BCL2L1, ACP1, NAA35, PDSS2, ADAP1, SH3BP5L, RILPL1, RAC1, RCHY1, C19ORF24, TCF3, RANBP17, ZC3H15, MKI67, ACACA, GARS, FNIP1, FNIP2, UPF3A, SRSF3, SRSF5, AIDA, WDR61, PARPBP, PKP4, CDC42BPA, TGFBR3, PPP2R3C, SRSF1, CREBRF, HSF2, EEF2K, ANP32A, EPG5, MASTL, BRD4, TARSL2, USP15, ATF7IP, RAP2C, ERLIN2, KIAA0586, CCT6A, RFTN1, FMN1, PJA2, FANCD2, RRM2, OSBPL10, TXK, ZNF480, USP24, ARL4A, SRGAP2, SNAP29, EXOC8, POLA1, EPB41L4A, ERI1, ZNF655, MTMR2, SRRT, LRRTM4, DGKE, MTMR9, PER3, SNAP23, ACSL4, ZNF263, HIST1H2BD, PPHLN1, NUCKS1, HIST1H2BG, ATRN, CAPN2, APPL2, RPL28, MID2, RPS6KA3, DUSP3, RPL22, GSK3B, SFPQ, DYM, USP48, MPHOSPH6, KATNAL1, MPHOSPH8, SRP14, METTL21B, AP1G1, EIF5, RBM4, STYX, IL11, ATAT1, CDKN2C, DNAJC9, BPNT1, ASPM, EGFR, BCL10, RBFOX2, TWF1, RELB, RPS6KC1, TOPBP1, FADD, PKIA, TACC1, NABP1, HIF1A, HSPB8, STMN1, ACTBL2, EID1, ARFGAP3, MPLKIP, EID3, STAM2, SLF1, NHS, SESN2, AZI2, AKT1S1, PTK6, PRKRA, GMPPA, FBXW2, RPL4, ARHGDIB, ERCC6L, GINS1, PHACTR4, BRIP1, WHSC1, WIPI1, SAFB2, PRKAR1A, LVRN, ZNF318, FBXO32, HSPD1, CYB5R3, E2F3, GPBP1, ALG2, ANO1, DICER1, RPRM, FER, NBPF1, CASP8, LRWD1, CNTLN, KDM5B, CASP2, NFX1, CDK1, ARL1, DENND6A, KIF11, NUSAP1, IRF2BP2, ZFR, CHAMP1, CDK2, SDC1, TRNAU1AP, FAM120A, DDT, MAPRE2, EMC2, SNX19, HYPK, SLC7A6OS, HAUS6, HYLS1, GDAP1, RPS15A, NR3C1, NDC1, TSC22D1, CHD9, NSUN2, PPP4R3B, EXO1, WDFY3, BBOF1, NF1, RCAN1, RCAN3, ANXA5, UBE2Q2, SMC2, ANXA3, SMC3, SMC4, INVS, ZBED4, AKR1B1, JAK2, CUL4B, ALKBH3, ITGB3BP, RAB3GAP2, RAD51C, TMEM18, DZIP3, ALOXE3, PDLIM7, PTPN21, AQP7, HOOK3, G2E3, CD44, WWP2, RAB23, EIF2B2, YY1, WNK1, KRT10, POLB, OPTN, FARP1, TANK, CEP350, CDCA7L, EPS8L2, COASY, SRSF10, IGF2BP2, AFAP1L1, PXK, TIPRL, VRK2, AGGF1, HOXA10, FBXO5, KLF5, MSTO1, SMYD3, NDFIP2, SMYD2, NOTCH3, FAM101B, RNF7, C1ORF116, CCT8, GRK5, CLSPN, COPS2, WASF3, CPEB2, FERMT2, VPS37A, SHOC2, CAMKK2, PARN, BLZF1, FANCI, ANKRD11, AGAP1, FAM129A, CEP112, RBM44, DSN1, HERC6, MBD1, RBBP6, DNAJC24, FCRLB, GADD45B, GADD45A, PLEK2, USP3, CEP126, PPFIA1, FKBP1A, CEP128, MLF1, PLCL2, SUMO3, GALK2, STK40, SQSTM1, NCAPG, DTNB, KIF21A, SPATA5, MLLT4, RBM25, PLEC, UBXN1, BIRC5, HNRNPDL, RAPH1, COG3, PAPOLA, C4ORF46, SLC16A7, PSMD12, PYGL, KIF20B, APBB2, ATP6V0A2, CALM1, STIL, ZC3HAV1, EIF5B, PI4K2B, MCM10, SMNDC1, GSTM3, MCOLN3, ZNF185, ORC5, MLKL,	462	1.4	1.67E-15

			PDRG1, CUTC, NQO2, CEP89, DTL, RRP8, NUPL2, CDKL3, STK4, ELL2, PTHLH, TNS3, MCMBP, SLU7, RIPK4, CSNK1G3, DST, MAP7D3, SEPT9, ANAPC16, ZFAND5, BLM, PNPT1, SOX4, SNX4, CMPK1, RASAL2, BLOC1S4, CSE1L, MFAP3L, STRBP, RNF14, CFLAR, PARD6B, GABARAPL2, RPGRIP1L, CASC5, BRCA1, RIMKLB, UACA, PSMC4, SLAIN2, ITGA7, WDR4, CPNE3, TMPO, FPGS, SMC1A, PDCD6, C9ORF72, HECW2, CEP57L1, PDCD2, NFATC2IP, SLK, MAPKAP1, TPP2, TPR, PPP1R14C, AKT3, ELP2, RABL6, PROSC, CAMSAP3, UBE2H, TBCEL, ECT2, RTTN, DAPK1, UBE2N, LAP3, AMH, LARP6, XPC, UBE2K, BTG1, KRIT1, COMMD3, BUB1B, UBE2W, PRKCZ, PPP4R2, USP9X, NANOS1, KIAA0101, ZNF706, DDTL, TYMS, TUBGCP3, MOAP1, TUBGCP5, NPAS3, SPRR2D, POU2F3, ENO3, ERCC2, TXNIP, ICA1, DNM1L, MAP1B, RUFY1, KIF18A, MTL5, CENPE, CENPI, MON2, UBL5, SLC17A5, CEP68, SP4, ANXA11, BRE, CENPV, ACTR10			

	GO CC	GO:0005634~nucleus	TUBB2A, RPL15, NAA15, NAA16, CLK1, SART3, CDCA7, HIST1H2BN, CLK3, RAE1, CLK4, PATZ1, OGT, TIGD7, CCNA2, CDCA4, LUC7L3, ZNF101, KRR1, MAGI2, RCOR3, ZNF644, TIGD1, PIK3CB, ZNF48, LIG3, ZHX2, ZNF502, ESPL1, GEM, MECOM, ERGIC2, PTRF, MAPK6, JUN, TRAPPC2, CRTC2, ZNF611, ZNF79, ZSCAN5A, NTAN1, UBA5, PUS7, ADAP1, HESX1, ZNF226, RAC1, RCHY1, TCF3, NAT14, UNC45A, MKI67, PIBF1, NDC80, GCFC2, UPF3A, RERG, ZNF215, SRSF5, WDR61, PPP2R3C, SRSF1, ELF1, ZNF532, U2SURP, NAP1L1, ZNF347, CCNE1, HSF2, ANP32A, MASTL, BRD4, USP15, ATF7IP, MICAL2, ZSWIM7, ZNF138, FMN1, ZNF134, FANCD2, RRM2, GNB5, TXK, ZNF33B, CLOCK, ARL4A, SRGAP2, ZNF557, HIST1H2AE, POLA1, ERI1, NUFIP1, ZNF367, ZNF655, MYCBP2, MTMR2, ZNF169, SF3B1, SFR1, TCEA1, ZNF750, PER3, FBXW11, FEN1, TRIP13, ZNF267, ZNF263, SPATA33, ZNF566, HIST1H2BD, ZNF28, NUB1, NUCKS1, SWAP70, ZNF771, HIST1H2BG, CS, ZNF770, PHF10, CAPN2, APPL2, ZNF165, ATRX, DUSP3, RPL22, GSK3B, SFPQ, SYF2, ZNF461, MPHOSPH6, MPHOSPH8, AKNA, SRP14, ZNF580, EIF5, RBM4, STYX, ZNF451, TCEAL1, TCEAL4, CDKN2C, DNAJC9, ZNF302, CTDSP1, ASPM, MTUS1, EGFR, BCL10, RBFOX2, DFFB, NEIL3, RELB, TOPBP1, GRHL2, RMI1, PKIA, TACC1, NABP1, DCUN1D1, HIF1A, SYCP3, PRCC, HSPB8, ZNF586, HMGB1, EID1, CNBP, MPLKIP, BBS7, SLF2, SLF1, DSCR3, SESN2, ATF1, EPM2AIP1, TCERG1, PTK6, HIST1H4E, RPL4, HELLS, GINS1, FKTN, FOXA1, BRIP1, WHSC1, SPRYD4, CDKN1A, ATF3, EAF1, ZNF317, PNRC2, DNAJB2, RNPC3, HIST1H3E, NBN, GPBP1, ALG2, DICER1, E2F8, SLFN5, FER, MBP, PRMT7, LRWD1, CASP2, KDM5B, NFX1, KIF14, CDK1, CCNL1, NUSAP1, IRF2BP2, HMGA2, CHAMP1, CDK2, TMEM38B, TRNAU1AP, FAM120A, NSL1, TXNRD1, EMC2, UGP2, SNX10, KDM6B, SLC7A6OS, HYLS1, GDAP1, DCK, NR3C1, TSPYL4, TSC22D1, CHD9, TFAM, CHD2, VPS36, NSUN2, HSPA8, EXO1, NCDN, NF1, RCAN1, ANXA5, SMC2, SMC3, SMC4, INVS, ZBED4, ZRANB2, JAK2, ZRANB3, ALKBH3, SCAND1, ITGB3BP, RAD51C, PDLIM7, SLC35A2, ATP2B1, SFSWAP, N4BP2L2, H2AFV, WWP2, CREB3L2, H2AFX, FAM103A1, PAN2, YY1, KRT10, POLB, OPTN, ESCO2, TBRG1, CDCA7L, SRSF10, SRSF11, CHEK1, IGF2BP2, AFAP1L1, PXK, VRK2, HOXA10, FBXO5, TCF25, IKZF5, PELI1, TKT, SMYD2, NOP10, RAD54L, NOTCH2, RNF7, GRK5, NCOR1, CPEB2, EID2B, FERMT2, SOBP, SHOC2, SENP5, ARL2BP, CAMKK2, PARN, BLZF1, ANKRD11, NSMCE2, TOP2A, IP6K2, CTBP2, DSN1, UFD1L, HERC6, SF1, MBD4, FAM76B, FAM76A, RAD52, MBD1, ZCCHC17, GADD45B, GADD45A, MECR, USP3, POLR2K, LARP1B, MLF1, SUMO3, ZFP36L1, NCAPG, THAP1, ACTL6A, RAB2A, UBXN1, PDS5B, BIRC5, HNRNPDL, PAPOLA, SLC50A1, KIF20B, APBB2, CALM1, ZC3HAV1, EIF5B, SAE1, PMAIP1, MCM10, CBX5, SMNDC1, TOP1, ZNF181, GSTM3, ORC5, LOX, ATOH7, AKIRIN1, CUTC, RBMS1, DTL, USP1, TOR1AIP1, RRP8,	454	1.31	1.49E-09

			NUPL2, STK4, ZNF197, FGFR1OP, MCMBP, SLU7, AKAP7, DST, MAP7D3, CAV2, BLM, SOX4, SOX6, CMPK1, CSE1L, MTCH2, C12ORF10, MFAP3L, STRBP, SSX2IP, SLC30A9, RNF14, MAFG, PARD6B, CSTF3, CSTF2, KCTD1, ATAD2, CASC5, HEATR1, BRCA1, PRICKLE4, UACA, PSMC4, WDR4, CPNE3, TMPO, SMC1A, PDCD6, DUT, C9ORF72, ARHGAP19, HIST2H4A, PDCD2, NFATC2IP, PHC3, FUBP1, RANBP9, MAPKAP1, TPP2, SETMAR, CDK12, TPR, RABL6, ZNF92, ECT2, UBE2N, LAP3, LARP6, XPC, UBE2K, BTG1, COMMD3, UBE2W, MSANTD4, CUX1, SUPT3H, PPP4R2, KIAA0101, ZNF706, TYMS, ERCC8, NPAS2, POU2F3, ERCC2, TXNIP, DLST, KAT2B, RAD51AP1, RUFY1, KIF18A, MTL5, CENPE, CENPI, RALGDS, UBL5, ADNP2, CEP68, SP4, BRE, CENPV, CENPU, NFIC, NFIA, ZBTB8A			
	GO CC	GO:0005829~cytosol	ITGB3BP, MOCOS, EHHADH, RPL15, LPAR1, TPK1, CUL3, COL4A3BP, PIK3CA, DEPDC1B, OGT, EIF2B2, PAN2, PAN3, PIK3CB, MYH3, NUDT15, ESPL1, VPS41, OPTN, MECOM, FARP1, RPTOR, BCL2L11, TANK, PGM2, PGM3, PTRF, MAPK6, JUN, PUDP, MAPK9, NUP43, TRAPPC2, PFKFB4, UBA5, IGF2BP2, BCL2L2, CHEK1, BCL2L1, PPCDC, RIC1, EPHB2, TK1, GPD1L, NPHP3, RILPL1, STX17, RAC1, CDA, FBXO5, TNKS, AMD1, PELI1, OSBPL3, TGFBR2, GARS, ACACA, TRIO, CDC23, GAS2, NDC80, TKT, SMYD2, GART, NOTCH3, UPF3A, RERG, RPE, CCT8, SH3RF1, ENOX2, UBE2G2, FERMT2, LATS1, ARL2BP, CCNE2, CCNE1, PARN, AASDHPPT, FXN, EEF2K, ARHGAP11A, RAP2A, PRTFDC1, RAP2C, DSN1, POLR1D, UFD1L, RAB4A, HERC6, CCT6A, C8ORF44-SGK3, ARHGEF10, CHMP1B, PAPD4, MB21D1, SERPINB8, RRM2, EIF4A2, PSEN2, GNB5, THEM4, PARVA, SRGAP2, SERP1, BID, ATG10, LIMS1, SORD, EXOC7, EXOC8, POLR2K, PPFIA1, RPL27A, UROS, RPL37, FKBP1A, ZFP36L1, MTMR2, RPL32, KLC1, SQSTM1, NCAPG, CHM, FBXW11, MLLT4, PLEC, CSNK1A1, UBXN1, SPATA33, SLC8A1, PDS5B, SWAP70, BIRC5, CAPN2, RPL28, MSRB3, RPS6KA3, DUSP3,	311	1.41	3.15E-09

			PSMD12, RPL22, PYGL, GSK3B, GFPT1, NLN, PAICS, CALM1, SRP14, CEP72, STIL, OCLN, AP1G1, EIF5, CEP78, F2RL1, STYX, EIF5B, SAE1, PMAIP1, PI4K2B, VCL, GSTM3, ATAT1, CDKN2C, SLC2A1, MLKL, BPNT1, BCL10, CEP89, DFFB, RELB, CORO7, FADD, NUPL2, CDO1, STK4, TNNT3, HIF1A, FGFR1OP, NBR1, USO1, AKAP7, STMN1, DST, CHMP2A, ANAPC16, HMGB1, CNBP, ARFGAP3, BBS7, DIAPH2, STAM2, SESN2, CMPK1, RASAL2, BLOC1S4, AKT1S1, CSE1L, PRKRA, RPL4, SEC61A1, TRAF3, ARHGDIB, ERCC6L, PARD6B, GABARAPL2, CFLAR, RPGRIP1L, FN3KRP, CASC5, MYL12A, VAV2, ATG3, WIPI1, KCTD7, CDKN1A, PLK4, PSMC4, GLS, PRKAR1A, DNAJB2, CPNE3, HSPD1, FPGS, SMC1A, NBN, PRKAG2, DICER1, ARHGAP19, PPIP5K2, RHOQ, FER, MKLN1, RANBP9, PRMT7, TPP2, MAPKAP1, CASP8, RHOD, CASP2, SEC24D, KIF14, CDK1, KIF11, KIF15, ECT2, CDK2, UBE2N, EIF4G2, ATP6V1A, EIF4G3, NSL1, NUCB2, BUB1B, TXNRD1, INPP4B, CUX1, SMS, UGP2, PRKCZ, USP9X, CALD1, ADH5, DCK, RPS15A, NR3C1, TPM4, FAM13B, TYMS, TUBGCP3, TFAM, NPAS2, MOAP1, TUBGCP5, ENO3, BRK1, TNRC6B, VPS36, TNRC6A, HBB, HSPA8, CENPO, TXNIP, SCLT1, CENPN, ICA1, DNM1L, KAT2B, NCDN, NF1, MAP1B, KIF18A, AHI1, CENPE, TPMT, ANXA5, SMC2, SMC3, CDC25A, RALGDS, CENPI, SMC4, CADPS, MPI, GSPT1, AKR1B1, JAK2, CENPU, SH3D19, CUL4B			
	GO CC	GO:0005654~ nucleoplasm	ITGB3BP, RAD51C, FAM20B, PNISR, ZNF638, SART3, CUL3, HIST1H2BN, CDCA7, CLK3, COL4A3BP, CREB3L2, H2AFX, PATZ1, OGT, CCNA2, LUC7L3, LIG3, ZHX2, POLB, OPTN, MECOM, RPTOR, ESCO2, RFC5, DCAF7, PTRF, CEP350, MAPK6, JUN, MAPK9, SCAF8, COASY, CRTC2, SRSF10, SRSF11, CHEK1, RILPL1, FBXO5, RCHY1, TCF3, KLF5, GARS, SMYD3, CDC23, TKT, SMYD2, RAD54L, GCFC2, FNIP2, NOTCH3, UPF3A, SRSF3, NOTCH2, SRSF5, RNF7, WDR61, PARPBP, CCT8, NCOR1, CREBRF, SRSF1, CLSPN, COPS2, ELF1, FERMT2, U2SURP, VPS37A, SHOC2, TRMT10C, SENP5, BOD1L1, CCNE2, CCNE1, BLZF1, FANCI, ANKRD11, ANP32A, NSMCE2, MASTL, BRD4, TOP2A, DEDD2, IP6K2, ATF7IP, UFD1L, POLR1D, SF1, MBD4, RAD52, RBBP6, FANCD2, RRM2, ZNF480, RBM39, GADD45A, NSD1, CLOCK, ARL4A, CLUAP1, POLR2K, POLA1, ZNF367, FAAP20, SUMO3, SF3B1, SRRT, MRPL10, STK40, SQSTM1, TCEA1, ACTL6A, SNAP23, MLLT4, FEN1, RBM25, ZNF263, ECI2, TRMU, HIST1H2BD, PDS5B, PPHLN1, HIST1H2BG, BIRC5, HNRNPDL, COG3, RPS6KA3, DUSP3, PAPOLA, PSMD12, SFPQ, KIF20B, USP48, RBM15, CALM1, RBM4, SAE1, MCM10, TCEAL1, PNN, CBX5, TOP1, KLHL8, ORC5, CTDSP1, AKIRIN1, NQO2, ORC3, ARGLU1, RBFOX2, DTL, DFFB, USP1, NEIL3, RELB, TOPBP1, RRP8, NUPL2, GRHL2, RMI1, ELL2, PTHLH, NABP1, HIF1A, HSPB8, MCMBP, SLU7, MAP7D3, ANAPC16, EID1, HMGB1, MPLKIP, EID3, BLM,	283	1.61	2.66E-15

			STAM2, SOX4, SOX6, NR2C2, ATF1, AKT1S1, CSE1L, POLE2, C12ORF10, PTK6, PRKRA, HIST1H4E, ERCC6L, GINS1, MAFG, CSTF3, CSTF2, BRIP1, ATAD2, CASC5, WHSC1, BRCA1, SAFB2, TRNT1, CDKN1A, ATF3, EAF1, PSMC4, SMARCC1, WDR4, C2ORF49, FBXO32, ZNF318, HIST1H3E, RNPC3, SMC1A, DUT, C9ORF72, NBN, E2F3, GPBP1, PRKAG2, HIST2H4A, FAM63B, PHC3, FUBP1, PRMT7, MAPKAP1, CASP8, TPR, KDM5B, AKT3, CDK1, BANP, HMGA2, CHAMP1, ZFR, CDK2, UBE2N, LAP3, XPC, CUX1, KDM6B, MATR3, HYPK, SMARCAD1, SUPT3H, PPP4R2, HAUS6, KIAA0101, NR3C1, TYMS, CHD9, ERCC8, NPAS2, NPAS3, POU2F3, CHD2, NSUN2, TNRC6A, HSPA8, ERCC2, PPP4R3B, EXO1, CENPO, CENPN, KAT2B, RAD51AP1, MSH2, FAM188A, SMC2, SMC3, CDC25A, CENPI, SMC4, SP4, AKR1B1, ANXA11, BRE, ZRANB2, CENPV, JAK2, CUL4B, MIS18BP1, SH3D19, CENPU, SETD2, ALKBH3, NFIA			
	GO CC	GO:0016020~membrane	ITGB3BP, AKNA, IMPAD1, AP1G1, HBS1L, RPL15, NAA15, STRN, PI4K2B, MTHFD1L, PNN, ATP2B1, CUL3, CISD2, SLC16A1, CLK3, WWP2, SLC2A1, LRRC59, RNF149, EGFR, KRR1, SLC33A1, RPS6KC1, KRT10, CORO7, VPS41, CHPT1, ERGIC1, GCC2, TACC1, ERGIC2, PARP16, CEP350, LRP10, ATP2C1, NBR1, ACAP2, USO1, SLU7, RIPK4, STMN1, ARL8B, MAP7D3, CHMP2A, CAV2, ARFGAP3, BBS7, PNPT1, SNX4, PRRC2C, RIC1, IKBIP, MIA3, KIAA2013, CSE1L, MTCH2, RAC1, PRKRA, HIST1H4E, HLA-DPB1, RPL4, ARL6IP5, SEC61A1, ERCC6L, ARHGDIB, OSBPL3, MKI67, TGFBR1, NDC80, HEATR1, GAS2, PPIF, RERG, APOL2, NOTCH2, DDX55, ATP2A2, PSMC4, PRKAR1A, HIST1H3E, HSPD1, TMPO, ALG11, NCOR1, CYB5R3, SLC20A1, ALG2, ATL3, KIAA0430, NAP1L1, TMEM237, DNAJC10, NUP188, HIST2H4A, SLC26A2, MMP25, PIGK, SRPX, FANCI, DENND5B, FAM129A, PPP1R14C, CASP2, PIGA, AP3B1, KIF14, CDK1, KIF11, MAN1A2, KIF15, PIGT, PIGN, EIF4G2, FAM120A, PSEN2, AVEN, SEC23B, MATR3, BID, MFSD6, PRKCZ, SORD, EXOC7, GALNT7, EXOC8, USP9X, GDAP1, RPL27A, RPS15A, FKBP1A, NR3C1, ESYT1, TPM4, MYCBP2, NDC1, TUBGCP3, DGKE, RPL32, NCAPG, KLC1, BCAP29, PCSK6, ACSL4, INPP5A, HSPA8, FEN1, CSNK1A1, DLST, ECI2, DNM1L, NCDN, MSH2, NF1, CENPE, ANXA5, RPL28, ANXA3, ITPR2, SLC17A5, INVS, PSMD12, MBOAT7, ANXA11, TENM3, DYM, DPM3, SYNM, APBB2, PAICS	170	1.3	0.0178
	GO CC	GO:0005813~centrosome	STIL, CEP72, CEP57L1, CEP78, VPS37A, ARL2BP, HOOK3, CCNE1, SLC16A1, CCSAP, MASTL, CEP112, CDK1, CEP89, DTL, KIF15, ESPL1, TOPBP1, KIAA0586, CAMSAP3, ARHGEF10, CDK2, RTTN, ELL2, ANKRD26, CEP350, FGFR1OP, PSEN2, SNX10, MAP7D3, SNAP29, CLUAP1, PPP4R2, HAUS6, MPLKIP,	63	2.21	6.99E-07

			BBS7, HYLS1, CEP126, SLF1, CHEK1, BCL2L1, TUBGCP3, RILPL1, TUBGCP5, NCAPG, FBXW11, TBC1D31, ERCC6L, CSNK1A1, PPP4R3B, SCLT1, NIN, RPGRIP1L, AHI1, PIBF1, PLK4, CEP68, GSK3B, SLAIN2, CCT8, KIF20B, PPP2R3C, CALM1			
	GO CC	GO:0005694~ chromosome	PDS5B, DTL, PPHLN1, NUSAP1, TOPBP1, WHSC1, CENPE, RBBP6, FAAP20, ZFR, SMC3, BRCA1, BOD1L1, BRD4, SETD2, SMC1A, NSD1, CLOCK	18	3.16	4.40E-03

Supplementary Table 3. Target transcripts of miR182 experimentally validated from miRTarBase. The logFC of expression in TC22 and M14 for the anti-miR-182-5p vs control cells contrasts and the average expression across all samples are indicated for all differentially expressed genes already experimentally validated according to miRTarBase database, with the two validation evidence strength categories (strong and less strong evidence). LRA, Luciferase Reporter Assay; WB, Western Blot, NGS, Next-Gen Sequencing.

Gene symbol	Gene description	RefSeq transcript.ID	LogFC TC22	Average expression TC22	LogFC M14	Average expression M14	LRA	WB	qRT-PCR	Micro-array	NGS
ATF1	activating transcription factor 1	NM_005171 /// XM_011538386 /// XM_011538387 /// XM_011538388	0,41	8,52	0,38	8,52	V				
ATF1	activating transcription factor 1	NM_005171 /// XM_011538386 /// XM_011538387 /// XM_011538388	0,25	8,07	0,31	8,07	V				
ANKRD36	ankyrin repeat domain 36	NM_001164315 /// NM_198555 /// XM_006712514 /// XM_006712516 /// XM_011511130 /// XM_011511131 /// XM_011511132 /// XM_011511133 /// XM_011511134 /// XM_011511135 /// XM_011511136 /// XM_011511137 /// XM_011511138 /// XM_011511139 /// XM_011511140 /// XM_011511141 /// XM_011511142 /// XM_011511143 /// XM_011511144 /// XM_011511145 /// XR_427086 /// XR_922917 /// XR_922918 /// XR_922919 /// XR_922920 /// XR_922921 /// XR_922922 /// XR_922923 /// XR_922924 /// XR_922925	0,54	6,28	0,08	6,28					V
ANKRD36	ankyrin repeat domain 36	NM_001164315 /// NM_198555 /// XM_006712514 /// XM_006712516 /// XM_011511130 /// XM_011511131 /// XM_011511132 /// XM_011511133 /// XM_011511134 /// XM_011511135 /// XM_011511136 /// XM_011511137 /// XM_011511138 /// XM_011511139 /// XM_011511140 /// XM_011511141 /// XM_011511142 /// XM_011511143 /// XM_011511144 /// XM_011511145 /// XR_427086 /// XR_922917 /// XR_922918 /// XR_922919 /// XR_922920 /// XR_922921 /// XR_922922 /// XR_922923 /// XR_922924 /// XR_922925	0,49	6,08	0,09	6,08					V
BRWD1	bromodomain and WD repeat domain containing 1	NM_001007246 /// NM_018963 /// NM_033656 /// XM_011529611 /// XM_011529612 /// XM_011529613	0,49	6,08	0,32	6,08					V
BRWD1	bromodomain and WD repeat domain	NM_001007246 /// NM_018963 /// NM_033656 /// XM_011529611 /// XM_011529612 /// XM_011529613	0,49	6,08	0,32	6,08					V

	containing 1										
BRWD1	bromodomain and WD repeat domain containing 1	NM_001007246 /// NM_018963 /// NM_033656 /// XM_011529611 /// XM_011529612 /// XM_011529613	0,49	6,08	0,32	6,08					V
BRWD1	bromodomain and WD repeat domain containing 1	NM_001007246 /// NM_018963 /// NM_033656 /// XM_011529611 /// XM_011529612 /// XM_011529613	0,49	6,08	0,32	6,08					V
DDAH1	dimethylarginine dimethylaminohydrolase 1	NM_001134445 /// NM_012137 /// XM_005270707 /// XM_005270709 /// XM_005270710 /// XM_006710544 /// XM_011541158	0,54	6,24	0,41	6,24					V
DDAH1	dimethylarginine dimethylaminohydrolase 1	NM_001134445 /// NM_012137 /// XM_005270707 /// XM_005270709 /// XM_005270710 /// XM_006710544 /// XM_011541158	0,50	6,50	0,41	6,50					V
DDAH1	dimethylarginine dimethylaminohydrolase 1	NM_001134445 /// NM_012137 /// XM_005270707 /// XM_005270709 /// XM_005270710 /// XM_006710544 /// XM_011541158	0,32	9,41	0,35	9,41					V
FAM193A	family with sequence similarity 193. member A	NM_001256666 /// NM_001256667 /// NM_001256668 /// NM_003704 /// NR_046335 /// NR_046336 /// XM_006713930 /// XM_006713932 /// XM_011513590 /// XM_011513591 /// XM_011513592 /// XM_011513593	0,43	5,92	0,09	5,92					V
FLOT1	flotillin 1	NM_005803 /// XM_005248780 /// XM_005248781 /// XM_005272759 /// XM_005272760 /// XM_005274909 /// XM_005274910 /// XM_005275335 /// XM_005275336 /// XM_005275502 /// XM_005275503 /// XM_006714947 /// XM_006725465 /// XM_006725672 /// XM_006725971 /// XM_006726072	0,40	8,06	0,24	8,06	V	V	V		V
FLOT1	flotillin 1	NM_005803 /// XM_005248780 /// XM_005248781 /// XM_005272759 /// XM_005272760 /// XM_005274909 /// XM_005274910 /// XM_005275335 /// XM_005275336 /// XM_005275502 /// XM_005275503 /// XM_006714947 /// XM_006725465 /// XM_006725672 /// XM_006725971 /// XM_006726072	0,40	8,06	0,24	8,06	V	V	V		V
FLOT1	flotillin 1	NM_005803 /// XM_005248780 /// XM_005248781 /// XM_005272759 /// XM_005272760 /// XM_005274909 ///	0,40	8,06	0,24	8,06	V	V	V		V

		XM_005274910 /// XM_005275335 /// XM_005275336 /// XM_005275502 /// XM_005275503 /// XM_006714947 /// XM_006725465 /// XM_006725672 /// XM_006725971 /// XM_006726072									
FLOT1	flotillin 1	NM_005803 /// XM_005248780 /// XM_005248781 /// XM_005272759 /// XM_005272760 /// XM_005274909 /// XM_005274910 /// XM_005275335 /// XM_005275336 /// XM_005275502 /// XM_005275503 /// XM_006714947 /// XM_006725465 /// XM_006725672 /// XM_006725971 /// XM_006726072	0,35	8,83	0,23	8,83	V	V	V		V
FLOT1	flotillin 1	NM_005803 /// XM_005248780 /// XM_005248781 /// XM_005272759 /// XM_005272760 /// XM_005274909 /// XM_005274910 /// XM_005275335 /// XM_005275336 /// XM_005275502 /// XM_005275503 /// XM_006714947 /// XM_006725465 /// XM_006725672 /// XM_006725971 /// XM_006726072	0,35	8,83	0,23	8,83	V	V	V		V
FLOT1	flotillin 1	NM_005803 /// XM_005248780 /// XM_005248781 /// XM_005272759 /// XM_005272760 /// XM_005274909 /// XM_005274910 /// XM_005275335 /// XM_005275336 /// XM_005275502 /// XM_005275503 /// XM_006714947 /// XM_006725465 /// XM_006725672 /// XM_006725971 /// XM_006726072	0,35	8,83	0,23	8,83	V	V	V		V
FLOT1	flotillin 1	NM_005803 /// XM_005248780 /// XM_005248781 /// XM_005272759 /// XM_005272760 /// XM_005274909 /// XM_005274910 /// XM_005275335 /// XM_005275336 /// XM_005275502 /// XM_005275503 /// XM_006714947 /// XM_006725465 /// XM_006725672 /// XM_006725971 /// XM_006726072	0,33	9,80	0,22	9,80	V	V	V		V
FLOT1	flotillin 1	NM_005803 /// XM_005248780 /// XM_005248781 /// XM_005272759 /// XM_005272760 /// XM_005274909 /// XM_005274910 /// XM_005275335 /// XM_005275336 /// XM_005275502 /// XM_005275503 /// XM_006714947 /// XM_006725465 /// XM_006725672 /// XM_006725971 /// XM_006726072	0,33	9,80	0,22	9,80	V	V	V		V
FLOT1	flotillin 1	NM_005803 /// XM_005248780 /// XM_005248781 /// XM_005272759 /// XM_005272760 /// XM_005274909 /// XM_005274910 /// XM_005275335 /// XM_005275336 /// XM_005275502 /// XM_005275503 /// XM_006714947 /// XM_006725465 /// XM_006725672 /// XM_006725971 /// XM_006726072	0,33	9,80	0,22	9,80	V	V	V		V
NR3C1	nuclear receptor subfamily 3. group C. member 1	NM_000176 /// NM_001018074 /// NM_001018075 /// NM_001018076 /// NM_001018077 /// NM_001020825 /// NM_001024094 /// NM_001204258 /// NM_001204259 /// NM_001204260 /// NM_001204261 /// NM_001204262 /// NM_001204263 /// NM_001204264 /// NM_001204265 ///	0,33	7,72	0,28	7,72					V

	(glucocorticoid receptor)	XM_005268419 /// XM_005268420 /// XM_005268422 /// XM_005268423 /// XM_011537636 /// XM_011537637									
NR3C1	nuclear receptor subfamily 3. group C. member 1 (glucocorticoid receptor)	NM_000176 /// NM_001018074 /// NM_001018075 /// NM_001018076 /// NM_001018077 /// NM_001020825 /// NM_001024094 /// NM_001204258 /// NM_001204259 /// NM_001204260 /// NM_001204261 /// NM_001204262 /// NM_001204263 /// NM_001204264 /// NM_001204265 /// XM_005268419 /// XM_005268420 /// XM_005268422 /// XM_005268423 /// XM_011537636 /// XM_011537637	0,33	7,72	0,28	7,72					V
NR3C1	nuclear receptor subfamily 3. group C. member 1 (glucocorticoid receptor)	NM_000176 /// NM_001018074 /// NM_001018075 /// NM_001018076 /// NM_001018077 /// NM_001020825 /// NM_001024094 /// NM_001204258 /// NM_001204259 /// NM_001204260 /// NM_001204261 /// NM_001204262 /// NM_001204263 /// NM_001204264 /// NM_001204265 /// XM_005268419 /// XM_005268420 /// XM_005268422 /// XM_005268423 /// XM_011537636 /// XM_011537637	0,22	8,05	0,40	8,05					V
NR3C1	nuclear receptor subfamily 3. group C. member 1 (glucocorticoid receptor)	NM_000176 /// NM_001018074 /// NM_001018075 /// NM_001018076 /// NM_001018077 /// NM_001020825 /// NM_001024094 /// NM_001204258 /// NM_001204259 /// NM_001204260 /// NM_001204261 /// NM_001204262 /// NM_001204263 /// NM_001204264 /// NM_001204265 /// XM_005268419 /// XM_005268420 /// XM_005268422 /// XM_005268423 /// XM_011537636 /// XM_011537637	0,22	8,05	0,40	8,05					V
NR3C1	nuclear receptor subfamily 3. group C. member 1 (glucocorticoid receptor)	NM_000176 /// NM_001018074 /// NM_001018075 /// NM_001018076 /// NM_001018077 /// NM_001020825 /// NM_001024094 /// NM_001204258 /// NM_001204259 /// NM_001204260 /// NM_001204261 /// NM_001204262 /// NM_001204263 /// NM_001204264 /// NM_001204265 /// XM_005268419 /// XM_005268420 /// XM_005268422 /// XM_005268423 /// XM_011537636 /// XM_011537637	0,21	7,42	0,37	7,42					V
NR3C1	nuclear receptor subfamily 3. group C. member 1 (glucocorticoid receptor)	NM_000176 /// NM_001018074 /// NM_001018075 /// NM_001018076 /// NM_001018077 /// NM_001020825 /// NM_001024094 /// NM_001204258 /// NM_001204259 /// NM_001204260 /// NM_001204261 /// NM_001204262 /// NM_001204263 /// NM_001204264 /// NM_001204265 /// XM_005268419 /// XM_005268420 /// XM_005268422 /// XM_005268423 /// XM_011537636 /// XM_011537637	0,21	7,42	0,37	7,42					V
PNISR	PNN-interacting serine/arginine-rich protein	NM_015491 /// NM_032870 /// XM_005266912 /// XM_005266913 /// XM_005266914 /// XM_005266915 /// XM_005266916 /// XM_005266917	0,40	8,24	0,14	8,24					V
PNISR	PNN-interacting serine/argini	NM_015491 /// NM_032870 /// XM_005266912 /// XM_005266913 /// XM_005266914 /// XM_005266915 /// XM_005266916 /// XM_005266917	0,32	9,53	0,11	9,53					V

	ne-rich protein										
QSER1	glutamine and serine rich 1	NM_001076786 /// NM_024774 /// XM_006718323 /// XM_006718325	0,35	7,48	-0,05	7,48					V
RBM12	RNA binding motif protein 12	NM_001198838 /// NM_001198840 /// NM_006047 /// NM_152838	0,23	9,33	0,44	9,33					V
SESN2	sestrin 2	NM_031459 /// XR_946773	0,64	8,79	112098700799447,00	8,79					V
SESN2	sestrin 2	NM_031459 /// XR_946773	0,62	8,06	112195821748955,00	8,06					V
TNRC6A	trinucleotide repeat containing 6A	NM_014494 /// XM_005255254 /// XM_005255257 /// XM_006721039 /// XM_011545791 /// XM_011545792 /// XM_011545793 /// XM_011545794 /// XM_011545795 /// XM_011545796	0,41	8,37	0,40	8,37					V
TNRC6A	trinucleotide repeat containing 6A	NM_014494 /// XM_005255254 /// XM_005255257 /// XM_006721039 /// XM_011545791 /// XM_011545792 /// XM_011545793 /// XM_011545794 /// XM_011545795 /// XM_011545796	0,39	9,17	0,40	9,17					V

Supplementary Table 4. List of potential miR-182 direct target genes with transcripts significantly up-regulated after miR-182 inhibition. For each gene, the table indicated the average expression and the logFC observed in each comparison (anti-miR-182 *vs* anti-miR-NC treated cells) for associated significantly up-regulated probesets and transcripts with TargetScan predicted target sites, along with total cumulative context ++ score and the number of conserved and non-conserved target sites.

Gene symbol	Total number of conserved sites	Total number of non-conserved sites	Transcript ID	Total context ++ score	Probeset ID	Gene description	Ensembl ID	RefSeq transcript ID	LogFC TC22	Average expression TC22	Adjusted P-value TC22	LogFC M14	Average expression M14	Adjusted P value M14	Validated target transcripts (miRTarBase
ACP6	0	1	ENST0000 0369238.6	-0.030	11721112 _a_at	acid phosphatase 6, lysophosphatidi c	ENSG0000016283 6 /// OTTHUMG000000 14019	NM_016361	0,35	8,29	0,0006014	0,29	8,29	0,0033224	
ADAMTS9	0	2	ENST0000 0295903.4	-0.140	11745589 _a_at	ADAM metallopeptida se with thrombospondi n type 1 motif 9	ENSG0000016363 8 /// OTTHUMG000001 58722	NM_182920	0,35	5,25	0,0025149	0,10	5,25	0,3375300	
ADTRP	0	1	ENST0000 0414691.3	-0.263	11731981 _a_at	androgen-dependent TFPI-regulating protein	ENSG0000011186 3 /// OTTHUMG000000 14260	NM_00114394 8 /// NM_032744	0,41	5,29	0,0201324	0,06	5,29	0,7086656	
AHSA2	0	1	ENST0000 0394457.3	-0.140	11730312 _a_at	AHA1, activator of heat shock 90kDa protein ATPase homolog 2 (yeast)	ENSG0000017320 9 /// OTTHUMG000001 29437	NM_152392	0,46	7,42	0,0025995	0,35	7,42	0,0146383	
AKAP11	0	2	ENST0000 0025301.2	-0.233	11763810 _a_at	A kinase (PRKA) anchor protein 11	ENSG0000002351 6 /// OTTHUMG000000 16805	NM_016248 /// NM_144490	0,30	6,88	0,0123632	-0,20	6,88	0,0838473	
ANKRD13C	0	1	ENST0000 0370944.4	-0.155	11759780 _at	ankyrin repeat domain 13C	---	NM_030816	0,56	8,03	0,0017520	0,80	8,03	0,0000551	
ANKRD36	0	1	ENST0000 0357042.4	-0.108	11762617 _x_at	ankyrin repeat domain 36	---	NM_00116431 5 /// NM_198555	0,49	6,08	0,0001316	0,09	6,08	0,3696595	Less strong evidence
ANKRD36	0	1	ENST0000 0357042.4	-0.108	11753238 _x_at	ankyrin repeat domain 36	ENSG0000013597 6 /// OTTHUMG000001 55256	NM_00116431 5 /// NM_198555	0,54	6,28	0,0000010	0,08	6,28	0,2585233	Less strong evidence
APPBP2	0	2	ENST0000 0083182.3	-0.160	11724570 _at	amyloid beta precursor protein (cytoplasmic tail) binding protein 2	ENSG0000006272 5 /// OTTHUMG000001 80048	NM_00128247 6 /// NM_006380	0,32	7,66	0,0034529	0,29	7,66	0,0060652	
APPBP2	0	2	ENST0000 0083182.3	-0.160	11724573 _at	amyloid beta precursor protein (cytoplasmic tail) binding	ENSG0000006272 5 /// OTTHUMG000001 80048	NM_00128247 6 /// NM_006380	0,35	6,84	0,0441612	0,25	6,84	0,1477062	

						protein 2									
ARGLU1	0	1	ENST0000 0400198.3	-0.226	11761385 _a_at	arginine and glutamate rich 1	---	NM_018011	0,56	4,99	0,0001303	0,43	4,99	0,0015540	
ARL14	0	1	ENST0000 0320767.2	-0.237	11735743 _at	ADP-ribosylation factor like GTPase 14	ENSG0000017967 4 /// OTTHUMG000001 59031	NM_025047	0,57	11,04	0,0000757	0,89	11,04	0,0000003	
ARL4A	0	1	ENST0000 0396663.1	-0.157	11756387 _x_at	ADP-ribosylation factor like GTPase 4A	ENSG0000012264 4 /// OTTHUMG000000 23374	NM_00103716 4 /// NM_00119539 6 /// NM_005738 /// NM_212460	0,23	9,49	0,0274238	0,36	9,49	0,0015715	
ARL4A	0	1	ENST0000 0396663.1	-0.157	11733140 _s_at	ADP-ribosylation factor like GTPase 4A	ENSG0000012264 4 /// OTTHUMG000000 23374	NM_00103716 4 /// NM_00119539 6 /// NM_005738 /// NM_212460	0,29	10,06	0,0047540	0,35	10,06	0,0010161	
ARL4A	0	1	ENST0000 0396663.1	-0.157	11739230 _a_at	ADP-ribosylation factor like GTPase 4A	ENSG0000012264 4 /// OTTHUMG000000 23374	NM_00103716 4 /// NM_00119539 6 /// NM_005738 /// NM_212460	0,37	8,97	0,0010066	0,37	8,97	0,0009208	
ARL8B	0	1	ENST0000 0419534.2	-0.128	11753615 _a_at	ADP-ribosylation factor like GTPase 8B	ENSG0000013410 8 /// OTTHUMG000000 90463	NM_018184	0,35	9,69	0,0000827	0,13	9,69	0,0674360	
ARL8B	0	1	ENST0000 0419534.2	-0.128	11753616 _s_at	ADP-ribosylation factor like GTPase 8B	ENSG0000013410 8 /// OTTHUMG000000 90463	NM_018184	0,36	9,33	0,0011946	0,12	9,33	0,2160679	
ARRDC3	1	0	ENST0000 0265138.3	-0.168	11718723 _at	arrestin domain containing 3	ENSG0000011336 9 /// OTTHUMG000001 62616	NM_020801	0,41	7,71	0,0000217	0,24	7,71	0,0032226	
ATF1	0	1	ENST0000 0262053.3	-0.340	11743163 _at	activating transcription factor 1	ENSG0000012326 8 /// OTTHUMG000001 69482	NM_005171	0,25	8,07	0,0174433	0,31	8,07	0,0046038	Strong evidence
ATF1	0	1	ENST0000 0262053.3	-0.340	11751694 _a_at	activating transcription factor 1	ENSG0000012326 8 /// OTTHUMG000001 69482	NM_005171	0,41	8,52	0,0003003	0,38	8,52	0,0005412	Strong evidence
ATF7IP	2	1	ENST0000 0261168.4	-0.804	11752314 _a_at	activating transcription factor 7 interacting protein	ENSG0000017168 1 /// OTTHUMG000001 68656	NM_00128651 4 /// NM_00128651 5 /// NM_018179 /// NM_181352	0,34	7,42	0,0000857	0,09	7,42	0,2017515	
BCL10	2	2	ENST0000 0370580.1	-0.948	11726703 _a_at	B-cell CLL/lymphoma	ENSG0000014286 7 ///	NM_003921	0,31	9,20	0,0003312	0,15	9,20	0,0490427	

						10	OTTHUMG00000009965								
BCL10	2	2	ENST00000370580.1	-0.948	11753497_a_at	B-cell CLL/lymphoma 10	ENSG00000142867 /// OTTHUMG00000009965	NM_003921	0,33	7,93	0,0003016	0,28	7,93	0,0014928	
BCL2L1	0	1	ENST00000376062.2	-0.123	11759514_at	BCL2-like 1	ENSG00000171552 /// OTTHUMG00000032192	NM_001191 /// NM_138578	0,34	6,92	0,0002305	0,14	6,92	0,0816082	
BIRC5	0	1	ENST00000301633.4	-0.317	11760008_at	baculoviral IAP repeat containing 5	ENSG00000089685 /// OTTHUMG00000177505	NM_001012270 /// NM_001012271 /// NM_001168	0,31	4,43	0,0010400	0,14	4,43	0,1040423	
BOD1L1	1	1	ENST00000040738.5	-0.416	11736591_at	biorientation of chromosomes in cell division 1-like 1	ENSG00000038219 /// OTTHUMG00000090659	NM_148894	0,41	8,10	0,0006476	0,01	8,10	0,8893996	
BRD4	0	1	ENST00000263377.2	-0.010	11743990_at	bromodomain containing 4	ENSG00000141867 /// OTTHUMG00000183252	NM_014299 /// NM_058243	0,35	7,34	0,0003132	0,32	7,34	0,0007066	
BRWD1	2	1	ENST00000342449.3	-0.300	11728438_a_at	bromodomain and WD repeat domain containing 1	ENSG00000185658 /// OTTHUMG00000066030	NM_001007246 /// NM_018963 /// NM_033656	0,49	6,08	0,0044200	0,32	6,08	0,0482111	Less strong evidence
BTG1	0	1	ENST00000256015.3	-0.174	11733023_s_at	B-cell translocation gene 1, anti-proliferative	ENSG00000133639 /// OTTHUMG00000170092	NM_001731	0,49	11,32	0,0001252	0,33	11,32	0,0035710	
BTG1	0	1	ENST00000256015.3	-0.174	11733024_x_at	B-cell translocation gene 1, anti-proliferative	ENSG00000133639 /// OTTHUMG00000170092	NM_001731	0,58	10,57	0,0000371	0,35	10,57	0,0045176	
C11orf71	0	1	ENST00000325636.4	-0.928	11759623_at	chromosome 11 open reading frame 71	ENSG00000180425	NM_001271562 /// NM_019021	1,22	6,95	0,0000010	1,41	6,95	0,0000002	
C11orf71	0	1	ENST00000325636.4	-0.928	11738248_a_at	chromosome 11 open reading frame 71	ENSG00000180425	NM_001271562 /// NM_019021	0,98	6,95	0,0000021	0,83	6,95	0,0000167	
C12orf76	0	1	ENST00000546651.2	-0.296	11754802_s_at	chromosome 12 open reading frame 76	ENSG00000174456 /// OTTHUMG00000169315	NM_207435	0,38	5,72	0,0007279	0,40	5,72	0,0005031	
C16orf72	0	1	ENST00000327827.7	-0.065	11743154_at	chromosome 16 open reading frame 72	ENSG00000182831 /// OTTHUMG00000178147	NM_014117	0,25	8,02	0,0184329	0,34	8,02	0,0028969	
C16orf91	0	1	ENST00000442039.2	-0.231	11744385_a_at	chromosome 16 open reading frame	ENSG00000174109 /// OTTHUMG00000	NM_001010878 /// NM_00127205	0,32	9,11	0,0151661	0,33	9,11	0,0120841	

						91	76551	1							
C19orf25	0	1	ENST0000 0436106.2	-0.190	11720619 _a_at	chromosome 19 open reading frame 25	ENSG0000011955 9 /// OTTHUMG000001 80092	NM_152482	0,29	7,96	0,0075921	0,39	7,96	0,0008603	
C1orf50	0	1	ENST0000 0372525.5	-0.176	11748882 _a_at	chromosome 1 open reading frame 50	ENSG0000016400 8 /// OTTHUMG000000 07568	NM_024097	0,39	7,98	0,0000083	0,31	7,98	0,0001044	
CALCR	1	0	ENST0000 0359558.2	-0.235	11736981 _a_at	calcitonin receptor	ENSG0000000494 8 /// OTTHUMG000000 23599	NM_00116473 7 /// NM_00116473 8 /// NM_001742	0,31	3,63	0,0161040	-0,08	3,63	0,5156071	
CCDC71L	0	1	ENST0000 0523505.1	-0.182	11739442 _s_at	coiled-coil domain containing 71-like	ENSG0000025327 6 /// OTTHUMG000001 64150	NM_175884	0,40	5,87	0,0043952	0,45	5,87	0,0017101	
CCDC71L	0	1	ENST0000 0523505.1	-0.182	11750185 _a_at	coiled-coil domain containing 71-like	ENSG0000025327 6 /// OTTHUMG000001 64150	NM_175884	0,31	9,13	0,0403660	0,33	9,13	0,0305670	
CCNG1	0	1	ENST0000 0340828.2	-0.153	11715675 _a_at	cyclin G1	ENSG0000011332 8 /// OTTHUMG000001 30380	NM_004060 /// NM_199246	0,27	8,52	0,0195800	0,33	8,52	0,0049574	
CCNG1	0	1	ENST0000 0340828.2	-0.153	11749306 _a_at	cyclin G1	ENSG0000011332 8 /// OTTHUMG000001 30380	NM_004060 /// NM_199246	0,27	7,59	0,0092608	0,42	7,59	0,0002945	
CEACAM6	0	1	ENST0000 0199764.6	-0.145	11729153 _at	carcinoembryonic antigen-related cell adhesion molecule 6 (non-specific cross reacting antigen)	ENSG0000008654 8 /// OTTHUMG000001 51064	NM_002483	0,43	9,82	0,0443482	0,03	9,82	0,8861897	
CELF1	3	0	ENST0000 0395290.2	-0.461	11736054 _a_at	CUGBP, Elav-like family member 1	ENSG0000014918 7 /// OTTHUMG000001 66526	NM_00102559 6 /// NM_00117263 9 /// NM_00117264 0 /// NM_006560 /// NM_198700	0,44	8,38	0,0028304	0,33	8,38	0,0171911	
CGGBP1	1	1	ENST0000 0309534.6	-0.425	11742899 _a_at	CGG triplet repeat binding protein 1	ENSG0000016332 0 /// OTTHUMG000001 59009	NM_00100839 0 /// NM_00119530 8 /// NM_003663	0,39	10,11	0,0047334	0,26	10,11	0,0427666	
CHMP1B	1	0	ENST0000 0526991.2	-0.370	11731477 _at	charged multivesicular body protein 1B	ENSG0000025511 2 /// OTTHUMG000001	NM_020412	0,43	9,77	0,0001058	0,25	9,77	0,0085624	

							65820								
CHMP2B	1	1	ENST0000 0263780.4	-0.690	11724747 _a_at	charged multivesicular body protein 2B	ENSG0000008393 7 /// OTTHUMG000001 58982	NM_00124464 4 /// NM_014043	0,32	10,44	0,0166781	0,02	10,44	0,8992290	
CHORDC1	0	1	ENST0000 0320585.6	-0.170	11743053 _a_at	cysteine and histidine rich domain containing 1	---	NM_00114407 3 /// NM_012124	0,46	6,91	0,0000778	0,20	6,91	0,0376627	
CHORDC1	0	1	ENST0000 0320585.6	-0.170	11743052 _a_at	cysteine and histidine rich domain containing 1	---	NM_00114407 3 /// NM_012124	0,39	7,02	0,0016253	0,11	7,02	0,2876560	
CHORDC1	0	1	ENST0000 0320585.6	-0.170	11742061 _a_at	cysteine and histidine rich domain containing 1	---	NM_00114407 3 /// NM_012124	0,47	6,54	0,0000027	0,22	6,54	0,0048704	
CLK4	0	1	ENST0000 0316308.4	-0.020	11748024 _a_at	CDC like kinase 4	ENSG0000011324 0 /// OTTHUMG000001 30893	NM_020666	0,56	6,38	0,0000207	0,52	6,38	0,0000561	
CLK4	0	1	ENST0000 0316308.4	-0.020	11756853 _a_at	CDC like kinase 4	ENSG0000011324 0 /// OTTHUMG000001 30893	NM_020666	0,37	7,18	0,0010914	0,33	7,18	0,0029331	
COG3	1	0	ENST0000 0349995.5	-0.249	11745418 _a_at	component of oligomeric golgi complex 3	ENSG0000013615 2 /// OTTHUMG000000 16855	NM_00120447 6 /// NM_031431	0,57	5,01	0,0014701	0,52	5,01	0,0026724	
COPS2	0	1	ENST0000 0388901.5	NULL	11724191 _a_at	COP9 signalosome subunit 2	ENSG0000016620 0 /// OTTHUMG000001 72324	NM_00114388 7 /// NM_004236	0,31	9,31	0,0003849	0,25	9,31	0,0029005	
CPEB2	0	1	ENST0000 0538197.1	-0.138	11724951 _s_at	cytoplasmic polyadenylation element binding protein 2	ENSG0000013744 9 /// OTTHUMG000000 90669	NM_00117738 1 /// NM_00117738 2 /// NM_00117738 3 /// NM_00117738 4 /// NM_182485 /// NM_182646	0,35	7,37	0,0041408	0,40	7,37	0,0016010	
CPEB2	0	1	ENST0000 0538197.1	-0.138	11724950 _a_at	cytoplasmic polyadenylation element binding protein 2	ENSG0000013744 9 /// OTTHUMG000000 90669	NM_00117738 1 /// NM_00117738 2 /// NM_00117738 3 /// NM_00117738 4 /// NM_182485 /// NM_182646	0,55	5,78	0,0003785	0,40	5,78	0,0054466	
CPNE3	0	1	ENST0000	-0.020	11719103	copine III	ENSG0000008571	NM_003909	0,45	9,49	0,0000067	-0,06	9,49	0,3811705	

			0198765.4		_at		9 /// OTTHUMG00000163725								
CREB3L2	1	1	ENST00000330387.6	-0.196	11759649_x_at	cAMP responsive element binding protein 3-like 2	ENSG00000182158 /// OTTHUMG00000155744	NM_001253775 /// NM_194071	0,39	5,65	0,0029089	0,03	5,65	0,7878171	
CSGALNACT1	0	1	ENST00000454498.2	-0.108	11727223_a_at	chondroitin sulfate N-acetylgalactosaminyltransferase 1	ENSG00000147408 /// OTTHUMG00000130827	NM_001130518 /// NM_018371	0,34	5,15	0,0116945	-0,04	5,15	0,7634296	
CSGALNACT1	0	1	ENST00000454498.2	-0.108	11732526_s_at	chondroitin sulfate N-acetylgalactosaminyltransferase 1	ENSG00000147408 /// OTTHUMG00000130827	NM_001130518 /// NM_018371	0,37	4,33	0,0277911	-0,06	4,33	0,6911918	
CTTNBP2NL	0	1	ENST00000271277.6	-0.144	11730863_at	CTTNBP2 N-terminal like	ENSG00000143079 /// OTTHUMG00000011154	NM_018704	0,20	6,86	0,0295691	0,30	6,86	0,0024227	
CXorf38	0	1	ENST00000378426.1	-0.179	11756170_a_at	chromosome X open reading frame 38	ENSG00000185753 /// OTTHUMG00000024104	NM_144970	0,42	7,65	0,0000316	0,44	7,65	0,0000203	
CXorf38	0	1	ENST00000378426.1	-0.179	11736519_x_at	chromosome X open reading frame 38	ENSG00000185753 /// OTTHUMG00000024104	NM_144970	0,34	8,33	0,0001033	0,32	8,33	0,0001956	
CYP1B1	1	0	ENST00000260630.3	-0.126	11747104_s_at	cytochrome P450, family 1, subfamily B, polypeptide 1	ENSG00000138061 /// OTTHUMG00000100970	NM_000104	0,62	7,10	0,0407793	0,63	7,10	0,0371504	
DCAF4L1	0	1	ENST00000333141.5	-0.124	11733379_at	DDB1 and CUL4 associated factor 4-like 1	ENSG00000182308	NM_001029955	0,43	3,44	0,0074300	-0,11	3,44	0,4534228	
DCAF7	0	1	ENST00000310827.4	-0.130	11729626_a_at	DDB1 and CUL4 associated factor 7	ENSG00000136485 /// OTTHUMG00000178902	NM_001003725 /// NM_005828	0,30	8,30	0,0006949	0,11	8,30	0,1367297	
DCLK1	0	3	ENST00000379892.4	-0.285	11745757_a_at	doublecortin-like kinase 1	ENSG00000133083 /// OTTHUMG00000016729	NM_001195415 /// NM_001195416 /// NM_001195430 /// NM_004734	-0,42	3,94	0,0121705	0,32	3,94	0,0474467	
DDAH1	1	0	ENST00000535924.2	-0.221	11748534_a_at	dimethylarginine dimethylaminohydrolase 1	ENSG00000153904 /// OTTHUMG00000191181	NM_001134445 /// NM_012137	0,54	6,24	0,0172490	0,41	6,24	0,0599540	Less strong evidence
DDAH1	1	0	ENST00000535924.2	-0.221	11716917_a_at	dimethylarginine	ENSG00000153904 ///	NM_001134445 ///	0,50	6,50	0,0166737	0,41	6,50	0,0409196	Less strong evidence

						dimethylamino hydrolase 1	OTTHUMG00000191181	NM_012137							
DDAH1	1	0	ENST00000535924.2	-0.221	11757504_a_at	dimethylarginine dimethylamino hydrolase 1	ENSG00000153904 /// OTTHUMG00000191181	NM_001134445 /// NM_012137	0,32	9,41	0,0477781	0,35	9,41	0,0338837	
DDTL	1	0	ENST00000215770.5	-0.244	11761623_at	D-dopachrome tautomerase-like	---	NM_001084393	0,38	5,57	0,0030650	0,14	5,57	0,2284160	
DDTL	1	0	ENST00000215770.5	-0.244	11760188_x_at	D-dopachrome tautomerase-like	---	NM_001084393	0,59	5,23	0,0009133	0,33	5,23	0,0363485	
DIO2	0	1	ENST00000438257.4	-0.144	11749826_a_at	deiodinase, iodothyronine, type II	ENSG00000211448 /// OTTHUMG00000171443	NM_000793 /// NM_001007023 /// NM_001242502 /// NM_001242503 /// NM_013989	0,78	5,48	0,0307058	1,07	5,48	0,0048859	
DIO2	0	1	ENST00000438257.4	-0.144	11721580_a_at	deiodinase, iodothyronine, type II	ENSG00000211448 /// OTTHUMG00000171443	NM_000793 /// NM_001007023 /// NM_001242502 /// NM_001242503 /// NM_013989	0,96	6,87	0,0146868	1,10	6,87	0,0064344	
DIO2	0	1	ENST00000438257.4	-0.144	11741639_a_at	deiodinase, iodothyronine, type II	ENSG00000211448 /// OTTHUMG00000171443	NM_000793 /// NM_001007023 /// NM_001242502 /// NM_001242503 /// NM_013989	0,57	6,28	0,0161472	0,99	6,28	0,0002356	
DSE	0	1	ENST00000452085.3	-0.020	11749976_a_at	dermatan sulfate epimerase	ENSG00000111817 /// OTTHUMG00000015434	NM_001080976 /// NM_013352	0,39	6,61	0,0003428	0,33	6,61	0,0013593	
DUSP3	0	1	ENST00000226004.3	-0.075	11748476_a_at	dual specificity phosphatase 3	ENSG00000108861 /// OTTHUMG00000180889	NM_004090	0,35	8,04	0,0013398	0,10	8,04	0,3009323	
DUSP3	0	1	ENST00000226004.3	-0.075	11753617_a_at	dual specificity phosphatase 3	ENSG00000108861 /// OTTHUMG00000180889	NM_004090	0,33	7,80	0,0007787	0,11	7,80	0,1960146	
DUSP3	0	1	ENST00000226004.3	-0.075	11733776_a_at	dual specificity phosphatase 3	ENSG00000108861 /// OTTHUMG00000180889	NM_004090	0,33	7,81	0,0002882	0,11	7,81	0,1679882	
DUSP6	0	1	ENST00000279488.7	-0.181	11741980_a_at	dual specificity phosphatase 6	ENSG00000139318 ///	NM_001946 /// NM_022652	0,31	9,87	0,0104763	0,13	9,87	0,2514303	

							OTTHUMG00000169912								
DUSP6	0	1	ENST00000279488.7	-0.181	11744435_a_at	dual specificity phosphatase 6	ENSG00000139318 /// OTTHUMG00000169912	NM_001946 /// NM_022652	0,32	9,44	0,0067973	0,20	9,44	0,0691023	
DUSP6	0	1	ENST00000279488.7	-0.181	11722049_a_at	dual specificity phosphatase 6	ENSG00000139318 /// OTTHUMG00000169912	NM_001946 /// NM_022652	0,31	9,37	0,0136092	0,20	9,37	0,0923864	
EID2B	0	1	ENST00000326282.4	-0.411	11730510_at	EP300 interacting inhibitor of differentiation 2B	ENSG00000176401 /// OTTHUMG00000183068	NM_152361	0,43	5,57	0,0000775	0,44	5,57	0,0000680	
EIF5	2	0	ENST00000216554.3	-0.630	11724724_a_at	eukaryotic translation initiation factor 5	ENSG00000100664 /// OTTHUMG00000171839	NM_001969 /// NM_183004	0,31	11,45	0,0029186	0,22	11,45	0,0250325	
EIF5	2	0	ENST00000216554.3	-0.630	11758020_s_at	eukaryotic translation initiation factor 5	ENSG00000100664 /// OTTHUMG00000171839	NM_001969 /// NM_183004	0,31	11,01	0,0072287	0,35	11,01	0,0035285	
ELL2	1	0	ENST00000237853.4	-0.209	11749208_a_at	elongation factor, RNA polymerase II, 2	ENSG00000118985 /// OTTHUMG00000122085	NM_012081	0,33	6,39	0,0050864	0,37	6,39	0,0021910	
ELL2	1	0	ENST00000237853.4	-0.209	11752840_a_at	elongation factor, RNA polymerase II, 2	ENSG00000118985 /// OTTHUMG00000122085	NM_012081	0,33	6,73	0,0043212	0,27	6,73	0,0165581	
ELL2	1	0	ENST00000237853.4	-0.209	11736478_a_at	elongation factor, RNA polymerase II, 2	ENSG00000118985 /// OTTHUMG00000122085	NM_012081	0,55	6,67	0,0001089	0,32	6,67	0,0099191	
EPM2AIP1	0	2	ENST00000322716.5	-0.318	11725354_at	EPM2A (laforin) interacting protein 1	ENSG00000178567 /// OTTHUMG00000185486	NM_014805	0,33	5,13	0,0011535	0,24	5,13	0,0113509	
ERLIN2	0	2	ENST00000276461.5	-0.121	11745026_a_at	ER lipid raft associated 2	ENSG00000147475 /// OTTHUMG00000164005	NM_001003790 /// NM_001003791 /// NM_007175	0,34	6,06	0,0063772	-0,06	6,06	0,6037844	
ERLIN2	0	2	ENST00000276461.5	-0.121	11735259_a_at	ER lipid raft associated 2	ENSG00000147475 /// OTTHUMG00000164005	NM_001003790 /// NM_001003791 /// NM_007175	0,38	5,07	0,0293111	0,03	5,07	0,8481693	
ERLIN2	0	2	ENST00000276461.5	-0.121	11745025_a_at	ER lipid raft associated 2	ENSG00000147475 /// OTTHUMG00000164005	NM_001003790 /// NM_001003791 /// NM_007175	0,38	6,39	0,0004220	0,07	6,39	0,4202836	

ERLIN2	0	2	ENST0000 0276461.5	-0.121	11741587 _x_at	ER lipid raft associated 2	ENSG0000014747 5 /// OTTHUMG000001 64005	NM_00100379 0 /// NM_00100379 1 /// NM_007175	0,30	6,85	0,0205214	0,05	6,85	0,6706815	
ERLIN2	0	2	ENST0000 0276461.5	-0.121	11741586 _a_at	ER lipid raft associated 2	ENSG0000014747 5 /// OTTHUMG000001 64005	NM_00100379 0 /// NM_00100379 1 /// NM_007175	0,38	7,07	0,0001459	0,18	7,07	0,0324895	
ESCO1	1	0	ENST0000 0269214.5	-0.153	11725203 _a_at	establishment of sister chromatid cohesion N-acetyltransferase 1	ENSG0000014144 6 /// OTTHUMG000001 78919	NM_052911	0,36	7,20	0,0026321	0,01	7,20	0,9561131	
FADD	0	1	ENST0000 0301838.4	-0.178	11760883 _at	Fas (TNFRSF6)-associated via death domain	---	NM_003824	0,72	5,15	0,0000019	0,31	5,15	0,0071619	
FAM120AOS	0	1	ENST0000 0423591.1	-0.067	11717406 _a_at	family with sequence similarity 120A opposite strand	ENSG0000018893 8 /// OTTHUMG000000 20251	NM_198841	0,31	5,66	0,0024322	0,37	5,66	0,0004856	
FAM122A	1	2	ENST0000 0394264.3	-0.447	11752722 _a_at	family with sequence similarity 122A	ENSG0000018786 6 /// OTTHUMG000000 19971	NM_138333	0,35	5,56	0,0006599	0,12	5,56	0,1570986	
FAM122A	1	2	ENST0000 0394264.3	-0.447	11728317 _a_at	family with sequence similarity 122A	ENSG0000018786 6 /// OTTHUMG000000 19971	NM_138333	0,26	7,44	0,0010666	0,34	7,44	0,0000700	
FAM193A	0	1	ENST0000 0505311.1	-0.020	11746034 _a_at	family with sequence similarity 193, member A	ENSG0000012538 6	NM_00125666 6 /// NM_00125666 7 /// NM_00125666 8 /// NM_003704	0,43	5,92	0,0000126	0,09	5,92	0,1948433	Less strong evidence
FAM198B	0	1	ENST0000 0585682.1	-0.122	11739380 _a_at	family with sequence similarity 198, member B	ENSG0000016412 5 /// OTTHUMG000001 61537	NM_00103170 0 /// NM_00112842 4 /// NM_016613	0,34	6,16	0,0042866	0,19	6,16	0,0908887	
FBLN1	0	1	ENST0000 0327858.6	-0.176	11744152 _a_at	fibulin 1	ENSG0000007794 2 /// OTTHUMG000001 51340	NM_001996 /// NM_006485 /// NM_006486 /// NM_006487	0,28	4,95	0,0407736	0,32	4,95	0,0219881	
FBXO32	0	1	ENST0000 0517956.1	-0.114	11719394 _a_at	F-box protein 32	ENSG0000015680 4 /// OTTHUMG000001 64981	NM_00124246 3 /// NM_058229 /// NM_148177	0,71	7,61	0,0002297	0,35	7,61	0,0346743	
FLOT1	1	2	ENST0000 0376389.3	-0.820	11748081 _a_at	flotillin 1	ENSG0000013731 2 /// ENSG0000020637	NM_005803	0,40	8,06	0,0020014	0,24	8,06	0,0402630	Strong evidence

							9 /// ENSG00000206480 /// ENSG00000224740 /// ENSG00000230143 /// ENSG00000232280 /// ENSG00000236271 /// OTTHUMG00000004837 /// OTTHUMG00000031151 /// OTTHUMG00000031433 /// OTTHUMG00000133717 /// OTTHUMG00000148942 /// OTTHUMG00000149221 /// OTTHUMG00000149457									
FLOT1	1	2	ENST00000376389.3	-0.820	11743047_x_at	flotillin 1	ENSG00000137312 /// ENSG00000206379 /// ENSG00000206480 /// ENSG00000223654 /// ENSG00000224740 /// ENSG00000230143 /// ENSG00000232280 /// ENSG00000236271 /// OTTHUMG00000004837 /// OTTHUMG00000031151 /// OTTHUMG00000031433 /// OTTHUMG00000133717 /// OTTHUMG00000148753 /// OTTHUMG00000148942 /// OTTHUMG00000149221 ///	NM_005803	0,33	9,80	0,0052240	0,22	9,80	0,0465985	Strong evidence

							OTTHUMG00000149457								
FLOT1	1	2	ENST00000376389.3	-0.820	11748082_x_at	flotillin 1	ENSG00000137312 /// ENSG00000206379 /// ENSG00000206480 /// ENSG00000224740 /// ENSG00000230143 /// ENSG00000232280 /// ENSG00000236271 /// OTTHUMG00000004837 /// OTTHUMG00000031151 /// OTTHUMG00000031433 /// OTTHUMG00000133717 /// OTTHUMG00000148942 /// OTTHUMG00000149221 /// OTTHUMG00000149457	NM_005803	0,35	8,83	0,0057140	0,23	8,83	0,0468651	Strong evidence
FNDC3B	2	0	ENST00000336824.4	-0.354	11759612_at	fibronectin type III domain containing 3B	ENSG00000075420 /// OTTHUMG00000156761	NM_001135095 /// NM_022763	0,45	8,13	0,0025175	0,60	8,13	0,0001979	
FRS2	4	0	ENST00000550389.1	-0.849	11750929_a_at	fibroblast growth factor receptor substrate 2	ENSG00000166225 /// OTTHUMG00000169373	NM_001042555 /// NM_001278351 /// NM_001278353 /// NM_001278354 /// NM_001278355 /// NM_001278356 /// NM_001278357 /// NM_006654	0,30	5,69	0,0170435	0,28	5,69	0,0267237	
GABRE	0	1	ENST00000370328.3	-0.020	11761105_at	gamma-aminobutyric acid (GABA) A receptor, epsilon	ENSG00000102287 /// OTTHUMG00000024176	NM_004961 /// NM_021984 /// NM_021987 /// NM_021990	0,35	3,44	0,0280018	0,26	3,44	0,0863885	

GMFB	1	0	ENST0000 0358056.3	-0.296	11753719 _a_at	glia maturation factor, beta	ENSG0000019704 5 /// OTTHUMG000001 40307	NM_004124	0,38	7,35	0,0034624	0,22	7,35	0,0691798	
GMFB	1	0	ENST0000 0358056.3	-0.296	11753720 _x_at	glia maturation factor, beta	ENSG0000019704 5 /// OTTHUMG000001 40307	NM_004124	0,37	7,77	0,0001883	0,16	7,77	0,0533150	
GNA13	1	1	ENST0000 0439174.2	-0.281	11717682 _a_at	guanine nucleotide binding protein (G protein), alpha 13	ENSG0000012006 3 /// OTTHUMG000001 79316	NM_00128242 5 /// NM_006572	0,42	5,01	0,0079938	0,53	5,01	0,0016359	
GNA13	1	1	ENST0000 0439174.2	-0.281	11748689 _a_at	guanine nucleotide binding protein (G protein), alpha 13	ENSG0000012006 3 /// OTTHUMG000001 79316	NM_00128242 5 /// NM_006572	0,28	6,33	0,0031380	0,32	6,33	0,0010624	
GOLM1	0	2	ENST0000 0388712.3	-0.152	11715721 _a_at	golgi membrane protein 1	ENSG0000013505 2 /// OTTHUMG000000 20130	NM_00109926 8 /// NM_016548 /// NM_177937	0,33	7,96	0,0001559	0,19	7,96	0,0145542	
GRHL2	1	0	ENST0000 0251808.3	-0.225	11752934 _a_at	grainyhead-like transcription factor 2	ENSG0000008330 7 /// OTTHUMG000001 49915	NM_024915	0,38	5,75	0,0009940	0,16	5,75	0,1141654	
GRK5	0	1	ENST0000 0392870.2	-0.030	11760785 _s_at	G protein-coupled receptor kinase 5	ENSG0000019887 3 /// OTTHUMG000000 19149	NM_005308	0,36	4,10	0,0031549	-0,07	4,10	0,5016964	
GSTM3	0	1	ENST0000 0540225.1	-0.180	11746129 _a_at	glutathione S-transferase mu 3 (brain)	ENSG0000013420 2 /// OTTHUMG000000 11640	NM_000849	0,32	5,25	0,0049526	-0,15	5,25	0,1368202	
GTF2E1	0	1	ENST0000 0283875.5	-0.020	11749079 _a_at	general transcription factor IIE subunit 1	ENSG0000015376 7 /// OTTHUMG000001 59667	NM_005513	0,30	5,91	0,0199783	0,19	5,91	0,1257279	
GXYLT1	2	1	ENST0000 0398675.3	-0.493	11724161 _a_at	glucoside xylosyltransferase 1	ENSG0000015123 3 /// OTTHUMG000001 69379	NM_00109965 0 /// NM_173601	0,33	6,74	0,0004924	0,32	6,74	0,0006881	
GXYLT1	2	1	ENST0000 0398675.3	-0.493	11724160 _a_at	glucoside xylosyltransferase 1	ENSG0000015123 3 /// OTTHUMG000001 69379	NM_00109965 0 /// NM_173601	0,35	7,03	0,0014851	0,51	7,03	0,0000369	
HCFC2	0	2	ENST0000 0229330.4	-0.042	11724545 _at	host cell factor C2	ENSG0000011172 7 /// OTTHUMG000001 70175	NM_013320	0,26	5,96	0,0117407	0,35	5,96	0,0015263	
HIST1H2AC	0	1	ENST0000 0602637.1	-0.191	11736244 _s_at	histone cluster 1, H2ac	ENSG0000018057 3 /// OTTHUMG000000 14428	NM_003512	0,37	7,64	0,0278937	0,44	7,64	0,0119751	

HIST1H2BG	0	1	ENST0000 0244601.3	-0.106	11734796 _s_at	histone cluster 1, H2bg	ENSG0000027380 2 /// OTTHUMG000000 14446	NM_003518	1,01	7,36	0,0012304	0,47	7,36	0,0904719	
HIST1H2BG	0	1	ENST0000 0244601.3	-0.106	11734797 _x_at	histone cluster 1, H2bg	ENSG0000027380 2 /// OTTHUMG000000 14446	NM_003518	1,20	6,83	0,0010329	0,59	6,83	0,0670775	
HIST1H2BH	1	0	ENST0000 0356350.2	-0.352	11759111 _x_at	histone cluster 1, H2bh	ENSG0000027571 3 /// OTTHUMG000000 14447	NM_003524	0,65	6,41	0,0347095	1,06	6,41	0,0016312	
HMGA2	0	1	ENST0000 0403681.2	-0.205	11762062 _x_at	high mobility group AT-hook 2	ENSG0000014994 8 /// OTTHUMG000001 68936	NM_00101588 6 /// NM_00130091 8 /// NM_00130091 9 /// NM_003483 /// NM_003484	0,42	3,41	0,0000093	0,07	3,41	0,3107378	
HMGA2	0	1	ENST0000 0403681.2	-0.205	11762061 _at	high mobility group AT-hook 2	ENSG0000014994 8 /// OTTHUMG000001 68936	NM_00101588 6 /// NM_00130091 8 /// NM_00130091 9 /// NM_003483 /// NM_003484	0,38	3,24	0,0020291	0,05	3,24	0,6394929	
HMGA2	0	1	ENST0000 0403681.2	-0.205	11732032 _a_at	high mobility group AT-hook 2	ENSG0000014994 8 /// OTTHUMG000001 68936	NM_00101588 6 /// NM_00130091 8 /// NM_00130091 9 /// NM_003483 /// NM_003484	0,81	4,92	0,0000101	0,16	4,92	0,2416214	
HSD17B12	0	1	ENST0000 0278353.4	-0.068	11759794 _at	hydroxysteroid (17-beta) dehydrogenase 12	ENSG0000014908 4 /// OTTHUMG000001 66403	NM_016142	0,53	5,56	0,0019252	0,32	5,56	0,0415132	
HSPA13	1	0	ENST0000 0285667.3	-0.171	11749913 _a_at	heat shock protein 70kDa family, member 13	ENSG0000015530 4 /// OTTHUMG000000 74261	NM_006948	0,34	7,29	0,0205270	0,27	7,29	0,0597372	
IDS	0	1	ENST0000 0422081.2	-0.173	11760820 _at	iduronate 2-sulfatase	ENSG0000001040 4 /// OTTHUMG000000 22615	NM_000202 /// NM_00116655 0 /// NM_006123	0,65	3,96	0,0002165	0,10	3,96	0,5019361	
IL6R	0	1	ENST0000 0344086.4	-0.052	11736509 _x_at	interleukin 6 receptor	ENSG0000016071 2 /// OTTHUMG000000 36073	NM_000565 /// NM_00120686 6 /// NM_181359	0,33	4,43	0,0330130	0,02	4,43	0,9096618	
IL6R	0	1	ENST0000 0344086.4	-0.052	11741959 _x_at	interleukin 6 receptor	ENSG0000016071 2 /// OTTHUMG000000	NM_000565 /// NM_00120686 6 ///	0,54	4,87	0,0039633	0,23	4,87	0,1656933	

							36073	NM_181359							
IL6ST	0	1	ENST0000 0381287.4	-0.115	11730758 _a_at	interleukin 6 signal transducer	ENSG0000013435 2 /// OTTHUMG000000 97043	NM_00119098 1 /// NM_002184 /// NM_175767	0,39	6,20	0,0388091	0,16	6,20	0,3747794	
INTS6	1	1	ENST0000 0311234.4	-0.373	11734299 _at	integrator complex subunit 6	ENSG0000010278 6 /// OTTHUMG000000 16945	NM_00103993 7 /// NM_00103993 8 /// NM_00130609 1 /// NM_012141	0,43	5,66	0,0046312	0,78	5,66	0,0000205	
INTS6	1	1	ENST0000 0311234.4	-0.373	11751762 _s_at	integrator complex subunit 6	ENSG0000010278 6 /// OTTHUMG000000 16945	NM_00103993 7 /// NM_00103993 8 /// NM_00130609 1 /// NM_012141	0,21	5,75	0,0458483	0,45	5,75	0,0002305	
INTS6	1	1	ENST0000 0311234.4	-0.373	11751761 _a_at	integrator complex subunit 6	ENSG0000010278 6 /// OTTHUMG000000 16945	NM_00103993 7 /// NM_00103993 8 /// NM_00130609 1 /// NM_012141	0,30	6,54	0,0210498	0,13	6,54	0,3029833	
ITGB8	1	0	ENST0000 0222573.4	-0.142	11749103 _a_at	integrin beta 8	ENSG0000010585 5 /// OTTHUMG000000 23594	NM_002214	0,36	7,01	0,0042622	0,22	7,01	0,0610550	
ITGB8	1	0	ENST0000 0222573.4	-0.142	11747473 _a_at	integrin beta 8	ENSG0000010585 5 /// OTTHUMG000000 23594	NM_002214	0,31	6,62	0,0391752	0,12	6,62	0,3996721	
ITGB8	1	0	ENST0000 0222573.4	-0.142	11751989 _a_at	integrin beta 8	ENSG0000010585 5 /// OTTHUMG000000 23594	NM_002214	0,33	5,06	0,0076011	0,06	5,06	0,6038452	
JRKL	0	1	ENST0000 0458427.1	-0.226	11749734 _s_at	JRK-like	ENSG0000018334 0 /// OTTHUMG000001 54950	NM_00126183 3 /// NM_003772	0,25	6,60	0,0047784	0,61	6,60	0,0000005	
JRKL	0	1	ENST0000 0458427.1	-0.226	11740266 _at	JRK-like	ENSG0000018334 0 /// OTTHUMG000001 54950	NM_00126183 3 /// NM_003772	0,21	7,07	0,0435480	0,32	7,07	0,0043549	
JRKL	0	1	ENST0000 0458427.1	-0.226	11749733 _a_at	JRK-like	ENSG0000018334 0 /// OTTHUMG000001 54950	NM_00126183 3 /// NM_003772	0,21	5,55	0,0242839	0,36	5,55	0,0006925	
KIAA0753	0	1	ENST0000 0361413.3	-0.010	11752031 _a_at	KIAA0753	ENSG0000019892 0 /// OTTHUMG000001 77928	NM_014804	0,26	6,03	0,0387318	0,32	6,03	0,0125877	

KLF5	0	1	ENST0000 0377687.4	-0.146	11744572 _a_at	Kruppel-like factor 5 (intestinal)	ENSG0000010255 4 /// OTTHUMG000000 17074	NM_00128681 8 /// NM_001730	0,40	10,34	0,0002555	0,21	10,34	0,0276966	
LAMA4	0	1	ENST0000 0230538.7	-0.010	11722282 _a_at	laminin, alpha 4	ENSG0000011276 9 /// OTTHUMG000000 15386	NM_00110520 6 /// NM_00110520 7 /// NM_00110520 8 /// NM_00110520 9 /// NM_002290	0,56	7,21	0,0000009	0,09	7,21	0,2269368	
LRP10	1	0	ENST0000 0359591.4	-0.212	11763484 _x_at	LDL receptor related protein 10	ENSG0000019732 4 /// OTTHUMG000000 28705	NM_014045	0,37	5,81	0,0014111	0,15	5,81	0,1350842	
MAP3K2	0	4	ENST0000 0409947.1	-0.179	11739317 _at	mitogen-activated protein kinase kinase kinase 2	ENSG0000016996 7 /// OTTHUMG000001 53397	NM_006609	0,31	7,42	0,0027957	0,19	7,42	0,0511446	
MET	1	2	ENST0000 0397752.3	-0.297	11754144 _a_at	MET proto-oncogene, receptor tyrosine kinase	ENSG0000010597 6	NM_000245 /// NM_00112750 0	0,56	5,92	0,0105157	0,25	5,92	0,2167070	
MFNG	0	1	ENST0000 0416983.3	-0.033	11724498 _a_at	MFNG O-fucosylpeptide 3-beta-N-acetylglucosaminyltransferase	ENSG0000010006 0 /// OTTHUMG000001 50560	NM_00116634 3 /// NM_002405	0,24	4,55	0,0428382	0,41	4,55	0,0013938	
MFNG	0	1	ENST0000 0416983.3	-0.033	11724499 _at	MFNG O-fucosylpeptide 3-beta-N-acetylglucosaminyltransferase	ENSG0000010006 0 /// OTTHUMG000001 50560	NM_00116634 3 /// NM_002405	0,31	5,97	0,0012214	0,02	5,97	0,7861669	
MOSPD1	0	1	ENST0000 0370783.3	-0.338	11747759 _a_at	motile sperm domain containing 1	ENSG0000010192 8 /// OTTHUMG000000 35315	NM_00130618 8 /// NM_019556	0,35	7,17	0,0361316	0,11	7,17	0,4698189	
MPLKIP	0	1	ENST0000 0306984.6	-0.127	11717999 _at	M-phase specific PLK1 interacting protein	ENSG0000016830 3 /// OTTHUMG000001 28797	NM_138701	0,45	11,00	0,0000125	0,26	11,00	0,0023035	
MPLKIP	0	1	ENST0000 0306984.6	-0.127	11718000 _x_at	M-phase specific PLK1 interacting protein	ENSG0000016830 3 /// OTTHUMG000001 28797	NM_138701	0,42	10,70	0,0000114	0,25	10,70	0,0018010	
MPLKIP	0	1	ENST0000 0306984.6	-0.127	11717998 _a_at	M-phase specific PLK1 interacting protein	ENSG0000016830 3 /// OTTHUMG000001 28797	NM_138701	0,43	10,44	0,0000133	0,24	10,44	0,0034200	
MRPS25	0	1	ENST0000 0253686.2	-0.072	11725634 _at	mitochondrial ribosomal protein S25	ENSG0000013136 8 /// OTTHUMG000001	NM_022497	0,34	6,68	0,0007171	0,32	6,68	0,0013057	

							29836								
MRRF	0	1	ENST0000 0344641.3	-0.065	11760918 _a_at	mitochondrial ribosome recycling factor	ENSG0000014818 7 /// OTTHUMG000000 20600	NM_00117351 2 /// NM_138777 /// NM_199176 /// NM_199177	0,25	4,65	0,0081153	0,39	4,65	0,0002366	
MSANTD4	0	1	ENST0000 0301919.4	-0.082	11722271 _at	Myb/SANT-like DNA-binding domain containing 4 with coiled-coils	ENSG0000017090 3 /// OTTHUMG000001 66240	NM_032424	0,33	6,38	0,0012050	0,41	6,38	0,0001439	
MSL2	1	0	ENST0000 0309993.2	-0.208	11736379 _at	male-specific lethal 2 homolog (Drosophila)	ENSG0000017457 9 /// OTTHUMG000001 59793	NM_00114541 7 /// NM_018133	0,24	6,67	0,0048221	0,32	6,67	0,0004823	
NABP1	1	4	ENST0000 0410026.2	-0.843	11726727 _a_at	nucleic acid binding protein 1	ENSG0000017355 9 /// OTTHUMG000001 32720	NM_00103171 6 /// NM_00125473 6 /// NM_022837	0,72	8,61	0,0000112	0,75	8,61	0,0000064	
NABP1	1	4	ENST0000 0410026.2	-0.843	11726728 _a_at	nucleic acid binding protein 1	ENSG0000017355 9 /// OTTHUMG000001 32720	NM_00103171 6 /// NM_00125473 6 /// NM_022837	0,50	5,73	0,0000776	0,48	5,73	0,0001199	
NABP1	1	4	ENST0000 0410026.2	-0.843	11726726 _s_at	nucleic acid binding protein 1	ENSG0000017355 9 /// OTTHUMG000001 32720	NM_00103171 6 /// NM_00125473 6 /// NM_022837	0,76	9,55	0,0000011	0,71	9,55	0,0000026	
NABP1	1	4	ENST0000 0410026.2	-0.843	11726725 _a_at	nucleic acid binding protein 1	ENSG0000017355 9 /// OTTHUMG000001 32720	NM_00103171 6 /// NM_00125473 6 /// NM_022837	0,81	9,49	0,0000130	0,75	9,49	0,0000316	
NEDD9	0	1	ENST0000 0379446.5	-0.118	11730320 _a_at	neural precursor cell expressed, developmentally down-regulated 9	ENSG0000011185 9 /// OTTHUMG000000 14255	NM_00114239 3 /// NM_00127103 3 /// NM_006403 /// NM_182966	0,67	6,44	0,0138651	0,41	6,44	0,1098398	
NF1	1	0	ENST0000 0358273.4	-0.167	11763503 _a_at	neurofibromin 1	ENSG0000019671 2 /// OTTHUMG000001 32871	NM_000267 /// NM_00104249 2 /// NM_00112814 7	0,40	5,07	0,0410392	0,16	5,07	0,3927691	
NHS	1	0	ENST0000 0380060.3	-0.030	11745631 _a_at	Nance-Horan syndrome (congenital cataracts and dental anomalies)	ENSG0000018815 8 /// OTTHUMG000000 22799	NM_00113602 4 /// NM_00129186 7 /// NM_00129186 8 /// NM_198270	0,38	5,52	0,0005965	0,02	5,52	0,8535513	

NID1	1	0	ENST0000 0366595.3	-0.170	11743137 _a_at	nidogen 1	ENSG0000011696 2 /// OTTHUMG000000 40071	NM_002508	0,35	5,22	0,0184732	0,05	5,22	0,7034751	
NR3C1	0	2	ENST0000 0394464.2	-0.203	11751289 _a_at	nuclear receptor subfamily 3, group C, member 1 (glucocorticoid receptor)	ENSG0000011358 0 /// OTTHUMG000001 29677	NM_000176 /// NM_00101807 4 /// NM_00101807 5 /// NM_00101807 6 /// NM_00101807 7 /// NM_00102082 5 /// NM_00102409 4 /// NM_00120425 8 /// NM_00120425 9 /// NM_00120426 0 /// NM_00120426 1 /// NM_00120426 2 /// NM_00120426 3 /// NM_00120426 4 /// NM_00120426 5	0,22	8,05	0,0224108	0,40	8,05	0,0002286	Less strong evidence
NR3C1	0	2	ENST0000 0394464.2	-0.203	11743739 _a_at	nuclear receptor subfamily 3, group C, member 1 (glucocorticoid receptor)	ENSG0000011358 0 /// OTTHUMG000001 29677	NM_000176 /// NM_00101807 4 /// NM_00101807 5 /// NM_00101807 6 /// NM_00101807 7 /// NM_00102082 5 /// NM_00102409 4 /// NM_00120425 8 /// NM_00120425 9 /// NM_00120426 0 /// NM_00120426 1 /// NM_00120426	0,21	7,42	0,0499569	0,37	7,42	0,0018873	Less strong evidence

								2 /// NM_001204263 /// NM_001204264 /// NM_001204265							
NR3C1	0	2	ENST00000394464.2	-0.203	11743738_a_at	nuclear receptor subfamily 3, group C, member 1 (glucocorticoid receptor)	ENSG00000113580 /// OTTHUMG00000129677	NM_000176 /// NM_001018074 /// NM_001018075 /// NM_001018076 /// NM_001018077 /// NM_001020825 /// NM_001024094 /// NM_001204258 /// NM_001204259 /// NM_001204260 /// NM_001204261 /// NM_001204262 /// NM_001204263 /// NM_001204264 /// NM_001204265	0,33	7,72	0,0007652	0,28	7,72	0,0035327	Less strong evidence
NRAS	0	1	ENST00000369535.4	-0.242	11719188_at	neuroblastoma RAS viral (v-ras) oncogene homolog	ENSG00000213281 /// OTTHUMG00000012059	NM_002524	0,22	8,98	0,0057770	0,33	8,98	0,0001844	
NRP1	0	1	ENST00000374875.1	-0.188	11728215_a_at	neuropilin 1	ENSG00000099250 /// OTTHUMG00000019343	NM_001024628 /// NM_001024629 /// NM_001244972 /// NM_001244973 /// NM_003873	0,34	7,71	0,0022252	0,14	7,71	0,1669616	
NSD1	1	0	ENST00000439151.2	-0.027	11763489_a_at	nuclear receptor binding SET domain protein 1	ENSG00000165671 /// OTTHUMG00000130846	NM_022455 /// NM_172349	0,42	7,59	0,0015497	0,12	7,59	0,3042065	

NUPL2	0	1	ENST0000 0258742.5	-0.034	11746950 _a_at	nucleoporin like 2	ENSG0000013624 3 /// OTTHUMG000000 96955	NM_007342	0,33	9,13	0,0003849	0,15	9,13	0,0562936	
NUPL2	0	1	ENST0000 0258742.5	-0.034	11747896 _a_at	nucleoporin like 2	ENSG0000013624 3 /// OTTHUMG000000 96955	NM_007342	0,38	7,54	0,0022972	0,10	7,54	0,3538680	
NUPL2	0	1	ENST0000 0258742.5	-0.034	11760676 _at	nucleoporin like 2	---	NM_007342	0,31	5,28	0,0049753	0,14	5,28	0,1565988	
NXT2	1	0	ENST0000 0372106.1	-0.123	11756310 _a_at	nuclear transport factor 2-like export factor 2	ENSG0000010188 8 /// OTTHUMG000000 22185	NM_00124261 7 /// NM_00124261 8 /// NM_018698	0,32	6,96	0,0031752	0,29	6,96	0,0063995	
OGT	1	0	ENST0000 0373719.3	-0.172	11746064 _a_at	O-linked N-acetylglucosamine (GlcNAc) transferase	ENSG0000014716 2 /// OTTHUMG000000 33316	NM_003605 /// NM_181672 /// NM_181673	0,42	6,86	0,0000063	0,07	6,86	0,2808004	
OGT	1	0	ENST0000 0373719.3	-0.172	11760246 _at	O-linked N-acetylglucosamine (GlcNAc) transferase	ENSG0000014716 2 /// OTTHUMG000000 33316	NM_003605 /// NM_181672 /// NM_181673	0,94	4,42	0,0000004	0,35	4,42	0,0081433	
OTUD6B	1	1	ENST0000 0285420.4	-0.617	11723733 _a_at	OTU domain containing 6B	ENSG0000015510 0 /// OTTHUMG000001 50758	NM_00128674 5 /// NM_016023	0,26	6,68	0,0274484	0,37	6,68	0,0034135	
PAPPA	1	1	ENST0000 0328252.3	-0.094	11754579 _at	pregnancy-associated plasma protein A, pappalysin 1	ENSG0000018275 2 /// OTTHUMG000000 21045	NM_002581	0,35	6,10	0,0269173	-0,11	6,10	0,4459306	
PAPPA	1	1	ENST0000 0328252.3	-0.094	11727017 _s_at	pregnancy-associated plasma protein A, pappalysin 1	ENSG0000018275 2 /// OTTHUMG000000 21045	NM_002581	0,31	5,68	0,0103358	-0,05	5,68	0,6197608	
PARD6B	0	1	ENST0000 0371610.2	-0.142	11753786 _a_at	par-6 family cell polarity regulator beta	ENSG0000012417 1 /// OTTHUMG000000 32732	NM_032521	0,60	7,84	0,0000011	0,34	7,84	0,0006978	
PARPBP	1	0	ENST0000 0378128.3	-0.085	11760870 _at	PARP1 binding protein	ENSG0000018548 0	NM_017915	0,41	3,84	0,0111420	0,25	3,84	0,1077365	
PDE7A	1	0	ENST0000 0401827.3	-0.261	11720870 _a_at	phosphodiesterase 7A	ENSG0000020526 8 /// OTTHUMG000001 64469	NM_00124231 8 /// NM_002603 /// NM_002604	0,32	5,85	0,0260705	0,04	5,85	0,7682111	
PFDN6	0	1	ENST0000 0395131.1	-0.159	11727890 _a_at	prefoldin subunit 6	ENSG0000020422 0 /// ENSG0000020628 3 /// ENSG0000022478 2 /// ENSG0000023569 2 /// ENSG0000023733	NM_00118518 1 /// NM_00126559 5 /// NM_00126559 6 /// NM_014260	0,36	9,11	0,0033261	0,10	9,11	0,3388563	

							5 /// OTTHUMG00000012977 /// OTTHUMG00000031247 /// OTTHUMG00000031547 /// OTTHUMG00000149092 /// OTTHUMG00000149607								
PIGA	0	1	ENST00000542278.1	-0.159	11746260_x_at	phosphatidylinositol glycan anchor biosynthesis class A	ENSG00000165195 /// OTTHUMG00000021174	NM_002641 /// NM_020472 /// NM_020473	0,39	5,99	0,0019494	0,41	5,99	0,0014730	
PIGA	0	1	ENST00000542278.1	-0.159	11746259_a_at	phosphatidylinositol glycan anchor biosynthesis class A	ENSG00000165195 /// OTTHUMG00000021174	NM_002641 /// NM_020472 /// NM_020473	0,37	6,41	0,0007631	0,30	6,41	0,0038120	
PKIA	0	1	ENST00000396418.2	-0.303	11763261_x_at	protein kinase (cAMP-dependent, catalytic) inhibitor alpha	ENSG00000171033 /// OTTHUMG00000164618	NM_006823 /// NM_181839	0,55	5,53	0,0000870	0,25	5,53	0,0329941	
PKIA	0	1	ENST00000396418.2	-0.303	11754172_a_at	protein kinase (cAMP-dependent, catalytic) inhibitor alpha	ENSG00000171033 /// OTTHUMG00000164618	NM_006823 /// NM_181839	0,37	4,95	0,0028661	0,20	4,95	0,0834187	
PKIA	0	1	ENST00000396418.2	-0.303	11741174_s_at	protein kinase (cAMP-dependent, catalytic) inhibitor alpha	ENSG00000171033 /// OTTHUMG00000164618	NM_006823 /// NM_181839	0,31	7,45	0,0005952	0,11	7,45	0,1596052	
PLSCR1	0	3	ENST00000342435.4	-0.209	11759765_at	phospholipid scramblase 1	ENSG00000188313 /// OTTHUMG00000159427	NM_021105	0,58	7,38	0,0044472	0,58	7,38	0,0046003	
PNISR	1	0	ENST00000369239.5	-0.100	11755634_x_at	PNN-interacting serine/arginine-rich protein	ENSG00000132424 /// OTTHUMG00000015262	NM_015491 /// NM_032870	0,32	9,53	0,0000471	0,11	9,53	0,0857874	Less strong evidence
PNISR	1	0	ENST00000369239.5	-0.100	11744502_a_at	PNN-interacting serine/arginine-rich protein	ENSG00000132424 /// OTTHUMG00000015262	NM_015491 /// NM_032870	0,40	8,24	0,0000009	0,14	8,24	0,0191202	Less strong evidence
PNRC2	0	1	ENST00000334351.7	-0.224	11716988_s_at	proline-rich nuclear receptor coactivator 2	ENSG00000189266 /// OTTHUMG00000013891	NM_017761	0,30	10,26	0,0018098	0,34	10,26	0,0006623	
PNRC2	0	1	ENST00000334351.7	-0.224	11758304_s_at	proline-rich nuclear receptor	ENSG00000189266 /// OTTHUMG00000	NM_017761	0,43	9,29	0,0001841	0,46	9,29	0,0000824	

						coactivator 2	13891								
PNRC2	0	1	ENST0000 0334351.7	-0.224	11716989 _s_at	proline-rich nuclear receptor coactivator 2	ENSG0000018926 6 /// OTTHUMG000000 13891	NM_017761	0,43	9,70	0,0004964	0,44	9,70	0,0004010	
PPIL6	1	0	ENST0000 0521072.2	-0.030	11760036 _at	peptidylprolyl isomerase (cyclophilin)-like 6	---	NM_00111129 8 /// NM_00128636 0 /// NM_00128636 1 /// NM_173672	0,35	5,45	0,0076088	0,27	5,45	0,0310999	
PPP1R1C	1	2	ENST0000 0409137.3	-1.008	11763834 _a_at	protein phosphatase 1, regulatory (inhibitor) subunit 1C	ENSG0000015072 2 /// OTTHUMG000001 54326	NM_00108054 5 /// NM_00126142 4 /// NM_00126142 5	0,31	6,69	0,0112330	-0,10	6,69	0,3935510	
PPP4R2	2	0	ENST0000 0356692.5	-0.448	11736432 _x_at	protein phosphatase 4, regulatory subunit 2	ENSG0000016360 5 /// OTTHUMG000001 58816	NM_174907	0,40	8,25	0,0009800	0,22	8,25	0,0422454	
PPP4R2	2	0	ENST0000 0356692.5	-0.448	11759561 _s_at	protein phosphatase 4, regulatory subunit 2	ENSG0000016360 5 /// OTTHUMG000001 58816	NM_174907	0,35	6,85	0,0022546	0,20	6,85	0,0523487	
PRKAR1A	1	2	ENST0000 0589228.1	-0.519	11722007 _a_at	protein kinase, cAMP-dependent, regulatory, type I, alpha	ENSG0000010894 6 /// OTTHUMG000001 80128	NM_00127628 9 /// NM_00127629 0 /// NM_00127843 3 /// NM_002734 /// NM_212471 /// NM_212472	0,34	9,93	0,0001903	0,23	9,93	0,0050871	
PRKAR1A	1	2	ENST0000 0589228.1	-0.519	11753791 _s_at	protein kinase, cAMP-dependent, regulatory, type I, alpha	ENSG0000010894 6 /// OTTHUMG000001 80128	NM_00127628 9 /// NM_00127629 0 /// NM_00127843 3 /// NM_002734 /// NM_212471 /// NM_212472	0,39	8,04	0,0003057	0,25	8,04	0,0106420	
PRR3	1	0	ENST0000 0376560.3	-0.282	11723382 _a_at	proline rich 3	ENSG0000020457 6 /// ENSG0000020649 1 /// ENSG0000022376 6 /// ENSG0000022388 7 /// ENSG0000022818 6 ///	NM_00107749 7 /// NM_025263	0,53	6,65	0,0017048	0,32	6,65	0,0380391	

							ENSG00000229202 /// ENSG00000233564 /// OTTHUMG00000004919 /// OTTHUMG00000031037 /// OTTHUMG00000031307 /// OTTHUMG00000133026 /// OTTHUMG00000149025 /// OTTHUMG00000149307 /// OTTHUMG00000149538								
PRR3	1	0	ENST00000376560.3	-0.282	11723383_a_at	proline rich 3	ENSG00000204576 /// ENSG00000206491 /// ENSG00000223766 /// ENSG00000223887 /// ENSG00000228186 /// ENSG00000229202 /// ENSG00000233564 /// OTTHUMG00000004919 /// OTTHUMG00000031037 /// OTTHUMG00000031307 /// OTTHUMG00000133026 /// OTTHUMG00000149025 /// OTTHUMG00000149307 /// OTTHUMG00000149538	NM_001077497 /// NM_025263	0,48	6,81	0,0010655	0,45	6,81	0,0017399	
PRRT3	1	0	ENST00000412055.1	-0.254	11762802_at	proline-rich transmembrane protein 3	---	NM_207351	0,31	5,07	0,0094761	0,12	5,07	0,2552349	
PTHLH	0	1	ENST00000395872.1	-0.285	11731897_a_at	parathyroid hormone-like hormone	ENSG00000087494 /// OTTHUMG00000169221	NM_002820 /// NM_198964 /// NM_198965 /// NM_198966	0,61	5,28	0,0009013	0,64	5,28	0,0005515	
PTP4A1	1	0	ENST00000370651.3	-0.229	11717897_a_at	protein tyrosine phosphatase	ENSG00000112245 ///	NM_003463	0,36	10,10	0,0406770	0,42	10,10	0,0185931	

						type IVA, member 1	OTTHUMG00000014949								
PTP4A1	1	0	ENST00000370651.3	-0.229	11717892_a_at	protein tyrosine phosphatase type IVA, member 1	ENSG00000112245 /// OTTHUMG00000014949	NM_003463	0,35	9,60	0,0393288	0,36	9,60	0,0366605	
PXK	0	1	ENST00000463280.1	-0.206	11752623_x_at	PX domain containing serine/threonine kinase	ENSG00000168297 /// OTTHUMG00000159149	NM_001289095 /// NM_001289096 /// NM_001289098 /// NM_001289099 /// NM_001289100 /// NM_001289101 /// NM_017771	0,45	6,46	0,0001414	0,39	6,46	0,0005763	
PXK	0	1	ENST00000463280.1	-0.206	11752622_a_at	PX domain containing serine/threonine kinase	ENSG00000168297 /// OTTHUMG00000159149	NM_001289095 /// NM_001289096 /// NM_001289098 /// NM_001289099 /// NM_001289100 /// NM_001289101 /// NM_017771	0,38	6,12	0,0006871	0,31	6,12	0,0036459	
PXK	0	1	ENST00000463280.1	-0.206	11746685_x_at	PX domain containing serine/threonine kinase	ENSG00000168297 /// OTTHUMG00000159149	NM_001289095 /// NM_001289096 /// NM_001289098 /// NM_001289099 /// NM_001289100 /// NM_001289101 /// NM_017771	0,27	5,95	0,0069020	0,40	5,95	0,0002858	
QSER1	1	0	ENST00000399302.2	-0.096	11720906_a_at	glutamine and serine rich 1	ENSG00000060749 /// OTTHUMG00000166220	NM_001076786 /// NM_024774	0,35	7,48	0,0263717	-0,05	7,48	0,7328186	Less strong evidence
RBM12	0	1	ENST00000374114.3	-0.020	11719925_a_at	RNA binding motif protein 12	ENSG00000244462 /// OTTHUMG00000032350	NM_001198838 /// NM_001198840 /// NM_006047 /// NM_152838	0,23	9,33	0,0481512	0,44	9,33	0,0009554	Less strong evidence

RBM12B	0	1	ENST0000 0399300.2	-0.032	11732560 _s_at	RNA binding motif protein 12B	ENSG0000018380 8 /// OTTHUMG000001 64317	NM_203390	0,30	8,73	0,0034022	0,46	8,73	0,0000692	
RBM12B	0	1	ENST0000 0399300.2	-0.032	11732559 _at	RNA binding motif protein 12B	ENSG0000018380 8 /// OTTHUMG000001 64317	NM_203390	0,29	6,67	0,0001891	0,33	6,67	0,0000450	
RBM12B	0	1	ENST0000 0399300.2	-0.032	11756273 _a_at	RNA binding motif protein 12B	ENSG0000018380 8 /// OTTHUMG000001 64317	NM_203390	0,28	7,26	0,0117570	0,41	7,26	0,0007228	
RBM25	0	1	ENST0000 0261973.7	-0.027	11743410 _a_at	RNA binding motif protein 25	ENSG0000011970 7 /// OTTHUMG000001 67540	NM_021239	0,41	9,16	0,0000169	0,13	9,16	0,0765170	
RBM25	0	1	ENST0000 0261973.7	-0.027	11759711 _a_at	RNA binding motif protein 25	ENSG0000011970 7 /// OTTHUMG000001 67540	NM_021239	0,37	6,66	0,0039735	-0,21	6,66	0,0790573	
RCHY1	0	1	ENST0000 0451788.1	-0.093	11719571 _a_at	ring finger and CHY zinc finger domain containing 1, E3 ubiquitin protein ligase	ENSG0000016374 3 /// OTTHUMG000001 30105	NM_00100892 5 /// NM_00100992 2 /// NM_00127853 6 /// NM_00127853 7 /// NM_00127853 8 /// NM_00127853 9 /// NM_015436	0,34	8,32	0,0014380	0,35	8,32	0,0011669	
REEP3	0	2	ENST0000 0373758.4	-0.152	11722062 _at	receptor accessory protein 3	ENSG0000016547 6 /// OTTHUMG000000 18318	NM_00100133 0	0,35	9,83	0,0231653	0,00	9,83	0,9806522	
RGS2	0	1	ENST0000 0235382.5	-0.217	11715757 _a_at	regulator of G-protein signaling 2	ENSG0000011674 1 /// OTTHUMG000000 35600	NM_002923	0,40	7,10	0,0440384	0,16	7,10	0,3912035	
RIT1	0	1	ENST0000 0368323.3	-0.095	11725079 _a_at	Ras-like without CAAX 1	ENSG0000014362 2 /// OTTHUMG000000 14104	NM_00125682 0 /// NM_00125682 1 /// NM_006912	0,51	8,29	0,0000003	0,43	8,29	0,0000026	
RMND5A	1	1	ENST0000 0283632.4	-0.322	11743344 _a_at	required for meiotic nuclear division 5 homolog A	ENSG0000015356 1 /// OTTHUMG000001 30262	NM_022780	0,38	6,22	0,0000254	0,20	6,22	0,0071237	
RND3	1	0	ENST0000 0375734.2	-0.306	11753427 _a_at	Rho family GTPase 3	ENSG0000011596 3 /// OTTHUMG000001 31859	NM_00125473 8 /// NM_005168	0,43	9,04	0,0017935	0,35	9,04	0,0073675	

RPIA	0	1	ENST0000 0283646.4	-0.095	11744116 _s_at	ribose 5-phosphate isomerase A	ENSG0000015357 4 /// OTTHUMG000001 30333	NM_144563	0,31	9,28	0,0120026	0,24	9,28	0,0390263	
RSRC2	0	1	ENST0000 0331738.7	-0.099	11743272 _a_at	arginine/serine-rich coiled-coil 2	ENSG0000011101 1 /// OTTHUMG000001 67572	NM_023012 /// NM_198261 /// NM_198262	0,24	10,17	0,0006583	0,34	10,17	0,0000238	
RSRC2	0	1	ENST0000 0331738.7	-0.099	11743271 _s_at	arginine/serine-rich coiled-coil 2	ENSG0000011101 1 /// OTTHUMG000001 67572	NM_023012 /// NM_198261 /// NM_198262	0,35	9,73	0,0005734	0,35	9,73	0,0005753	
RSRC2	0	1	ENST0000 0331738.7	-0.099	11743490 _a_at	arginine/serine-rich coiled-coil 2	ENSG0000011101 1 /// OTTHUMG000001 67572	NM_023012 /// NM_198261 /// NM_198262	0,51	9,71	0,0000001	0,32	9,71	0,0000460	
RSRC2	0	1	ENST0000 0331738.7	-0.099	11743274 _x_at	arginine/serine-rich coiled-coil 2	ENSG0000011101 1 /// OTTHUMG000001 67572	NM_023012 /// NM_198261 /// NM_198262	0,24	9,68	0,0008751	0,39	9,68	0,0000061	
RSRC2	0	1	ENST0000 0331738.7	-0.099	11743270 _a_at	arginine/serine-rich coiled-coil 2	ENSG0000011101 1 /// OTTHUMG000001 67572	NM_023012 /// NM_198261 /// NM_198262	0,49	10,15	0,0000006	0,32	10,15	0,0001056	
SAMD12	1	2	ENST0000 0409003.4	-0.479	11737535 _at	sterile alpha motif domain containing 12	ENSG0000017757 0 /// OTTHUMG000000 59817	NM_00110167 6 /// NM_207506	0,45	3,60	0,0061237	0,04	3,60	0,7672591	
SCN9A	1	1	ENST0000 0409672.1	-0.335	11730102 _at	sodium channel, voltage gated, type IX alpha subunit	ENSG0000016943 2 /// OTTHUMG000001 54044	NM_002977	0,31	3,35	0,0410187	0,12	3,35	0,4189307	
SESN2	1	0	ENST0000 0253063.3	-0.141	11718325 _at	sestrin 2	ENSG0000013076 6 /// OTTHUMG000000 03532	NM_031459	0,64	8,79	0,0000668	1,12	8,79	0,0000001	Less strong evidence
SESN2	1	0	ENST0000 0253063.3	-0.141	11718324 _s_at	sestrin 2	ENSG0000013076 6 /// OTTHUMG000000 03532	NM_031459	0,62	8,06	0,0003221	1,12	8,06	0,0000003	Less strong evidence
SLAIN2	2	0	ENST0000 0264313.6	-0.425	11723723 _at	SLAIN motif family member 2	ENSG0000010917 1 /// OTTHUMG000001 61701	NM_020846	0,33	8,26	0,0014140	0,13	8,26	0,1435206	
SLAIN2	2	0	ENST0000 0264313.6	-0.425	11723721 _a_at	SLAIN motif family member 2	ENSG0000010917 1 /// OTTHUMG000001 61701	NM_020846	0,31	9,55	0,0001957	0,04	9,55	0,5344007	
SLC25A30	0	1	ENST0000 0539591.1	-0.199	11752963 _a_at	solute carrier family 25, member 30	ENSG0000017403 2 /// OTTHUMG000000 16853	NM_00101087 5 /// NM_00128680 6 /// NM_00128680	0,37	4,14	0,0169544	-0,02	4,14	0,9078344	

								7							
SLC4A7	1	1	ENST0000 0295736.5	-0.120	11747964 _a_at	solute carrier family 4, sodium bicarbonate cotransporter, member 7	ENSG0000003386 7 /// OTTHUMG000001 55679	NM_00125837 9 /// NM_00125838 0 /// NM_003615	0,43	8,46	0,0436401	-0,09	8,46	0,6538145	
SLC7A11	0	3	ENST0000 0280612.5	-0.169	11744680 _a_at	solute carrier family 7 (anionic amino acid transporter light chain, xc- system), member 11	ENSG0000015101 2 /// OTTHUMG000001 33396	NM_014331	0,49	8,41	0,0048250	0,48	8,41	0,0056479	
SNRNP48	0	1	ENST0000 0342415.5	-0.128	11736318 _a_at	small nuclear ribonucleoprot ein, U11/U12 48KDa subunit	ENSG0000016856 6 /// OTTHUMG000000 14213	NM_152551	0,30	6,86	0,0257810	0,30	6,86	0,0289860	
SNX19	0	2	ENST0000 0265909.4	-0.162	11750248 _x_at	sorting nexin 19	ENSG0000012045 1 /// OTTHUMG000001 65663	NM_00130108 9 /// NM_014758	0,36	5,23	0,0015346	0,17	5,23	0,0989727	
SOX6	2	0	ENST0000 0316399.6	-0.569	11726179 _a_at	SRY box 6	ENSG0000011069 3 /// OTTHUMG000001 65876	NM_00114581 1 /// NM_00114581 9 /// NM_017508 /// NM_033326	0,35	3,44	0,0015754	0,15	3,44	0,1209662	
SRSF1	0	2	ENST0000 0258962.4	-0.164	11747684 _a_at	serine/arginine- rich splicing factor 1	ENSG0000013645 0 /// OTTHUMG000001 78781	NM_00107816 6 /// NM_006924	0,35	10,88	0,0004264	0,23	10,88	0,0087623	
SRSF1	0	2	ENST0000 0258962.4	-0.164	11727811 _a_at	serine/arginine- rich splicing factor 1	ENSG0000013645 0 /// OTTHUMG000001 78781	NM_00107816 6 /// NM_006924	0,44	10,73	0,0000596	0,24	10,73	0,0099274	
SSU72	0	1	ENST0000 0291386.3	-0.222	11763451 _s_at	SSU72 homolog, RNA polymerase II CTD phosphatase	ENSG0000016007 5 /// OTTHUMG000000 00576	NM_014188	0,31	7,45	0,0272941	0,40	7,45	0,0061819	
SUB1	0	1	ENST0000 0265073.4	-0.182	11720598 _x_at	SUB1 homolog, transcriptional regulator	ENSG0000011338 7 /// OTTHUMG000001 31071	NM_006713	0,31	10,33	0,0022607	0,12	10,33	0,1614375	
SUCO	0	1	ENST0000 0367723.4	-0.122	11717623 _a_at	SUN domain containing ossification factor	ENSG0000009497 5 /// OTTHUMG000000 34839	NM_00128275 0 /// NM_00128275 1 /// NM_014283 /// NM_016227	0,27	7,64	0,0072148	0,42	7,64	0,0001947	
TAF1A	0	1	ENST0000 0543857.1	-0.214	11747455 _a_at	TATA box binding protein (TBP)-	ENSG0000014349 8 /// OTTHUMG000000	NM_00120153 6 /// NM_005681 ///	0,47	6,14	0,0027907	0,45	6,14	0,0042745	

						associated factor, RNA polymerase I, A, 48kDa	37544	NM_139352							
TAF1A	0	1	ENST0000 0543857.1	-0.214	11730540 _a_at	TATA box binding protein (TBP)-associated factor, RNA polymerase I, A, 48kDa	ENSG0000014349 8 /// OTTHUMG000000 37544	NM_00120153 6 /// NM_005681 /// NM_139352	0,35	6,86	0,0107824	0,40	6,86	0,0051901	
TAF1A	0	1	ENST0000 0543857.1	-0.214	11730541 _x_at	TATA box binding protein (TBP)-associated factor, RNA polymerase I, A, 48kDa	ENSG0000014349 8 /// OTTHUMG000000 37544	NM_00120153 6 /// NM_005681 /// NM_139352	0,32	7,90	0,0116383	0,42	7,90	0,0018710	
TAF1A	0	1	ENST0000 0543857.1	-0.214	11760914 _x_at	TATA box binding protein (TBP)-associated factor, RNA polymerase I, A, 48kDa	---	NM_00120153 6 /// NM_005681 /// NM_139352	0,32	6,14	0,0031829	0,26	6,14	0,0109889	
TBC1D23	0	1	ENST0000 0344949.5	-0.227	11718053 _a_at	TBC1 domain family, member 23	ENSG0000003605 4 /// OTTHUMG000001 59067	NM_00119919 8 /// NM_018309	0,36	8,57	0,0004819	0,07	8,57	0,3816669	
TCERG1	0	1	ENST0000 0296702.5	-0.030	11748475 _a_at	transcription elongation regulator 1	ENSG0000011364 9 /// OTTHUMG000001 29683	NM_00104000 6 /// NM_006706	0,38	8,72	0,0000224	0,11	8,72	0,1191300	
TGFBR2	1	2	ENST0000 0359013.4	-0.040	11750840 _s_at	transforming growth factor beta receptor II	ENSG0000016351 3 /// OTTHUMG000001 30569	NM_00102484 7 /// NM_003242	0,41	7,85	0,0001826	0,08	7,85	0,3530102	
THAP1	1	0	ENST0000 0345117.2	-0.213	11733906 _a_at	THAP domain containing, apoptosis associated protein 1	ENSG0000013193 1 /// OTTHUMG000001 65276	NM_018105 /// NM_199003	0,40	8,46	0,0000343	0,36	8,46	0,0001110	
TKT	0	1	ENST0000 0462138.1	-0.050	11719934 _a_at	transketolase	ENSG0000016393 1 /// OTTHUMG000001 58192	NM_001064 /// NM_00113505 5 /// NM_00113505 6 /// NM_00125802 8	0,68	7,07	0,0001022	0,63	7,07	0,0002210	
TMEM140	0	2	ENST0000 0275767.3	-0.473	11751628 _a_at	transmembrane protein 140	ENSG0000014685 9 /// OTTHUMG000001 55413	NM_018295	0,34	5,11	0,0004173	0,05	5,11	0,5635051	
TMEM167B	0	1	ENST0000 0338272.8	-0.382	11716229 _s_at	transmembrane protein 167B	ENSG0000021571 7 ///	NM_020141	0,33	7,39	0,0053516	0,26	7,39	0,0230324	

							OTTHUMG00000042364								
TMEM167B	0	1	ENST00000338272.8	-0.382	11758747_at	transmembrane protein 167B	ENSG00000215717 /// OTTHUMG00000042364	NM_020141	0,32	3,43	0,0112623	0,10	3,43	0,3989017	
TMEM236	0	1	ENST00000377495.1	-0.103	11758287_s_at	transmembrane protein 236	ENSG00000148483 /// OTTHUMG00000017753	NM_001013629 /// NM_001098844	0,48	5,74	0,0002270	0,18	5,74	0,0966127	
TMEM251	0	2	ENST00000415050.2	-0.091	11719419_a_at	transmembrane protein 251	ENSG00000153485 /// ENSG00000275947 /// OTTHUMG00000171265 /// OTTHUMG00000190208	NM_001098621 /// NM_015676	0,36	9,03	0,0000215	0,26	9,03	0,0005400	
TMEM261	0	1	ENST00000358227.4	-0.287	11716891_at	transmembrane protein 261	ENSG00000137038 /// OTTHUMG00000019539	NM_033428	0,31	5,72	0,0017638	0,05	5,72	0,5473809	
TMEM261	0	1	ENST00000358227.4	-0.287	11758682_s_at	transmembrane protein 261	ENSG00000137038 /// OTTHUMG00000019539	NM_033428	0,36	5,60	0,0111943	0,39	5,60	0,0061239	
TMEM30B	0	1	ENST00000555868.1	-0.179	11756750_a_at	transmembrane protein 30B	ENSG00000182107 /// OTTHUMG00000171426	NM_001017970	0,31	7,60	0,0009447	0,23	7,60	0,0072856	
TMEM42	0	1	ENST00000302392.4	-0.402	11756193_a_at	transmembrane protein 42	ENSG00000169964 /// ENSG00000280516 /// OTTHUMG00000133092	NM_144638	0,27	8,62	0,0031664	0,39	8,62	0,0001314	
TMEM67	1	0	ENST00000453321.3	-0.158	11763744_at	transmembrane protein 67	ENSG00000164953 /// OTTHUMG00000153119	NM_001142301 /// NM_153704	0,40	3,65	0,0068501	0,25	3,65	0,0739465	
TMEM68	1	0	ENST00000523073.1	-0.192	11760192_s_at	transmembrane protein 68	ENSG00000167904 /// OTTHUMG00000164293	NM_001286657 /// NM_001286660 /// NM_001286661 /// NM_152417	0,29	8,38	0,0458954	0,45	8,38	0,0045077	
TNRC6A	1	0	ENST00000395799.3	-0.204	11755871_s_at	trinucleotide repeat containing 6A	ENSG00000090905 /// OTTHUMG00000096999	NM_014494	0,41	8,37	0,0004016	0,40	8,37	0,0004190	Less strong evidence
TNRC6A	1	0	ENST00000395799.3	-0.204	11717817_a_at	trinucleotide repeat containing 6A	ENSG00000090905 /// OTTHUMG000000	NM_014494	0,39	9,17	0,0032144	0,40	9,17	0,0026024	Less strong evidence

							96999								
TPR	0	1	ENST0000 0367478.4	-0.185	11727484 _a_at	translocated promoter region, nuclear basket protein	ENSG0000004741 0 /// OTTHUMG000000 35580	NM_003292	0,33	8,17	0,0003802	-0,05	8,17	0,5256612	
TRIO	1	0	ENST0000 0344204.4	-0.276	11744590 _a_at	trio Rho guanine nucleotide exchange factor	ENSG0000003838 2 /// OTTHUMG000001 31057	NM_007118	0,40	8,14	0,0044831	0,14	8,14	0,2661869	
TRIO	1	0	ENST0000 0344204.4	-0.276	11724261 _a_at	trio Rho guanine nucleotide exchange factor	ENSG0000003838 2 /// OTTHUMG000001 31057	NM_007118	1,30	7,46	0,0000002	0,74	7,46	0,0001795	
TRMT13	0	1	ENST0000 0370141.2	-0.110	11760405 _x_at	tRNA methyltransfera se 13 homolog (S. cerevisiae)	ENSG0000012243 5 /// OTTHUMG000000 10841	NM_019083	0,43	7,64	0,0009904	0,25	7,64	0,0317208	
TRMT13	0	1	ENST0000 0370141.2	-0.110	11745452 _a_at	tRNA methyltransfera se 13 homolog (S. cerevisiae)	ENSG0000012243 5 /// OTTHUMG000000 10841	NM_019083	0,53	5,44	0,0005933	0,28	5,44	0,0395320	
TRMT13	0	1	ENST0000 0370141.2	-0.110	11745453 _x_at	tRNA methyltransfera se 13 homolog (S. cerevisiae)	ENSG0000012243 5 /// OTTHUMG000000 10841	NM_019083	0,50	6,96	0,0000390	0,32	6,96	0,0025149	
TRMT13	0	1	ENST0000 0370141.2	-0.110	11746421 _a_at	tRNA methyltransfera se 13 homolog (S. cerevisiae)	ENSG0000012243 5 /// OTTHUMG000000 10841	NM_019083	0,55	7,75	0,0000054	0,26	7,75	0,0064261	
TRMT13	0	1	ENST0000 0370141.2	-0.110	11761560 _x_at	tRNA methyltransfera se 13 homolog (S. cerevisiae)	ENSG0000012243 5 /// OTTHUMG000000 10841	NM_019083	0,40	8,00	0,0005903	0,22	8,00	0,0336779	
TSC22D2	0	1	ENST0000 0361875.3	-0.056	11750085 _a_at	TSC22 domain family, member 2	ENSG0000019642 8 /// OTTHUMG000001 59744	NM_00130326 4 /// NM_014779	0,36	7,32	0,0020318	0,24	7,32	0,0255453	
TSC22D2	0	1	ENST0000 0361875.3	-0.056	11748214 _a_at	TSC22 domain family, member 2	ENSG0000019642 8 /// OTTHUMG000001 59744	NM_00130326 4 /// NM_014779	0,42	8,15	0,0010860	0,18	8,15	0,1120323	
TSLP	0	1	ENST0000 0379706.4	-0.148	11744760 _s_at	thymic stromal lymphopoietin	ENSG0000014577 7 /// OTTHUMG000001 28791	NM_033035 /// NM_138551	0,47	3,41	0,0015137	0,53	3,41	0,0004835	
TXNRD1	1	0	ENST0000 0378070.4	-0.066	11750416 _a_at	thioredoxin reductase 1	ENSG0000019843 1 /// OTTHUMG000001 66481	NM_00109377 1 /// NM_00126144 5 /// NM_00126144 6 /// NM_003330 /// NM_182729 /// NM_182742 ///	0,34	11,15	0,0015979	0,34	11,15	0,0015537	

								NM_182743							
TXNRD1	1	0	ENST0000 0378070.4	-0.066	11715650 _a_at	thioredoxin reductase 1	ENSG0000019843 1 /// OTTHUMG000001 66481	NM_00109377 1 /// NM_00126144 5 /// NM_00126144 6 /// NM_003330 /// NM_182729 /// NM_182742 /// NM_182743	0,37	11,29	0,0003494	0,33	11,29	0,0009310	
UBE2W	1	0	ENST0000 0517608.1	-0.277	11750058 _a_at	ubiquitin-conjugating enzyme E2W (putative)	ENSG0000010434 3 /// OTTHUMG000001 64517	NM_00100148 1 /// NM_00100148 2 /// NM_00127101 5 /// NM_018299	0,47	7,27	0,0000107	0,20	7,27	0,0175297	
USP15	1	1	ENST0000 0353364.3	-0.242	11746454 _a_at	ubiquitin specific peptidase 15	ENSG0000013565 5 /// OTTHUMG000001 70186	NM_00125207 8 /// NM_00125207 9 /// NM_006313	0,33	8,12	0,0004378	0,15	8,12	0,0727080	
USP15	1	1	ENST0000 0353364.3	-0.242	11744582 _a_at	ubiquitin specific peptidase 15	ENSG0000013565 5 /// OTTHUMG000001 70186	NM_00125207 8 /// NM_00125207 9 /// NM_006313	0,30	4,93	0,0397156	0,15	4,93	0,2862970	
USP38	0	1	ENST0000 0307017.4	-0.129	11762389 _at	ubiquitin specific peptidase 38	ENSG0000017018 5 /// OTTHUMG000001 61420	NM_00129032 5 /// NM_00129032 6 /// NM_032557	0,70	4,26	0,0006797	0,66	4,26	0,0010789	
UTP23	0	1	ENST0000 0309822.2	-0.201	11731502 _at	UTP23, small subunit (SSU) processome component, homolog (yeast)	ENSG0000014767 9 /// OTTHUMG000001 64958	NM_032334	0,41	8,14	0,0001672	0,19	8,14	0,0356038	
VGLL3	1	1	ENST0000 0398399.2	-0.275	11757631 _s_at	vestigial-like family member 3	ENSG0000020653 8 /// OTTHUMG000001 58984	NM_016206	0,34	7,29	0,0205852	0,06	7,29	0,6744830	
WASL	1	0	ENST0000 0223023.4	-0.268	11717284 _a_at	Wiskott-Aldrich syndrome-like	ENSG0000010629 9 /// OTTHUMG000001 57346	NM_003941	0,41	8,54	0,0038344	0,00	8,54	0,9778441	
WASL	1	0	ENST0000 0223023.4	-0.268	11717285 _a_at	Wiskott-Aldrich syndrome-like	ENSG0000010629 9 /// OTTHUMG000001 57346	NM_003941	0,31	5,89	0,0092920	0,28	5,89	0,0146955	
WDR3	0	1	ENST0000 0349139.5	-0.031	11751592 _a_at	WD repeat domain 3	ENSG0000006518 3 /// OTTHUMG000000	NM_006784	0,55	6,65	0,0022737	0,18	6,65	0,2539747	

							12197								
WDR36	0	1	ENST0000 0506538.2	-0.109	11723738 _a_at	WD repeat domain 36	ENSG0000013498 7 /// OTTHUMG000001 28790	NM_139281	0,34	8,01	0,0005272	0,10	8,01	0,2389338	
WHSC1	1	0	ENST0000 0382895.3	-0.078	11762563 _at	Wolf-Hirschhorn syndrome candidate 1	ENSG0000010968 5 /// OTTHUMG000001 21147	NM_00104242 4 /// NM_007331 /// NM_014919 /// NM_133330 /// NM_133331 /// NM_133332 /// NM_133333 /// NM_133334 /// NM_133335 /// NM_133336	0,31	4,72	0,0081655	0,12	4,72	0,2469883	
WNK1	0	1	ENST0000 0315939.6	-0.049	11737175 _at	WNK lysine deficient protein kinase 1	ENSG0000006023 7 /// OTTHUMG000000 90321	NM_00118498 5 /// NM_014823 /// NM_018979 /// NM_213655	0,44	4,48	0,0036880	0,06	4,48	0,6305368	
WNK1	0	1	ENST0000 0315939.6	-0.049	11743280 _a_at	WNK lysine deficient protein kinase 1	ENSG0000006023 7 /// OTTHUMG000000 90321	NM_00118498 5 /// NM_014823 /// NM_018979 /// NM_213655	0,33	8,86	0,0015675	-0,03	8,86	0,7642621	
YWHAE	1	0	ENST0000 0264335.8	-0.302	11762793 _at	tyrosine 3-monooxygenas e/tryptophan 5-monooxygenas e activation protein, epsilon	ENSG0000010895 3 /// ENSG0000027447 4 /// OTTHUMG000001 34316 /// OTTHUMG000001 90126	NM_006761	0,31	4,87	0,0058799	0,27	4,87	0,0142832	
ZBTB21	0	1	ENST0000 0398505.3	-0.125	11758414 _s_at	zinc finger and BTB domain containing 21	ENSG0000017327 6 /// OTTHUMG000000 86789	NM_00109840 2 /// NM_00109840 3 /// NM_020727	0,30	7,35	0,0044343	0,45	7,35	0,0001228	
ZBTB21	0	1	ENST0000 0398505.3	-0.125	11749652 _a_at	zinc finger and BTB domain containing 21	ENSG0000017327 6 /// OTTHUMG000000 86789	NM_00109840 2 /// NM_00109840 3 /// NM_020727	0,26	5,00	0,0023555	0,39	5,00	0,0000515	
ZBTB6	1	0	ENST0000 0373659.3	-0.254	11729725 _at	zinc finger and BTB domain containing 6	ENSG0000018613 0 /// OTTHUMG000000 20628	NM_006626	0,37	5,50	0,0051811	0,27	5,50	0,0316776	
ZFAND5	1	0	ENST0000 0237937.3	-0.314	11743755 _s_at	zinc finger, AN1-type domain 5	ENSG0000010737 2	NM_00110242 0 /// NM_00110242 1 /// NM_00127824 3 ///	0,39	7,93	0,0004868	0,24	7,93	0,0155887	

								NM_001278244 /// NM_001278245 /// NM_006007							
ZFAND5	1	0	ENST00000237937.3	-0.314	11743753_x_at	zinc finger, AN1-type domain 5	ENSG00000107372	NM_001102420 /// NM_001102421 /// NM_001278243 /// NM_001278244 /// NM_001278245 /// NM_006007	0,41	7,49	0,0001095	0,21	7,49	0,0184423	
ZFAND5	1	0	ENST00000237937.3	-0.314	11736118_a_at	zinc finger, AN1-type domain 5	ENSG00000107372	NM_001102420 /// NM_001102421 /// NM_001278243 /// NM_001278244 /// NM_001278245 /// NM_006007	0,43	7,57	0,0000350	0,28	7,57	0,0020883	
ZFC3H1	1	0	ENST00000378743.3	-0.412	11762631_a_at	zinc finger, C3H1-type containing	ENSG00000133858 /// OTTHUMG00000169545	NM_144982	0,78	4,48	0,0001498	0,94	4,48	0,0000194	
ZFC3H1	1	0	ENST00000378743.3	-0.412	11762632_at	zinc finger, C3H1-type containing	ENSG00000133858 /// OTTHUMG00000169545	NM_144982	0,78	4,12	0,0002861	0,51	4,12	0,0086195	
ZFP36L1	2	0	ENST00000555997.1	-0.950	11726889_at	ZFP36 ring finger protein-like 1	ENSG00000185650	NM_001244698 /// NM_001244701 /// NM_004926	1,02	6,54	0,0000960	1,56	6,54	0,0000006	
ZKSCAN8	0	1	ENST00000330236.6	-0.050	11737829_at	zinc finger with KRAB and SCAN domains 8	ENSG00000198315	NM_001278119 /// NM_001278121 /// NM_001278122 /// NM_006298	0,39	3,56	0,0075427	0,07	3,56	0,5873911	
ZNF134	0	2	ENST00000396161.5	-0.108	11731497_a_at	zinc finger protein 134	ENSG00000213762 /// OTTHUMG00000183471	NM_003435	0,32	7,01	0,0012137	0,30	7,01	0,0021637	
ZNF134	0	2	ENST00000396161.5	-0.108	11731498_a_at	zinc finger protein 134	ENSG00000213762 /// OTTHUMG00000183471	NM_003435	0,30	6,70	0,0044673	0,36	6,70	0,0010167	

ZNF141	0	1	ENST0000 0240499.7	-0.205	11759239 _at	zinc finger protein 141	---	NM_003441	0,26	5,04	0,0344705	0,31	5,04	0,0123742	
ZNF226	0	2	ENST0000 0588883.1	-0.294	11743472 _a_at	zinc finger protein 226	ENSG0000016738 0 /// OTTHUMG000001 82351	NM_00103237 2 /// NM_00103237 3 /// NM_00103237 4 /// NM_00103237 5 /// NM_00114622 0 /// NM_015919 /// NM_016444	0,39	7,48	0,0001922	0,29	7,48	0,0022389	
ZNF226	0	2	ENST0000 0588883.1	-0.294	11743473 _x_at	zinc finger protein 226	ENSG0000016738 0 /// OTTHUMG000001 82351	NM_00103237 2 /// NM_00103237 3 /// NM_00103237 4 /// NM_00103237 5 /// NM_00114622 0 /// NM_015919 /// NM_016444	0,32	7,55	0,0009423	0,40	7,55	0,0001130	
ZNF234	0	3	ENST0000 0426739.2	-0.263	11732421 _at	zinc finger protein 234	ENSG0000026300 2 /// OTTHUMG000001 82337	NM_00114482 4 /// NM_006630	0,33	6,64	0,0475779	-0,17	6,64	0,3031015	
ZNF253	0	1	ENST0000 0589717.1	-0.117	11739672 _x_at	zinc finger protein 253	ENSG0000025677 1 /// OTTHUMG000001 82369	NM_021047	0,40	5,37	0,0244790	0,21	5,37	0,2089409	
ZNF254	0	1	ENST0000 0357002.4	-0.180	11749641 _x_at	zinc finger protein 254	ENSG0000021309 6 /// OTTHUMG000001 83394	NM_00127866 1 /// NM_00127866 2 /// NM_00127866 3 /// NM_00127866 4 /// NM_00127866 5 /// NM_00127867 7 /// NM_00127867 8 /// NM_004876 /// NM_203282	0,53	5,87	0,0082750	0,49	5,87	0,0140215	
ZNF267	0	1	ENST0000 0300870.1 0	-0.198	11754869 _s_at	zinc finger protein 267	ENSG0000018594 7 /// OTTHUMG000001 76535	NM_00126558 8 /// NM_003414	0,44	7,17	0,0001252	0,49	7,17	0,0000337	

ZNF267	0	1	ENST0000 0300870.1 0	-0.198	11727522 _a_at	zinc finger protein 267	ENSG0000018594 7 /// OTTHUMG000001 76535	NM_00126558 8 /// NM_003414	0,34	7,45	0,0036607	0,49	7,45	0,0001627	
ZNF267	0	1	ENST0000 0300870.1 0	-0.198	11727523 _x_at	zinc finger protein 267	ENSG0000018594 7 /// OTTHUMG000001 76535	NM_00126558 8 /// NM_003414	0,40	8,39	0,0005701	0,51	8,39	0,0000460	
ZNF451	1	0	ENST0000 0370708.4	-0.228	11760921 _a_at	zinc finger protein 451	ENSG0000011220 0 /// OTTHUMG000000 14916	NM_00103162 3 /// NM_00125727 3 /// NM_015555	0,43	5,65	0,0005783	0,16	5,65	0,1246583	
ZNF460	0	2	ENST0000 0360338.3	-0.069	11740310 _a_at	zinc finger protein 460	ENSG0000019771 4 /// OTTHUMG000001 83222	NM_006635	0,32	3,85	0,0103505	0,37	3,85	0,0041294	
ZNF460	0	2	ENST0000 0360338.3	-0.069	11740309 _a_at	zinc finger protein 460	ENSG0000019771 4 /// OTTHUMG000001 83222	NM_006635	0,42	3,50	0,0184184	0,28	3,50	0,1080020	
ZNF566	0	2	ENST0000 0454319.1	-0.248	11732294 _a_at	zinc finger protein 566	ENSG0000018601 7 /// OTTHUMG000000 48148	NM_00114534 3 /// NM_00114534 4 /// NM_00114534 5 /// NM_00130097 0 /// NM_032838	0,51	5,82	0,0000579	0,29	5,82	0,0073065	
ZSWIM7	0	1	ENST0000 0486655.1	-0.131	11755505 _a_at	zinc finger, SWIM-type containing 7	ENSG0000021494 1 /// OTTHUMG000000 59308	NM_00104269 7 /// NM_00104269 8	0,44	7,65	0,0000467	0,28	7,65	0,0027347	

Appendix 1

Circulating miR-182 is a biomarker of colorectal adenocarcinoma progression

Lisa Perilli[1,*], Caterina Vicentini[3,*], Marco Agostini[4,5], Silvia Pizzini[6], Marco Pizzi[7], Edoardo D'Angelo[3], Stefania Bortoluzzi[6], Susanna Mandruzzato[1,2], Enzo Mammano[4], Massimo Rugge[7], Donato Nitti[4], Aldo Scarpa[3,8], Matteo Fassan[3,8] and Paola Zanovello[1,2]

[1] Oncology and Immunology Section, Department of Surgery, Oncology and Gastroenterology, University of Padua, Padua, Italy

[2] Istituto Oncologico Veneto (IOV), IRCCS, Padua, Italy

[3] ARC-NET Research Centre, University of Verona, Verona, Italy

[4] Department of Surgery, Oncology and Gastroenterology, Surgery Section University of Padua, Padua, Italy

[5] Istituto di Ricerca Pediatrica - Citta' della Speranza, Padua, Italy

[6] Department of Biology, University of Padua, Padua, Italy

[7] Department of Medicine, Surgical Pathology & Cytopathology Unit, University of Padua, Padua, Italy

[8] Department of Pathology and Diagnostics, University of Verona, Verona, Italy

[*] These authors contributed equally to this work

***Correspondence to**: Matteo Fassan, **email**: matteo.fassan@gmail.com*

Keywords: miR-182, colon cancer, biomarkers, plasma

***Received**: June 03, 2014* ***Accepted**: July 22, 2014* ***Published**: July 23, 2014*

ABSTRACT

MiR-182 expression was evaluated by qRT-PCR and *in situ* hybridization in 20 tubular adenomas, 50 colorectal carcinoma (CRC), and 40 CRC liver metastases. Control samples obtained from patients with irritable bowel syndrome, or tumor-matched normal colon mucosa were analyzed (n=50). MiR-182 expression increased progressively and significantly along with the colorectal carcinogenesis cascade, and in CRC liver metastases. The inverse relation between miR-182 and the expression of its target gene *ENTPD5* was investigated by immunohistochemical analysis. We observed that normal colocytes featured a strong ENTPD5 cytoplasmic expression whereas a significantly and progressively lower expression was present along with dedifferentiation of the histologic phenotype. Plasma samples from 51 CRC patients and controls were tested for miR-182 expression. Plasma miR-182 concentrations were significantly higher in CRC patients than in healthy controls or patients with colon polyps at endoscopy. Moreover, miR-182 plasma levels were significantly reduced in post-operative samples after radical hepatic metastasectomy compared to preoperative samples. Our results strengthen the hypothesis of a central role of miR-182 dysregulation in colon mucosa transformation, demonstrate the concomitant progressive down-regulation of ENTPD5 levels during colon carcinogenesis, and indicate the potential of circulating miR-182 as blood based biomarker for screening and monitoring CRC during the follow-up.

INTRODUCTION

Colorectal cancer (CRC) is the third most common cancer and the third leading cause of cancer death in men and women in the United States [1]. Metastatic spread remains the ultimate cause of cancer-related death in most CRC cases, and 20-25% of patients present metastatic disease at diagnosis [2, 3]. While localized

CRC (stage I-II) is curable by surgical excision, only about 70% of stage III CRC cases with regional lymph node metastasis are curable by surgery combined with adjuvant chemotherapy. Metastatic disease (stage IV), despite improved survival due to recent advances in chemotherapy, is usually incurable [2, 3]. Therefore, it is of critical importance to understand the molecular alterations involved in CRC development and progression, and identify diagnostic and prognostic biomarkers for improving CRC patients' survival [4, 5].

MicroRNAs (miRNAs) are non-coding RNAs that control gene expression at the post-transcriptional level [6, 7]. Numerous studies have demonstrated that aberrant expressions of specific miRNAs are involved in many cancer types including CRC and can be associated with prognosis and therapeutic outcome [8, 9]. More recently, owing to miRNAs stability against degradation and their detectability in body fluids, the possibility that miRNAs may serve as a novel class of mini-invasive diagnostic biomarkers has been strongly suggested [10, 11]. Controversial data exist on miR-182 dysregulation in human cancer. miR-182 is up-regulated in ovarian cancer, melanoma, and hepatocellular carcinoma [12-14]; conversely, miR-182 is down-regulated in gastric adenocarcinoma and lung cancer [15-17]. These results suggest a key role of miR-182 in carcinogenesis, possibly with different mechanisms in various cancer subtypes.

In their seminal article, Sarver and colleagues reported an up-regulation of miR-182 in a small series of CRCs by using miRNA microarray expression analysis [18]. Surprisingly, two following studies have not found any difference in the expression of miR-182 between tumor and normal tissue [19, 20]. More recently, miR-182 expression has been associated to adverse CRC clinical characteristics and poor prognosis [21, 22]. By using a large data set of miRNAs expression profiles in normal colon mucosa, primary tumor and liver metastases of CRC samples, our group recently demonstrated that miR-182 was one of the most up-regulated in the transition from normal colon mucosa to primary tumor. Moreover, by integrating miRNAs and genes expression profiles, we identified ENTPD5 as a target gene of miR-182 [23].

In the present study, we further investigated the involvement of miR-182 in the transformation of the colon mucosa and CRC progression, and also extended the analysis of the relationship among miR-182 expression and its target gene ENTPD5. Moreover, we explored the diagnostic and prognostic value of circulating miR-182 as a potential biomarker for CRC patients monitoring.

RESULTS

miR-182 is up-regulated during colon carcinogenesis and metastatic process

To extend our previous findings on high miR-182 expression in CRC [24], we investigated its expressions in the colic adenoma-carcinoma sequence. To this aim, miR-182 expression was analyzed by qRT-PCR in a series of FFPE samples including 10 normal colic mucosa, 20 tubular adenomas low-grade [LG] and high-grade [HG] intraepithelial neoplasia [IEN, formerly known as dysplasia], and 10 early primary stages CRC. We observed a significant up-regulation of miR-182 in tubular adenomas with LG-IEN (2.35-fold change; *t*-test, p=0.006), tubular adenomas with HG-IEN (4.63-fold change; *t*-test, p=0.030), and in CRCs (15.2-fold change; *t*-test, p=0.020) (Figure 1A) in comparison to normal colic mucosa. Overall, miR-182 expression increased progressively and significantly along with the carcinogenesis cascade (ANOVA, p<0.001).

To study miR-182 dysregulation in CRC liver metastases, we investigated miR-182 expression by qRT-PCR in a series of 20 stage IV CRCs (Figure 1B). A significant overexpression of miR-182 was observed both in primary CRCs (5.3-fold change; paired *t*-test, p<0.0001), and CRC liver metastases (7.5-fold change; paired *t*-test, p=0.005) compared to normal tissues. Metastatic samples showed a higher, but not significant, miR-182 expression in comparison to primary tumors.

We also investigated miR-182 expression by ISH in 5 cases of stage IV CRCs. A consistently significant overexpression in paired primary tumors and CRC liver metastasis in comparison to normal colon mucosa was observed in all the tested samples (Figure 1C). miR-182 expression was detectable as a granular blue cytoplasmic staining consistently expressed by cancerous epithelia, whereas normal colocytes showed a negative or faint staining.

To further strengthen these results, we evaluated the prognostic impact of miR-182 expression on a large number of CRCs in The Cancer Genome Atlas (TCGA) CRC series (n=393). Interestingly, miR-182 expression was significantly higher in CRCs presenting lymph node (*t*-test, p=0.041) or liver metastases (*t*-test, p=0.022) at diagnosis. In univariate analysis, and considering the median miR-182 value as a cut-off limit, miR-182 expression levels negatively correlated with the overall survival of patients (Mantel-Cox log-rank test, p=0.035) (data not shown).

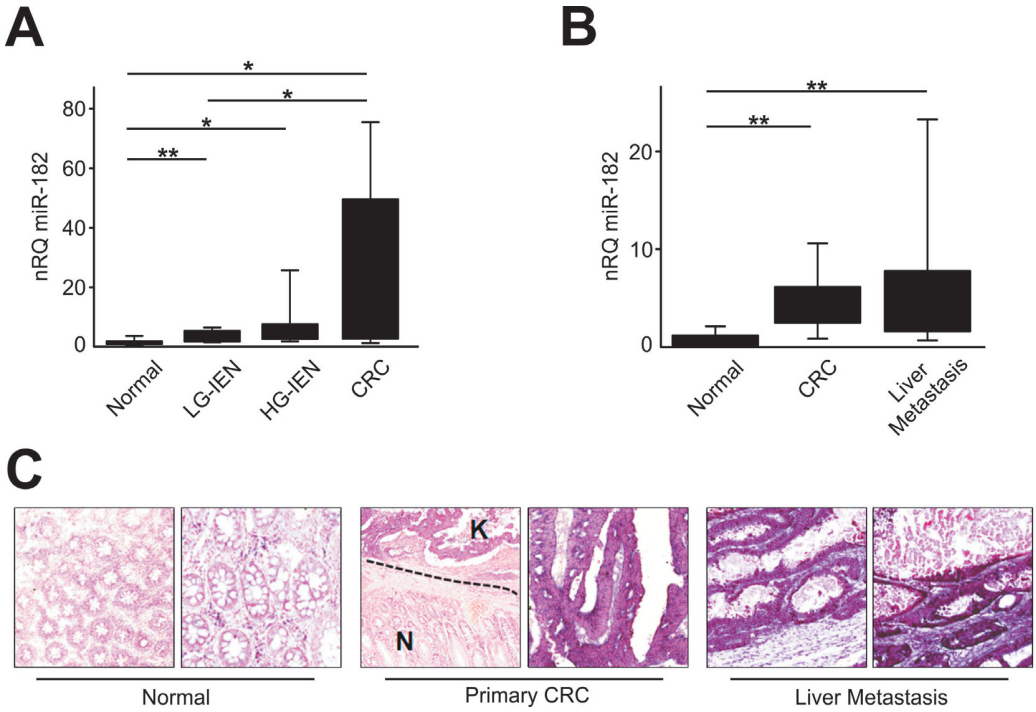

Figure 1: miR-182 is up-regulated during colon carcinogenesis. (A) miR-182 expression was evaluated by qRT-PCR after RNA extraction from FFPE samples of colon normal mucosa, LG-IEN, HG-IEN lesions and CRCs. **(B)** miR-182 expression was evaluated by qRT-PCR in matched surgical samples of normal colon mucosa, primary CRC and liver metastatis. **(C)** Representative ISH evaluation of miR-182 in matched tissue sections of normal colon, primary tumor and metastatic CRC (N= normal colon mucosa; K= primary CRC). The presence of miR-182 is shown by a grainy blue cytoplasmic stain; slides counterstained in fast red. (Original magnifications 10x and 20x). Significance (Student's *t* test); *p<0.05; **p<0.01. nRQ, normalized Relative Quantity. Data were expressed as mean values ± SD.

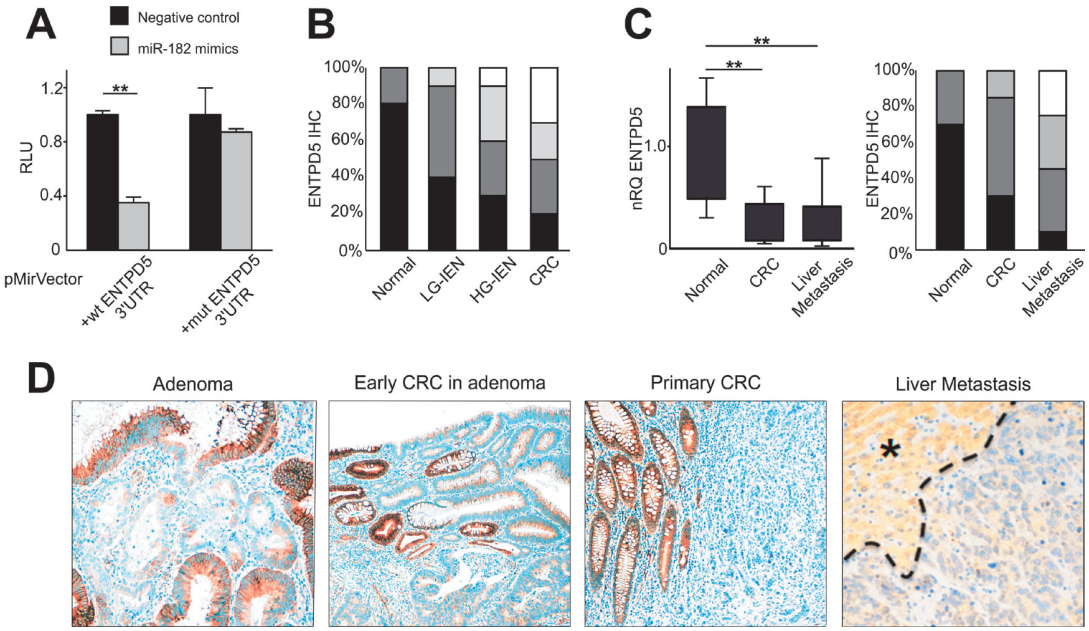

Figure 2: miR-182 targets ENTPD5 during colon carcinogenesis. (A) Luciferase reporter assay of miR-182 and 3′UTR ENTPD5 region. Relative light units (RLU) of biological replicates are shown as means ± standard deviation (SD) of three experiments performed in triplicate. Mutation of the binding site completely restored luciferase expression. (B) ENTPD5 IHC scores distribution (expressed as %) was significantly down-regulated during colorectal carcinogenesis (p<0.001). (C) ENTPD5 expression, as assessed by both qRT-PCR and IHC, is significantly lower in primary and metastatic CRCs in comparison to normal colic mucosa. (D) Representative examples of ENTPD5 expression during colon carcinogenesis. (Original magnifications 10x and 20x ; * liver parenchyma). Significance (Student's *t* test); *p<0.05; **p<0.01. Immunohistochemical scores: *black* = score 3 (% positive cases), *dark gray* = score 2, *light gray* = score 1, *white* = score 0 (% negative cases). nRQ, normalized Relative Quantity. Data were expressed as mean values ± SD.

miR-182 targets ENTPD5 during colon carcinogenesis

By means of luciferase mutagenesis reporter assay we confirmed the relationship between miR-182 and its target gene ENTPD5. Luciferase activity was reduced 2.0 fold by miR-182 expression in HEK293T cells transfected with wild-type ENTPD5-reporter. Mutation of the predicted MRE (miRNA response-element) completely restored luciferase expression, thus demonstrating a direct interaction between miR-182 and the 3' UTR of ENTPD5 transcript (Figure 2A).

To support this finding at protein level, we investigated by IHC the expression of ENTPD5 during colorectal carcinogenesis in a series of 20 normal colic mucosa samples, 40 tubular adenomas (LG-IEN and HG-IEN), and 20 early primary stages CRCs. Normal colocytes featured strong ENTPD5 cytoplasmic immunostaining whereas a significant and progressive lower expression was observed along with the dedifferentiation of the histologic phenotype (Kruskal-Wallis test for trend, $p<0.001$; Figure 2B and 2D). A heterogeneous pattern of staining was observed in colic adenomas (Figure 2D).

We tested ENTPD5 expression level also in CRC liver metastases (20 matched cases). By using qRT-PCR and IHC, we demonstrated at mRNA and protein level a significant down-regulation of ENTPD5 from normal colon mucosa, through primary CRC tumor to liver metastases (both $p<0.001$; Figure 2C). Overall, our results clearly indicate that the expression of ENTPD5 is significantly down-regulated in primary and metastatic CRC, as compared to normal tissue (Figure 2), thus confirming the relationship between miR-182 and its target.

Evaluation of plasma miR-182 levels in CRC patients

We hypothesized that the higher miR-182 expression in primary and metastatic CRC tissues could influence the miR-182 expression in the plasma of CRC patients. We thus analyzed miR-182 plasma levels in 10 healthy volunteers, 10 patients with colic adenomas at endoscopy, 10 early stages (stages I and II) and 10 late stages (stages III and IV) CRC patients.

Plasma miR-182 concentrations were significantly higher in CRC patients than in healthy controls (3.2-fold change; *t*-test, $p=0.008$) or patients with colic polyps at endoscopy (1.14-fold change; *t*-test, $p=0.013$) (Figure 3A). Considering tumor staging, miR-182 plasma expression in both early and advanced CRC patients was significantly higher than in normal controls (*t*-test, $p=0.041$ and $p=0.003$, respectively; Figure 3B).

We also evaluated miR-182 plasma levels before and 30 days after radical liver metastasectomy. Plasma miR-182 concentration was analyzed in paired pre- and post-operative samples from 11 CRC patients who underwent curative liver metastasectomy. We observed that miR-182 plasma levels were significantly reduced one month after surgery (paired *t*-test, $p=0.020$; Figure 3C).

DISCUSSION

The results of the present study can be summarized as follows: i) miR-182 is significantly up-regulated during colon carcinogenesis, and is associated to CRC patients prognosis; ii) miR-182 exerts a suppressive regulation on ENTPD5, suggesting novel molecular pathways in colon carcinogenesis; iii) miR-182 up-regulation can be detected in CRC plasma samples, and is therefore eligible as a novel diagnostic and non-invasive follow-up marker.

Reports on miR-182 involvement in human cancer

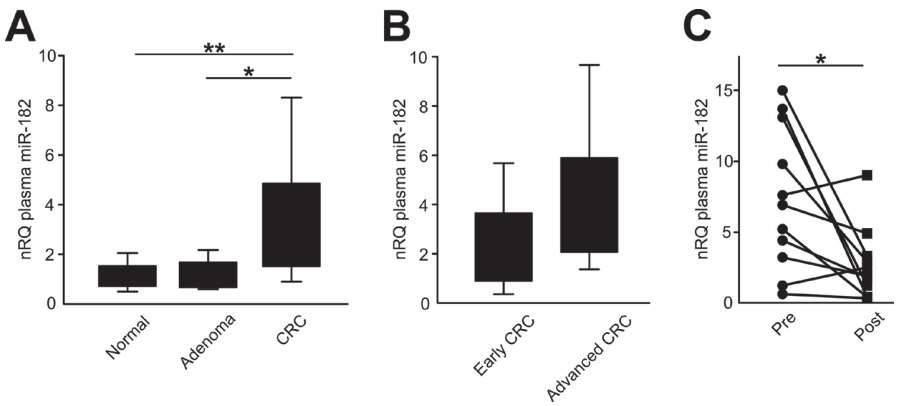

Figure 3: miR-182 plasma levels are significantly elevated in CRC patients. (A) miR-182 plasma levels were analyzed in 10 healthy volunteers, 10 patients with colic adenomas at endoscopy, 10 early stages (stages I and II) and 10 late stages (stages III and IV) CRC patients. **(B)** miR-182 plasma expression in advanced CRC patients and in early CRC patients. **(C)** Plasma miR-182 concentration before and after curative liver metastasectomy ($p=0.020$). Significance (Student's *t* test); *$p<0.05$; **$p<0.01$. nRQ, normalized Relative Quantity. Data were expressed as mean values ± SD.

have been discordant. For instance, miR-182 aberrant expression has been associated to tumor progression in melanoma, endometrial cancer and prostate carcinoma [13, 16, 25, 26]; in contrast, a tumor-suppressive role has been established in gastric adenocarcinoma, where miR-182 overexpression leads to the suppression of tumor cell growth [15].

More recently, miR-182 enhanced expression has been associated to adverse CRC clinical characteristics and poor prognosis [21, 22]. miR-182 prognostic impact is also supported by our elaboration of data from TCGA CRC cohort showing higher miR-182 expression in more advanced stages of CRC, and shorter survival in patients with high miR-182 expression levels. These findings are consistent with miR-182 plasma levels, which are higher in advanced CRC patients.

MiR-182 dysregulation in CRC has been associated to the targeting of the anti-angiogenic factor TSP-1. Moreover, anti-miR-182 exerts a transcriptional regulatory mechanism of TSP-1 modulating Egr-1 and Sp-1 function [27]. In our previous study, we identified post-transcriptional regulatory networks with miRNAs differentially expressed in the transition from normal mucosa through primary tumor to metastases. We observed that miR-182 is one of the most up-regulated miRNAs and, according to the reconstructed networks, has several putative target genes, some of which are significantly differentially expressed in the same comparisons [23]. Among these predicted interactions, a few have been already validated in cancer. For instance, it has been demonstrated that miR-182 acts as an oncogenic miRNA by interacting and negatively regulating PDCD4 in ovarian and lung cancer [28, 29]. Regarding other putative targets, such as SEMA6D, RGS2 and ANGPTL1, their involvement and modulation in cancer has been demonstrated but their interaction with miR-182 have yet to be explored. In the present paper, we definitively demonstrated that ENTPD5 is a target of miR-182 and confirmed the inverse correlation between miR-182 and ENTPD5 expression in CRC samples at both mRNA and protein level. Our results are in line with that recently published by Mikula *et al.* who showed that both ENTPD5 mRNA and protein levels progressively decrease during the transition from normal colon mucosa, through adenoma, to adenocarcinoma [30].

ENTPD5 belongs to a family of UDP-hydrolyzing enzymes and has been alternatively linked, depending on the different tumor cell system analyzed, to ATP consumption as well as protein folding [31]. Moreover, the expression of its mutated counterpart, better known as mt-PCPH, has been associated with its enhanced oncogenic activity, thus suggesting the proactive function of this enzyme as a proto-oncoprotein in tumor development [32]. However, owing to the discrepant results obtained in the different tumor types, the molecular functions played by ENTPD5 protein in CRC deserve further investigation.

We report here the first data about miR-182 plasma expression in CRC patients. Many studies have evaluated the feasibility of circulating miRNAs for detecting early stage cancer and as a prognostic/predictive marker. Ng *et al.* recently faced this issue by comparing miRNAs expression profiles in tissue and plasma, and evaluating miRNAs that were differentially expressed in both groups of samples [19]. MiR-17-3p and miR-92, belonging to the same miRNA gene cluster and classified as oncogenic, were validated as differentially expressed in CRC plasma and tissue, in comparison to their normal counterparts [19]. By miRNA profiling and subsequent validation, miR-601 and miR-760 were also suggested as potential diagnostic biomarkers of adenomas and CRC by the same group. Combining miR-29a, miR-92a, and miR-760, the detection sensitivity of early stages of CRC was further improved [33]. Another study which undertook a genome-wide miRNA profiling of plasma, identified miR-15b, miR-19a, miR-19b, miR-29a, and miR-335 as being able to differentiate CRC patients from healthy individuals, while miR-18a could do so also between advanced adenomas and healthy individuals [34].

In the present report, we pinpointed miR-182 plasma levels evaluation as a promising approach to enhance the repertoire for non-invasive CRC monitoring and screening. The main limitation of our analyses is the limited samples size, which affects any statistical evaluation of circulating miR-182 expression and its relationship to clinicopathological variables. Nevertheless, this study has several important clinical implications. First, the specific involvement of miR-182 in CRCs indicates its potential to be developed into a diagnostic marker for these patients. Secondly, miR-182 alone or in combination with its target genes (ENTPD5, TSP-1, PDCD4) may serve as prognostic marker for the monitoring of relapse of CRC patients. Thirdly, high miR-182 expression in advanced CRCs suggests that this miRNA could be an ideal candidate target for CRC treatment, though its diagnostic impact should be further tested in larger series of CRC patients.

MATERIAL AND METHODS

Patients

A total of 240 histopathological and 51 plasma samples from 211 patients (M/F 114/97; age 69.5 ± 12.3) were considered and included in this study, as schematized in Table 1.

All the histopathological samples were retrospectively collected from the files of the Surgical Pathology & Cytopathology Unit at the University of Padua. First 90 endoscopic biopsy samples were obtained from patients with different types of sporadic colonic polyps (i.e., 30 tubular adenomas with LG-IEN, 30 tubular

Table 1: Schematic diagram of the present study

Samples	# patients	Normal colon	LG-IEN	HG-IEN	CRC	CRC liver metastasis	Techniques applied
Endoscopic biopsies	40	10	10	10	10	-	qRT-PCR for miR-182
	80	20	20	20	20	-	IHC for ENTPD5
Surgical specimens	20	20	-	-	20	20	qRT-PCR for miR-182
	20	20	-	-	20	20	qRT-PCR and IHC for ENTPD5 ISH for miR-182
Plasma	51	10	10		31		qRT-PCR for miR-182
TOTAL		70 tissue 10 plasma	60 tissue 10 plasma		110 tissue 31 plasma		-

adenomas with HG-IEN), and 30 from patients with stage I-II CRCs. Another 30 normal colonic mucosa biopsy samples were obtained from patients who underwent colonoscopy for irritable bowel syndrome.

A further series of 40 stage IV CRCs were considered, and the following samples collected: i) normal colic mucosa taken at a minimum distance of 10 centimeters from the primary tumor site; ii) primary CRC; iii) CRC liver metastasis. Tumor characteristics were obtained both from the gross description of the specimen, as recorded at the time of surgery, and from the original histopathology report.

A series of 51 plasma samples were retrieved from the archives of the Surgery Unit at the University of Padua (Department of Surgery, Oncology and Gastroenterology). Plasma samples were collected from 10 healthy volunteers and at coloscopy from 10 patients with colic adenomas, 10 early stages (stages I and II) and 10 late stages (stages III and IV) CRC patients. A series of 11 stage IV CRC patients was also considered, and plasma samples were available at surgery and after 30 days from radical hepatic metastasectomy.

Patients with a known history of a hereditary colorectal cancer syndrome and which underwent neoadjuvant treatments were excluded. The Ethics Committee of the University Hospital of Padua approved the study on histopathological material (n. 57841 December 3rd 2013). All patients provided written informed consent.

TCGA data analysis

Data from TCGA pilot project established by the NCI and NHGR were explored (15th February 2014) for miR-182 expression in the TCGA colorectal cancer series [35]. Information about TCGA and the investigators and institutions that constitute the TCGA research network can be found at "http://cancergenome.nih.gov".

RNA isolation

Biopsy and tissue samples were manually microdissected to ensure that each sample contained at least 80% of tumor cells. The percentage of the target lesion as obtained by manual microdissection was further validated on an adjunctive hematoxylin and eosin histology section. Total RNA was extracted using the RecoverAll kit (Ambion, Austin, TX), according to the manufacturer's instructions.

In plasma samples, 500 µl of human plasma was thawed on ice and lysed with an equal volume of 2X Denaturing Solution (Ambion). To allow for normalization of sample-to-sample variation in RNA isolation, synthetic *C. elegans* miRNAs cel-miR-39, cel-miR-54, and cel-miR-238 (synthetic RNA oligonucleotides synthesized by Qiagen) were added (as a mixture of 7 pg/pl of each oligonucleotide) to each denatured sample (i.e., after combining the plasma sample with Denaturing Solution) with the exception of cel-miR-238, which was added after cDNA assembly. RNA was isolated using the mirVana PARIS kit following the manufacturer's protocol for liquid samples (Ambion). RNA was eluted with 50 µl of RNase-free H_2O.

qRT-PCR analysis

RNA extraction and quality controls were performed as previously described [23].

Total RNA (1 µg) was used for first-strand cDNA synthesis using the SuperScript™ II Reverse Transcriptase kit and Taqman Assay (Invitrogen by Life Technologies Inc., Monza, Italy) to detect and quantify ENTPD5 mRNA. To study mature hsa-miR-182 expression, the TaqMan MicroRNA Reverse Transcription Kit (Invitrogen) was used according to the manufacturer's instructions [23].

All reactions were run in triplicate, including no template controls, in a LightCycler 480 Real-Time System (Roche Diagnostics, Mannheim, Germany). Normalized expression was calculated using the comparative Ct method, and the fold change was expressed as $2^{-\Delta\Delta Ct}$.

For plasma samples, normalization was reached

using a median normalization procedure, as previously described with minor modifications [36]. For each sample, the Ct values obtained for the three spiked-in *C. elegans* miRNAs and for hsa-miR-16 were averaged to generate SpikeIn_Average_Ct values. The median of the SpikeIn_Average_Ct values obtained from all of the samples to be compared was next calculated (designated as the Median_SpikeIn_Ct value). The hsa-miR-182 raw Ct in a given sample was adjusted as follows: Normalized_Ct value for the miRNA in the sample = Raw_Ct value - [(SpikeIn_Average_Ct value of the given sample) - (Median_SpikeIn_Ct value)]. All reactions were run in triplicate, including no-template controls.

In situ RNA hybridization (ISH)

Locked nucleic acid (LNA) probes with complementarity to 21-bp sections of miR-182 were labeled with 5′-digoxigenin and synthesized by Exiqon (Copenhagen, Denmark). Tissue sections were digested with ISH protease 1 (Ventana Medical Systems, Milan, Italy) and ISH performed as described, with minor modifications [37]. Positive (U6; Exiqon) and negative scrambled LNA probes were used as controls.

Luciferase reporter assay

HEK293T cells transfection was carried out as previously described [23]. The pMir-ENTPD5 reporter construct with mutations in the seed sequence of miR-182 binding was synthesized using QuickChange Site-Directed Mutagenesis Kit (Stratagene, CA). Cells were cotransfected with miCENTURY OX miNatural for hsa-miR-182 or non-target RNA (Tema ricerca, Bologna, Italy) as negative control, in triplicate. Luciferase and Renilla activity were measured 30 h after transfection using the Dual-Glo Luciferase Assay System (Promega) according to the manufacturer's instructions. Three independent experiments were performed and the data are presented as the mean ± SD. Luciferase activity values were normalized to Renilla activity as relative light unit (RLU).

Statistical analysis

Differences in miR-182 expression were evaluated by t-test, paired t-test and ANOVA, as appropriate. IHC data were evaluated by Kruskal-Wallis test for trend. Survival analysis on TCGA data was carried out by applying the Log-rank Mantel-Cox test. The statistical analysis was performed using STATA software (Stata Corporation, College Station, Texas, USA).

ACKNOWLEDGEMENTS/GRANT SUPPORT

This research was supported by the Italian Association for Cancer Research (AIRC grants n. 12182 to AS, and 6421 to MR, AS, DN, and PZ). The funding agency had no role in the design and performance of the study. LP is recipient of an AIRC Fellowship.

Authors' contributions

All authors approved the final version of the manuscript. Study concept and design: LP, MF, PZ. Acquisition of data: LP, CV, MA, SP, MP, EDA, SB, EM. Analysis and interpretation of data: MA, SB, SM, MR, DN, AS, MF, PZ. Drafting of the manuscript: LP, CV, MF, MA, PZ.

Potential competing interests

The authors have no competing interests to declare.

REFERENCES

1. Siegel R, Desantis C and Jemal A. Colorectal cancer statistics, 2014. CA Cancer J Clin. 2014; 64(2):104-117.
2. Cunningham D, Atkin W, Lenz HJ, Lynch HT, Minsky B, Nordlinger B and Starling N. Colorectal cancer. Lancet. 2010; 375(9719):1030-1047.
3. Price TJ, Segelov E, Burge M, Haller DG, Ackland SP, Tebbutt NC, Karapetis CS, Pavlakis N, Sobrero AF, Cunningham D and Shapiro JD. Current opinion on optimal treatment for colorectal cancer. Expert Rev Anticancer Ther. 2013; 13(5):597-611.
4. Markowitz SD and Bertagnolli MM. Molecular origins of cancer: Molecular basis of colorectal cancer. N Engl J Med. 2009; 361(25):2449-2460.
5. Comprehensive molecular characterization of human colon and rectal cancer. Nature. 2012; 487(7407):330-337.
6. Valeri N, Croce CM and Fabbri M. Pathogenetic and clinical relevance of microRNAs in colorectal cancer. Cancer Genomics Proteomics. 2009; 6(4):195-204.
7. Lovat F, Valeri N and Croce CM. MicroRNAs in the pathogenesis of cancer. Semin Oncol. 2011; 38(6):724-733.
8. Schetter AJ and Harris CC. Alterations of microRNAs contribute to colon carcinogenesis. Semin Oncol. 2011; 38(6):734-742.
9. Fassan M, Croce CM and Rugge M. miRNAs in precancerous lesions of the gastrointestinal tract. World J Gastroenterol. 2011; 17(48):5231-5239.
10. Fassan M and Baffa R. MicroRNAs and targeted therapy: small molecules of unlimited potentials. Curr Opin Genet Dev. 2013; 23(1):75-77.

11. Schwarzenbach H, Nishida N, Calin GA and Pantel K. Clinical relevance of circulating cell-free microRNAs in cancer. Nat Rev Clin Oncol. 2014; 11(3):145-156.
12. Liu Z, Liu J, Segura MF, Shao C, Lee P, Gong Y, Hernando E and Wei JJ. MiR-182 overexpression in tumourigenesis of high-grade serous ovarian carcinoma. J Pathol. 2012; 228(2):204-215.
13. Segura MF, Hanniford D, Menendez S, Reavie L, Zou X, Alvarez-Diaz S, Zakrzewski J, Blochin E, Rose A, Bogunovic D, Polsky D, Wei J, Lee P, Belitskaya-Levy I, Bhardwaj N, Osman I, et al. Aberrant miR-182 expression promotes melanoma metastasis by repressing FOXO3 and microphthalmia-associated transcription factor. Proc Natl Acad Sci U S A. 2009; 106(6):1814-1819.
14. Wang J, Li J, Shen J, Wang C, Yang L and Zhang X. MicroRNA-182 downregulates metastasis suppressor 1 and contributes to metastasis of hepatocellular carcinoma. BMC Cancer. 2012; 12:227.
15. Kong WQ, Bai R, Liu T, Cai CL, Liu M, Li X and Tang H. MicroRNA-182 targets cAMP-responsive element-binding protein 1 and suppresses cell growth in human gastric adenocarcinoma. FEBS J. 2012; 279(7):1252-1260.
16. Sun Y, Fang R, Li C, Li L, Li F, Ye X and Chen H. Hsa-mir-182 suppresses lung tumorigenesis through down regulation of RGS17 expression in vitro. Biochem Biophys Res Commun. 2010; 396(2):501-507.
17. Yang WB, Chen PH, Hsu Ts, Fu TF, Su WC, Liaw H, Chang WC and Hung JJ. Sp1-mediated microRNA-182 expression regulates lung cancer progression. Oncotarget. 2014; 5(3):740-753.
18. Sarver AL, French AJ, Borralho PM, Thayanithy V, Oberg AL, Silverstein KA, Morlan BW, Riska SM, Boardman LA, Cunningham JM, Subramanian S, Wang L, Smyrk TC, Rodrigues CM, Thibodeau SN and Steer CJ. Human colon cancer profiles show differential microRNA expression depending on mismatch repair status and are characteristic of undifferentiated proliferative states. BMC Cancer. 2009; 9:401.
19. Ng EK, Chong WW, Jin H, Lam EK, Shin VY, Yu J, Poon TC, Ng SS and Sung JJ. Differential expression of microRNAs in plasma of patients with colorectal cancer: a potential marker for colorectal cancer screening. Gut. 2009; 58(10):1375-1381.
20. Schetter AJ, Leung SY, Sohn JJ, Zanetti KA, Bowman ED, Yanaihara N, Yuen ST, Chan TL, Kwong DL, Au GK, Liu CG, Calin GA, Croce CM and Harris CC. MicroRNA expression profiles associated with prognosis and therapeutic outcome in colon adenocarcinoma. JAMA. 2008; 299(4):425-436.
21. Rapti SM, Kontos CK, Papadopoulos IN and Scorilas A. Enhanced miR-182 transcription is a predictor of poor overall survival in colorectal adenocarcinoma patients. Clin Chem Lab Med. 2014.
22. Liu H, Du L, Wen Z, Yang Y, Li J, Wang L, Zhang X, Liu Y, Dong Z, Li W, Zheng G and Wang C. Up-regulation of miR-182 expression in colorectal cancer tissues and its prognostic value. Int J Colorectal Dis. 2013; 28(5):697-703.
23. Pizzini S, Bisognin A, Mandruzzato S, Biasiolo M, Facciolli A, Perilli L, Rossi E, Esposito G, Rugge M, Pilati P, Mocellin S, Nitti D, Bortoluzzi S and Zanovello P. Impact of microRNAs on regulatory networks and pathways in human colorectal carcinogenesis and development of metastasis. BMC Genomics. 2013; 14:589.
24. Fassan M, Baffa R and Kiss A. Advanced precancerous lesions within the GI tract: the molecular background. Best Pract Res Clin Gastroenterol. 2013; 27(2):159-169.
25. Myatt SS, Wang J, Monteiro LJ, Christian M, Ho KK, Fusi L, Dina RE, Brosens JJ, Ghaem-Maghami S and Lam EW. Definition of microRNAs that repress expression of the tumor suppressor gene FOXO1 in endometrial cancer. Cancer Res. 2010; 70(1):367-377.
26. Schaefer A, Jung M, Mollenkopf HJ, Wagner I, Stephan C, Jentzmik F, Miller K, Lein M, Kristiansen G and Jung K. Diagnostic and prognostic implications of microRNA profiling in prostate carcinoma. Int J Cancer. 2010; 126(5):1166-1176.
27. Amodeo V, Bazan V, Fanale D, Insalaco L, Caruso S, Cicero G, Bronte G, Rolfo C, Santini D and Russo A. Effects of anti-miR-182 on TSP-1 expression in human colon cancer cells: there is a sense in antisense? Expert Opin Ther Targets. 2013; 17(11):1249-1261.
28. Wang YQ, Guo RD, Guo RM, Sheng W and Yin LR. MicroRNA-182 promotes cell growth, invasion, and chemoresistance by targeting programmed cell death 4 (PDCD4) in human ovarian carcinomas. J Cell Biochem. 2013; 114(7):1464-1473.
29. Wang M, Wang Y, Zang W, Wang H, Chu H, Li P, Li M, Zhang G and Zhao G. Downregulation of microRNA-182 inhibits cell growth and invasion by targeting programmed cell death 4 in human lung adenocarcinoma cells. Tumour Biol. 2014; 35(1):39-46.
30. Mikula M, Rubel T, Karczmarski J, Goryca K, Dadlez M and Ostrowski J. Integrating proteomic and transcriptomic high-throughput surveys for search of new biomarkers of colon tumors. Funct Integr Genomics. 2010.
31. Fang M, Shen Z, Huang S, Zhao L, Chen S, Mak TW and Wang X. The ER UDPase ENTPD5 promotes protein N-glycosylation, the Warburg effect, and proliferation in the PTEN pathway. Cell. 2010; 143(5):711-724.
32. MacCarthy CM and Notario V. The ENTPD5/mt-PCPH oncoprotein is a catalytically inactive member of the ectonucleoside triphosphate diphosphohydrolase family. Int J Oncol. 2013; 43(4):1244-1252.
33. Wang Q, Huang Z, Ni S, Xiao X, Xu Q, Wang L, Huang D, Tan C, Sheng W and Du X. Plasma miR-601 and miR-760 are novel biomarkers for the early detection of colorectal cancer. PLoS One. 2012; 7(9):e44398.
34. Giraldez MD, Lozano JJ, Ramirez G, Hijona E, Bujanda

L, Castells A and Gironella M. Circulating microRNAs as biomarkers of colorectal cancer: results from a genome-wide profiling and validation study. Clin Gastroenterol Hepatol. 2012; 11(6):681-688 e683.